

V.I. Tsymbalyuk, R.Ya. Abdullaiev, I.A. Lurin,  
I.N. Dikan, R.V. Bubnov, O.I. Grechanyk

**Ultrasound  
of the spine, peripheral nerves  
and for pain management**

Kharkiv, 2024

УДК 615.8+616.8  
ББК 53.6+56.12  
У 51

Approved at the meeting of the Scientific Council of the state institution Institute of Neurosurgery named after Acad. A.P. Romodanova National Academy of Sciences of Ukraine  
Protocol No 11 of December 26, 2023

**Ultrasound** of the spine, peripheral nerves and for pain management  
[V.I. Tsybalyuk, R.Ya. Abdullaiev, I.A. Lurin, I.N. Dikan, R.V. Bubnov, O.I. Grechanyk,]. – Kharkiv: Fact, 2024. - 194 p

ISBN 978-617-568-032-2

The publication is devoted to ultrasound investigation of peripheral nerves and spinal cord. It presents more than 200 echograms demonstrating stenosis of the spinal canal with protrusions and herniated intervertebral discs, compression of rootlets of spinal nerves at various levels of the vertebral motor segment, traumatic lesions of peripheral nerves detecting and treatment myofascial trigger points for acute and chronic pain.

It is intended for medical doctors of ultrasonography, neurologists, neurosurgeons, vertebroneurologists, interns, students of higher medical educational institutions.

This work is subject to copyright. All rights reserved by the Authros. No part of this publication may be reproduced or transmitted in any form or by any means, electronically or mechanically, including photocopying, recording or any information storage or retrieval system, without either permission in writing from the publisher or a licence permitting restricted copying.

УДК 615.8+616.8  
ББК 53.6+56.12

ISBN 978-617-568-032-2

© V.I. Tsybalyuk, R.Ya. Abdullaiev, I.A. Lurin,  
I.N. Dikan, R.V. Bubnov, O.I. Grechanyk, 2024

# Content

Foreword .....	4
Chapter 1. Anatomy and ultrasound semiotics of the spinal canal, spinal cord and spinal nerves .....	5
1.1. <i>Cervical spine canal</i> .....	5
1.2. <i>Thoracic spinal canal</i> .....	17
1.3. <i>Lumbar spine</i> .....	18
Chapter 2. Ultrasonography in the diagnosis of causes of vertebral pain .....	30
Chapter 3. The use of Doppler ultrasound for degenerative changes in intervertebral discs .....	48
Chapter 4. Regional anesthesia of body under US guidance. Chapter 5 Spinal dyshammia .....	67
5.1. <i>Features of the blood circulation of the spinal cord</i> .....	67
5.2. <i>Anatomical and physiological prerequisites and clinic of spinal cord blood flow disorders</i> .....	71
5.3. <i>Neurovascular syndromes</i> .....	83
Chapter 6. Ultrasonography of peripheral nerves and regional anesthesia .....	90
Chapter 7. Trigger Points Dry Needling under Under Ultrasound Guidance for Pain Management. Personalized and Evidence- Based Concept .....	102
Chapter 8. Damage to peripheral nerves in gunshot wounds .....	124
Chapter 9. Regional anesthesia under ultrasound guidance .....	135
Chapter 10. Novel approaches of physical therapy and pain management .....	150
Chapter 11. Introduction to sonosurgery .....	164
Chapter 12. Clinical Application and Efficacy of Ultrasound in Combat-Related Neuropathies .....	171

# Foreword

The creation and further dramatic development of ultrasound methods truly revolutionized the diagnosis of many diseases. High resolution of ultrasound equipment, relative prostate and rapidity of research, its ease for the patient allow applying echography in various fields of medicine. The combination of two-dimensional and Doppler modes allows to study the anatomical structure of organs and determine the blood flow in them.

In recent years, the number of publications devoted to the study of intervertebral discs degeneration in at the cervical and lumbar levels has increased. However, due to the small number of experts in ultrasound imaging of these structures, the method is still not used enough.

The variety of clinical symptoms associated with the pathology of the spinal cord and peripheral nerves is the subject of research in the practice of a neurosurgeon, vertebrologist, neurologist. The greatest number of pathologies of the peripheral nervous system is due to compression of the spinal cord and roots of the spinal nerves in degenerative-dystrophic processes in the intervertebral discs, damage to the neurovascular bundle in various types of trauma. Current possibilities of ultrasound technologies open new prospects for studying these issues by this highly informative and inexpensive method. The advantages of ultrasonography include the possibility of conducting a real-time study, the ease of performing functional tests and concomitant vascular studies.

The capabilities of ultrasound to visualize the peripheral nerves, spinal cord and spinal nerves at the level of cervical and upper lumbar intervertebral motor segments is shown in this work. Interventions under ultrasound guidance including regional anesthesia, paravertebral block were also demonstrated. Innovative techniques of sonosurgery are presented in the book. The advance of visualizing myofascial trigger points allow to diagnose and treat acute and chronic pain at highly effective and evident-based level.

The authors hope that the publication will help to increase the awareness of a wide range of specialists regarding the possibilities of ultrasonography to solve many urgent problems. The book is designed for medical doctors of ultrasound diagnostics, orthopedics, traumatology, neurosurgery and neurology. The contribution of this manual can be used in the training of intern doctors in radiology, medical students and doctors-fellows at postgraduate education.

# Chapter 1

## Anatomy and ultrasound semiotics of the spinal canal, spinal cord and spinal nerves

### 1.1. Cervical spine canal

The vertebrae are located one above the other, with the participation of the arches, form the vertebral canal. Its surface is lined with a *dura mater*, between it and the posterior longitudinal ligament there is an anterior epidural space filled with a layer of loose fiber with veins of the anterior epidural plexus passing through it, collecting blood from the venous sinuses of the vertebral bodies.

In the vertebral canal there is a spinal cord (SC), its cervical part has an extent from the atlas to the middle of C7. In the cervical spine, spinal cord nerve roots 1–7 exit from the vertebral canal above the vertebra corresponding to them, and the spine C8 threads extend below the C7 body. The posterior leaflet of the *dura mater* closes the cerebrospinal space, forming a dural sac limited to the front and back of the *dura mater*, to the sides by dural funnels accompanied by radicular nerves and terminating at the level of the intervertebral foramen. Near the root nerves there is a dentate ligament attached to the wall of the spinal canal and SC. The canals, front limited by the posterior surface of the disc and the bone boundaries of the intervertebral foramen on the other sides, whose contents are the roots and leaves of the funnel, are sometimes called lateral, or radicular. Behind the posterior leaf of the *dura mater*, the posterior epidural cell space and the yellow ligament are located (Figure 1–3).

Yellow ligaments extend from the first cervical to the first sacral vertebra. Speaking in the spinal canal, they somewhat reduce its diameter. Given that these ligaments are most developed in the lumbar region, their hypertrophy can lead to pressure on the pony tail. Bundles consist of vertically extending elastic beams, giving them a yellow color (Fig. 4). The yellow liga-

ments are very elastic and elastic, so when the trunk is unbent, they shorten and act like muscles, causing the trunk to be held in the state of extension and thus reducing muscle tension. When bending, the yellow ligaments stretch and thereby also reduce the tension of the «torso rectifier». Such ligaments are absent between the arcs of the first and second cervical vertebrae. Here, the connective tissue Atlanto-osseum membrane is stretched, bounding behind the front edge of the intervertebral opening, through which the second cervical nerve emerges.

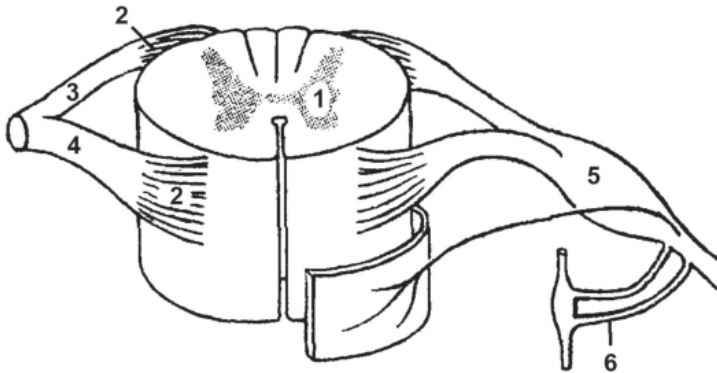


**Fig. 1.** Schematic representation of the spinal cord: 1 – spinal cord; 2 – radicular threads; 3 – posterior spine; 4 – the front spine; 5 – the spinal node; 6 – white branch; Preganglionic sympathetic fibers

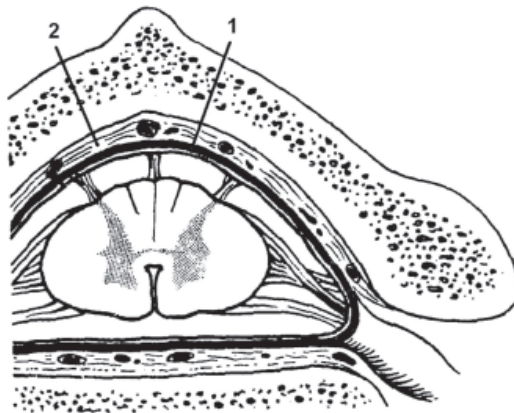


**Fig. 2.** Schematic representation of the spinal cord: 1 – epidural veins; 2 – epidural space

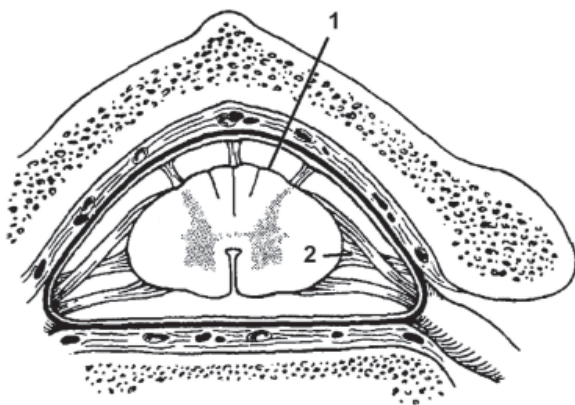


**Fig. 3.** Schematic representation of the spinal cord: 1 – soft dura mater; 2 – clogged ligament

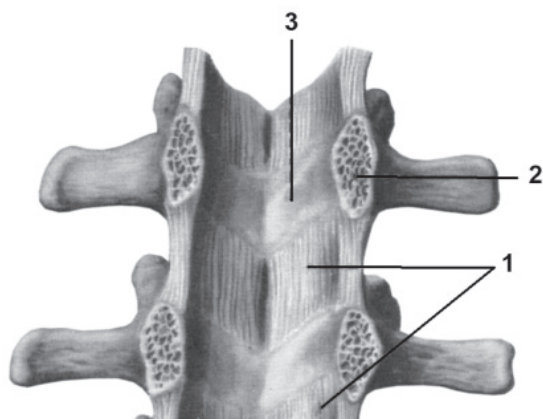


**Fig. 4.** Schematic representation of a fragment of the vertebral motor segment: 1 – yellow ligaments; 2 – a leg of an arch of a vertebra; 3 – arc of the vertebra

In the cervical region, transverse processes form openings through which the vertebral artery, vein and the accompanying sympathetic plexus accompany them. The transverse processes are short and directed to the sides. A deep furrow of the spinal nerve passes along the upper surface of each of them.

The ultrasonic tomography of the cervical spinal canal is capable to demonstrate:

A) vertebral artery syndrome, often caused by instability of the cervical motor segment and unco-vertebral arthrosis. This may be due to both degenerative-dystrophic changes in the discs, and the inconsistency of the ligamentous apparatus. It often occurs in young people, children and adolescents with an unchanged structure of intervertebral discs. The main causes of dysfunction of the ligamentous apparatus are dysplastic and dystrophic processes of connective tissue, traumas, including birth defects. In both cases, the main diagnostic method is triplex dopplerography with functional tests;

B) reflexive pain syndromes of osteochondrosis, the causes of which may be hernias of discs, protrusions, dislocations and osteophytes of vertebral bodies, as well as articular processes in spondylosis and spondyloarthrosis;

C) postoperative *cicatricial epiduritis*, varicose dilatation of the epidural veins.

Ultrasonic tomography of the cervical spinal canal is performed from the anterolateral and posterior approaches. Because of the slight convexity of the underlying and concavity of the vertebral body above the closure plate, anterolateral access is most effective for examining the disc and the spinal canal behind it. A significant part of the information on the state of the intervertebral motor segment can be obtained in the position of the patient lying on his back, having installed a sensor on both sides of the trachea in the longitudinal and transverse planes. The longitudinal section in the sagittal plane allows simultaneous visualization of the structure of the intervertebral disc, the vertebral canal. For good visualization of the studied structures, it is best to use a microconvex sensor with an operating frequency of 3–7 MHz, and in its absence, a combination of a 5-MHz convection sensor and a linear sensor with a 4 cm aperture and a working frequency of 7.5 MHz, Information.

The main ultrasound window for visualization of the spinal canal, SM and rootlets of the spinal nerves are intervertebral discs. The upper part of the spinal cord is better visualized from the occipital access. For all age groups of patients, a high-frequency microconvex sensor is suitable for the investigation of the cervical spinal cord. On the axial section in the center of the image, the spinal cord is located in the form of a hypo-anechogenous oval formation with a clear visualization of the membranes, jagged ligaments attached to it from the lateral sides (Fig. 5). On the longitudinal section, it is possible to better visualize the SC architecture as a fine-grained fibrillar structure (Fig. 6).

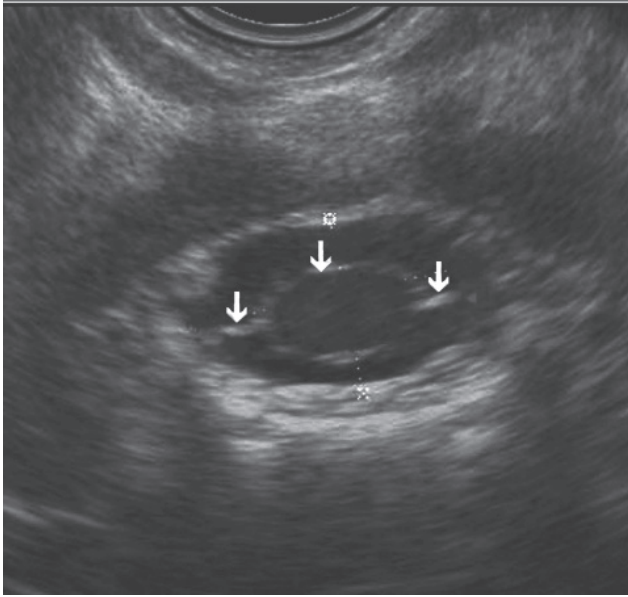


**Fig. 5.** Visualization of the spinal canal, spinal cord (*middle arrow*), jagged ligaments (*lateral arrows*) from the rear access in the axial section

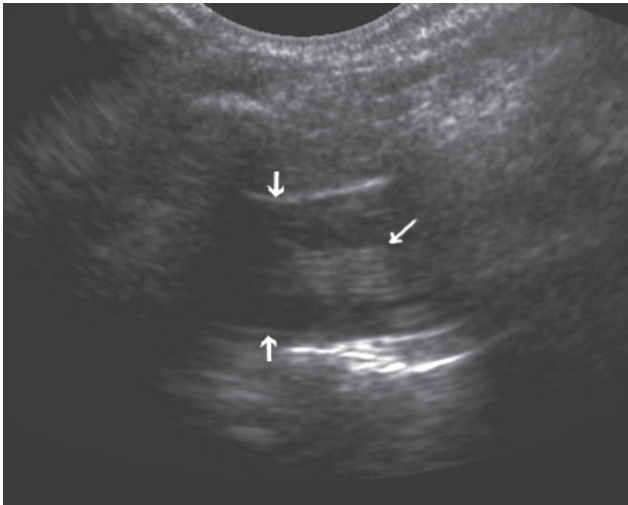


**Fig. 6.** Visualization of the internal structure of the spinal cord on the longitudinal section (*middle arrow*)

To correctly read the intervertebral disc, you should first visualize the body 7 of the cervical vertebra. When the sensor is located above the sternoclavicular junction, the body of C7 is located below all the discs available for later investigation in the sagittal plane, above it is C6–C7, and below it is C7–Th1. After revealing the natural anatomical landmark of the C7 body, the sensor is moved upwards in the sagittal plane, making identification of all the vertebral bodies and intervertebral discs. Inspection is best available four discs (D), easily identifiable because of the proximity to the sensor and the stability of the landmarks: C3–C4, C4–C5, C5–C6, C6–C7.

The longitudinal section in the sagittal plane allows simultaneous visualization of the anterior longitudinal ligament, the structures of the intervertebral discs, and the vertebral canal. From this access, vertebral bodies are determined on the hyperechogenic front surfaces, their height, thickness (height) of the discs is measured – the distance between the contours of their bodies. Inside the vertebral canal, at the level of the intervertebral discs, a SC with a characteristic architectonics is visualized (Fig. 7–9).

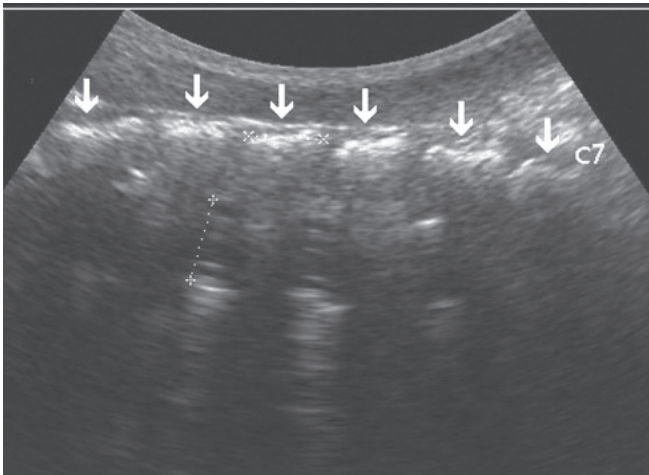


**Fig. 7.** Visualization of cervical vertebrae from C2 to C7 (*arrows*), intervertebral discs between them, spinal canal

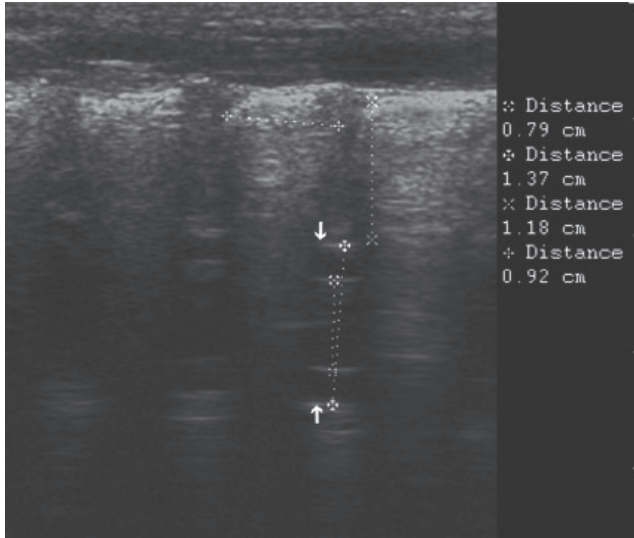


**Fig. 8.** Determination of sagittal size of vertebral body, vertebral canal

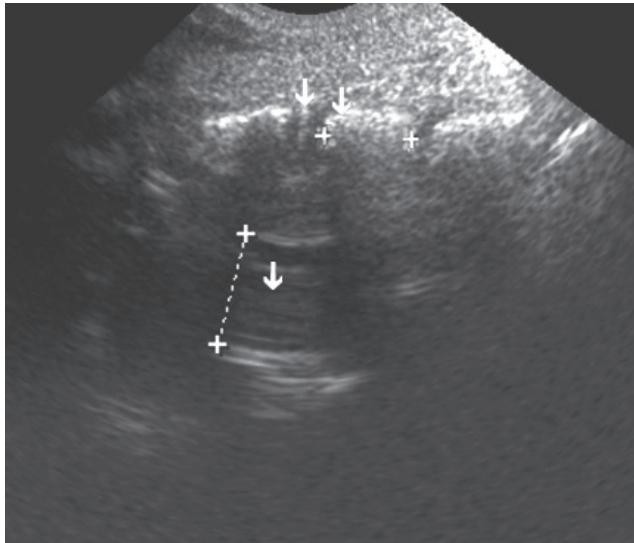


**Fig. 9.** Visualization of the spinal canal in a child from anterolateral access. Arrows from top to bottom show the intervertebral disc, vertebra and spinal cord. Well visible architectonics of the spinal cord (*arrow*)

After receiving the image of the disc in the sagittal plane, the sensor is rotated 90 degrees to visualize the axial section, on which it looks like a hypoechoic oval-rounded formation. The axial ultrasound tomogram clearly delineates the fibrous ring around the periphery of the disc as an average echogenicity of the circular fibrillar structure. The thickness of the fibrous ring is 5–7 mm. In the center of the intervertebral disc is a pulpous nucleus, which in young people has a hypo- or anechoic homogeneous structure and is clearly delineated with a fibrous ring. With age, the echogenicity of the pulpous nucleus rises, the border between it and the fibrous ring is not found. The posterior border of the intervertebral disc is defined as a clear, slightly concave hyperechoic line between the cartilaginous structure of the disc and cerebrospinal fluid in the vertebral canal.

On the sides of the spinal canal are channels of spinal nerves, which end at the level of the intervertebral foramen. From the SC, the anterior and posterior rootlets of the spinal nerves are separated, with jagged ligaments between them. They are attached from one side to the side walls of the spinal canal, on the other – to the spinal cord, holding it. With a good ultrasound window, the possibilities of ultrasonography are not inferior to magnetic resonance imaging (Fig. 10, 11)

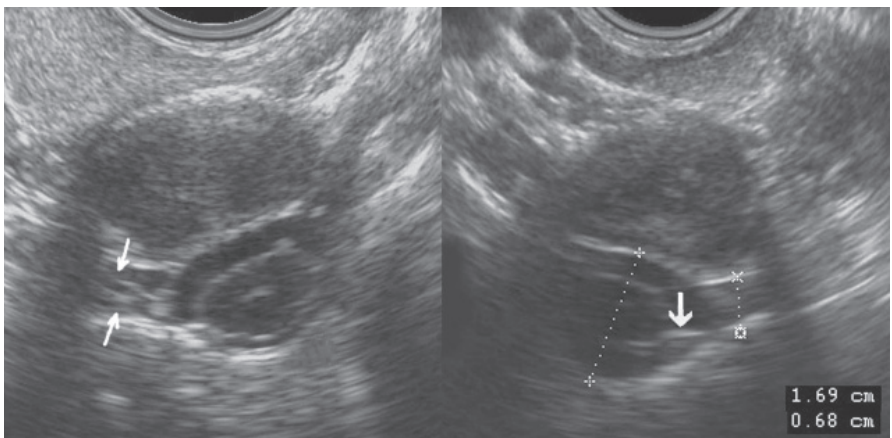


**Fig. 10.** Axial section of the intervertebral disc and spinal canal. On the right side of the echogram arrows indicate the spinal nerve in the lateral canal, the left part shows: the sagittal dimension of the central vertebral and lateral canals, as well as the dentate ligament (*arrow*)

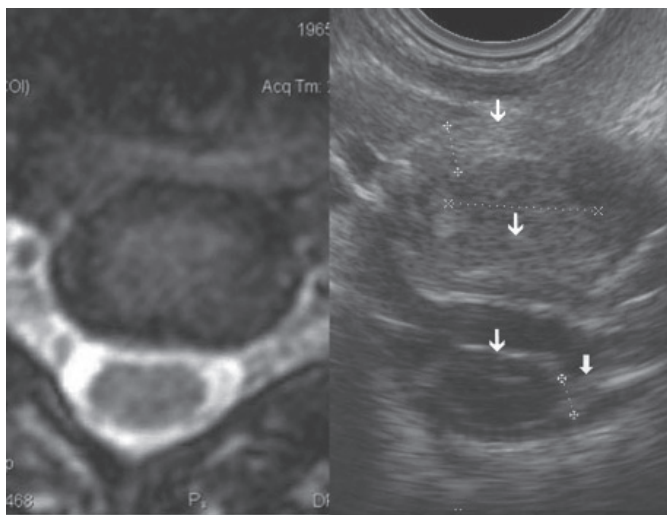


**Fig. 11.** Axial section of the intervertebral disc with magnetic resonance imaging and ultrasonography. Arrows from top to bottom show the fibrous ring, the pulposus nucleus, the spinal cord and the spine of the spinal nerve

In adults, the height (thickness) of the discs is 4–6 mm, the thickness of the fibrous ring is 4–5 mm, the anteroposterior size of the spinal canal is 13–15 mm, the canal of the spinal nerves is 5–7 mm, the thickness of the yellow ligament 2–3 mm.

With a slight lateral displacement of the sensor on the axial tomogram, it is possible to obtain an image of the hook-shaped process, the canal of the vertebral artery, and also the artery itself. Between the artery and the hook-shaped process, a layer of medium echogenicity is visualized, a hypoechoic articular gap is visible between the hyperechoic linear structure of the hook-shaped processes above and the underlying vertebrae. *Luschka's joints* are better visible when the sensor is located in the anterolateral region of the neck at an angle of 40–60 degrees in the cranio-caudal direction (Fig. 12).

When scanning on both sides at the level of each segment, the relationship between the hook-shaped process and the artery is established, the main criterion for evaluation is the symmetry of the distance between the artery and bone structures. Such an assessment is of particular importance at the level of segments C5–C6 and C4–C5, where unko-vertebral arthrosis most often occurs.

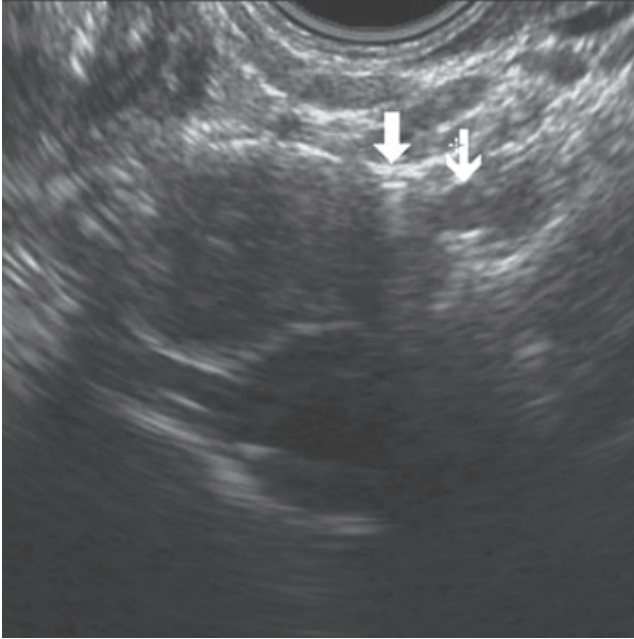


**Fig. 12.** Axial section of intervertebral disc and spinal canal. Clear visualization of the joint Lyushka (*left arrow*) and vertebral artery (*right arrow*)

In connection with the frequent damage to the atlanto-axial articulation, its instability in childhood is important visualization of this department. From the rear access, the most qualitative examination of the vertebral canal, arches and arcuate joints is carried out through the inter-gaps in the longitudinal and axial sections. Visualization of the dental process (*processus dentatus*, PD) of the second cervical vertebra (C2), the lateral masses (LM) of the first vertebra (C1), the *Cruveilhier`s joint* is best accomplished from the rear access. Sagittal sections with the location of the sensor on both sides of the spinous processes provide visualization of the spinal canal, and axial sections – LM, the tip of the DP, transverse ligament (TL) of the medial *atlanto-axial joint*. The thickness of PS in newborns varies within 1.8–2.2 mm, in older children 2.7–3.2 mm. The echogenicity of this ligament in newborns is lowered and comparable with the echogenicity of SM, in children 4–6 years old – with the pulposus core of the intervertebral disc, in older children – with echogenicity of the fibrous ring of the disc. The distance between LM in newborns is on the average  $15.0 \pm 1.8$  mm (Fig. 13–14).

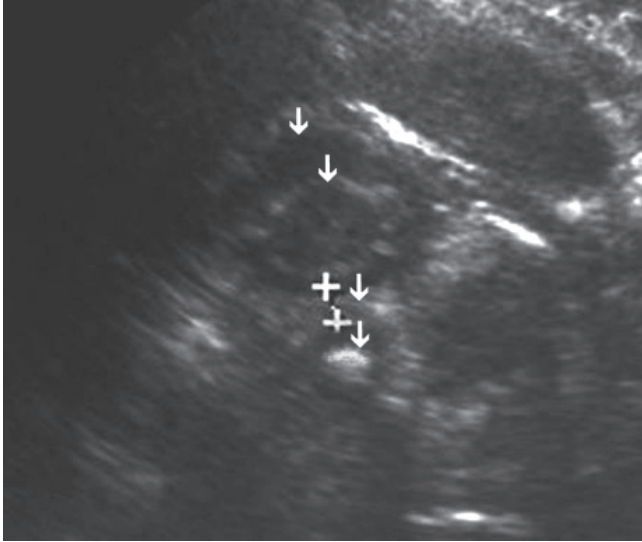


**Fig. 13.** Ultrasound tomogram of the spinal canal from the rear access in the infant at C1–C2 level. From the top down the arrows show the posterior dural space, spinal cord, transverse ligament, dentate process C2

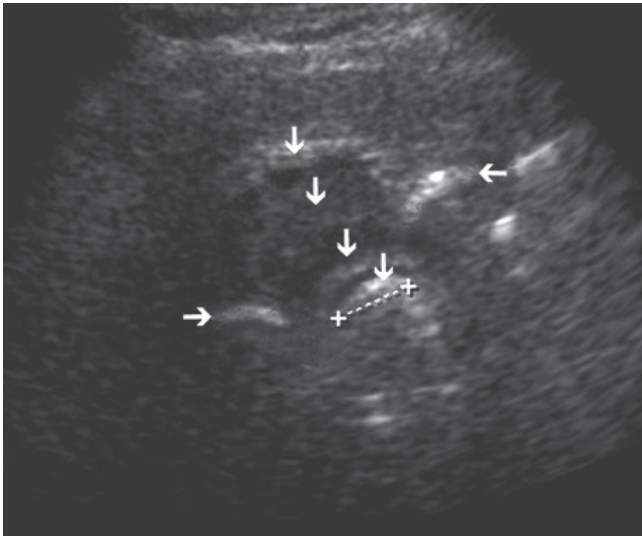


**Fig. 14.** The same for a child of 5 years. The lateral arrows show the lateral masses

The main criteria for the norm for the atlas-axial joint are: the central location of the PD with respect to the BM with asymmetry of no more than 12 %, the thickness of the synovial bag between the PDS and PS is more than 1.5 mm and the thickness of the anterior dural space (ADS) is about 2.0 mm for newborns and 2.5 mm – for children aged 4–6 years, posterior dural space (PDS) – about 3.0 and 3.5 mm, respectively, their ratio is 1.2–1.3 for all age groups, clear visualization Shells SM and its round-oval shape, the location of the BM at one level along the horizon hoists, uniform thickness of the transverse ligaments on both sides of the LP (Table. 1, 2).

Table 1.

**Ultrasound parameter of bone structures of atlanto-axial joints**

<b>Ultrasound parameter</b>	<b>Newborns (n = 12)</b>	<b>Healthy children aged 6–12 months (n = 15)</b>	<b>Healthy children aged 4–6 years old (n = 23)</b>
Width of LM, mm	16,19±0,78	18,01±1,08	27,87±0,98
D 1, mm	5,29±0,3	5,45±0,39	9,85±0,41
D 2, mm	5,87±0,41	6,09±0,41	10,98±0,45
Index D 1 / D 2	0,90±0,08	0,89±0,07	0,90±0,08
Width of DP, mm	5,03±0,36	6,47±0,39	7,04±0,41
Degree of ADS asymmetry	11,0±4,1	11,7±2,1	11,5±3,8

*Note. The abbreviations are explained in the text.*

Table 2.

**Ultrasound parameter of the spinal canal at the level of C1–C2**

<b>Ultrasound parameter</b>	<b>Newborns (n = 12)</b>	<b>Healthy children aged 6–12 months (n = 15)</b>	<b>Healthy children aged 4–6 years old (n = 23)</b>
Sagittal size SCC (C1-C2), mm	10,04 ± 0,42	11,23 ± 0,37	14,15 ± 0,51
Sagittal size of SC (C1-C2), mm	5,45 ± 0,26	5,63 ± 0,26	7,32 ± 0,42
Thickness PDS (C1-C2), mm	2,03 ± 0,21	2,49 ± 0,21	3,04 ± 0,7
thickness of ADS (C1-C2), mm	2,56 ± 0,27	3,11 ± 0,27	3,79 ± 0,34
PDS/ADS ratio	1,26 ± 0,13	1,25 ± 0,12	1,25 ± 0,12

*Note. The abbreviations are explained in the text.*

## 1.2. Thoracic spinal canal

The thoracic part of the spinal canal is formed by the body and the arms of twelve thoracic (T1–T12) vertebrae. The thoracic segments of the SM are located from the middle of C7 to the middle of T11. Ultrasonic tomography of the thoracic spinal canal can only be carried out from the rear access through the interstitial space by means of a microconvex sensor with a frequency of 3–5 MHz. In the longitudinal section, to identify the level of the spine, it is best to use a linear sensor with a working aperture of 4–5 cm. The spine can be counted from below from the first lumbar and from above from the seventh cervical vertebra. The sensor is located above the spinous process of the first lumbar vertebra and slowly moves upward. When moving from the first lumbar to the 12th thoracic vertebra on the monitor screen, the relatively long spinous process of the lumbar vertebra is replaced by a shorter process of the thoracic vertebra. Behind the *spinous processes*, acoustic shadows are visualized, between which is seen a vertebral canal with linearly located brain envelopes, the posterior contour of the disc (Fig. 15).

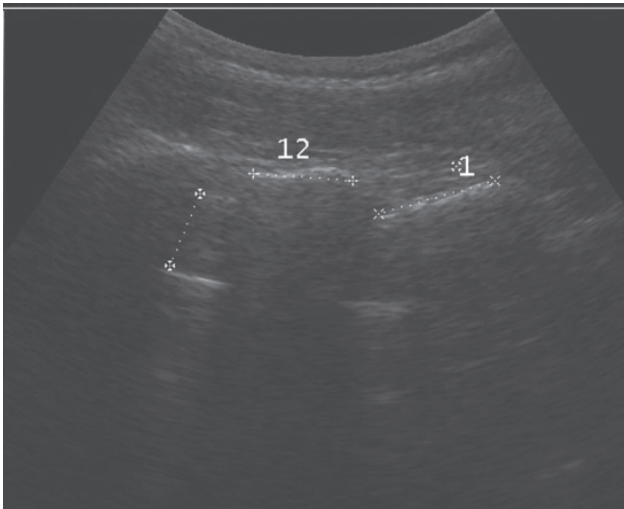


**Fig. 15.** The longitudinal section shows the difference in length and direction of the spinous process of the 12th thoracic and 1st lumbar vertebrae

On the axial ultrasound tomograms a spinous process, a vertebral canal, a back contour of the intervertebral disc, and in both directions from the center a channel of spinal nerves, an articular and transverse process can be visualized from top to bottom (Fig. 16).

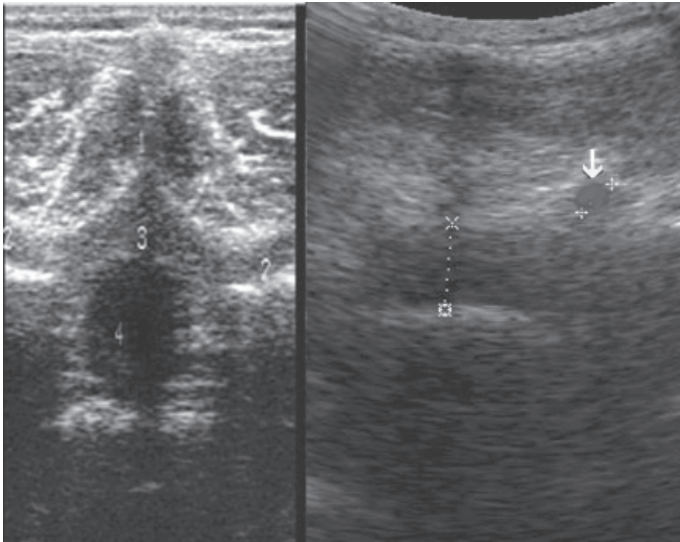


**Fig. 16.** The transverse section visualizes the vertebral canal (4), the arch (3), the transverse (2) and the spinous process (1) on the left side of the echogram, and the paravertebral longitudinal section shows the vertebral canal and the intervertebral foramen on the right side

### ***1.3. Lumbar spine***

The body of the lumbar vertebrae has a bean-shaped form, the arches are highly developed, the vertebral opening is larger than in the thoracic vertebrae, the anterior surface slightly concave in the sagittal direction. A vertebral canal forms between the posterior surface of the body and the arch. At the level of T11 – L1 is located the lumbar segment of the spinal cord, below it narrows and continues to the ponytail.

Lumbar intervertebral discs occupy a third of the body's height in accordance with the exercise performed. The most frequent localization of protrusions and disc herniations occurs at the most overloaded departments – L4–L5 and L5 and S1. The pelvic nucleus is located on the border of the posterior and middle third of the lumbar intervertebral discs. The fibrous ring in this region is much thicker in the front, where it is supported by a dense anterior longitudinal ligament, powerfully developed in the lumbar region. Behind the fibrous ring is thinner and separated from the vertebral canal by

a thin and more poorly developed posterior longitudinal ligament connected to the lumbar intervertebral disks more firmly than with the vertebral bodies. The ligament to the vertebral bodies is connected by a loose connective tissue, in which the venous plexus is laid (Fig. 17–20).

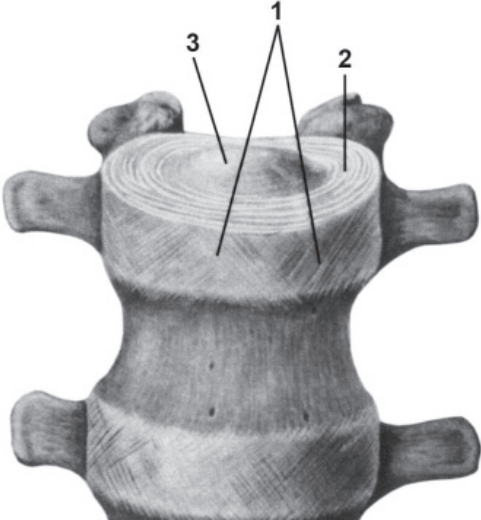


**Fig. 17.** Lumbar intervertebral disc: 1 – anterior longitudinal ligament; 2 – fibrous ring; 3 – pulposus nucleus

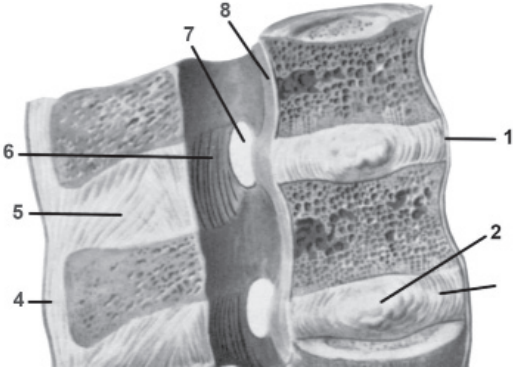


**Fig. 18.** Lumbar intervertebral disc: 1 – anterior longitudinal ligament; 2 – pulposus nucleus; 3 – fibrous ring; 4 – supramarginal ligaments; 5 – interstitial ligaments; 6 – yellow ligaments; 7 – intervertebral foramen; 8 – posterior longitudinal ligament

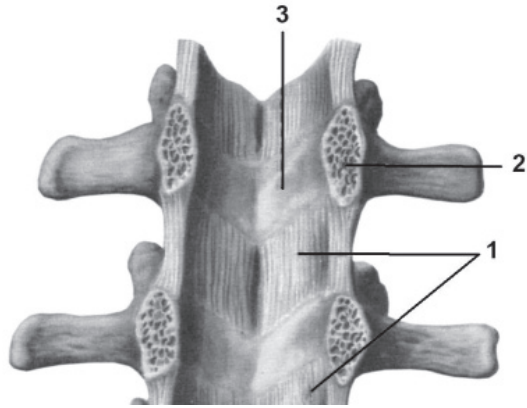


**Fig. 19.** Lumbar intervertebral disc: 1 – yellow ligaments; 2 – a leg of an arch of a vertebra; 3 – arc of the vertebra

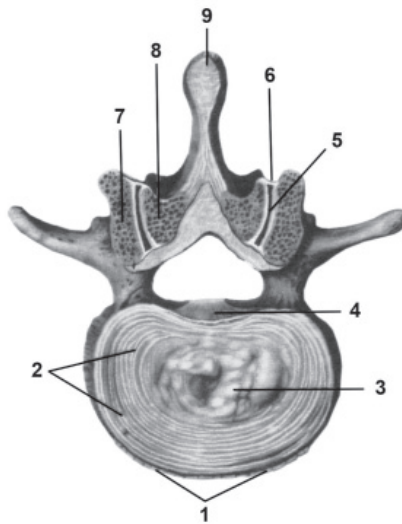


**Fig. 20.** Lumbar intervertebral disc: 1 – anterior longitudinal ligament; 2 – fibrous ring; 3 – pulposus nucleus; 5 – arcuate joint; 6 – articular cleft; 7 – articular process; 8 – arc of the vertebra; 9 – spinous process

Ultrasonic tomography of the lumbar vertebral motor segment is carried out from the anterior (transabdominal) and posterior approaches. Transabdominal access is most effective for examining the disc and the

spinal canal behind it. The longitudinal section in the sagittal plane allows simultaneous visualization of the intervertebral disc, vertebral canal, and vertebral bodies. The quality of visualization depends on the constitutional features and preparation of the patient. Convex electronic sensors with a frequency range of 2 to 5 MHz are used for the study. Qualitative visualization of studied structures in lean people is better performed at a high frequency (5 MHz), and in large and well-fed – low (2 MHz).

In the sagittal plane, the anterior contour of the vertebral bodies is defined as hyperechoic linear structures, between which the intervertebral discs are visualized as slit-like spaces between the vertebral bodies of different echogenicity and different degrees of homogeneity, which depends on the state of the pulpous substance. Behind the discs are bright linear hyperechoic echoes from the anterior and posterior borders of the vertebral canal, the yellow ligament, the vertebra arches. Between the hyperechoic linear signals from the hard and soft meninges there is an anechoic liquor space with small-line inclusions (Fig. 21). When counting the vertebral bodies, it should be taken into account that the lowest located hyperechoic linear structure with a height of 2.0–2.5 cm corresponds to the fifth lumbar vertebra (L5), then behind it is the sacrum whose surface lies at an angle to the scan plane, The reflection from its front contour is weakened. Below the navel is placed the fourth (L4), and above – the third lumbar vertebra (L3).

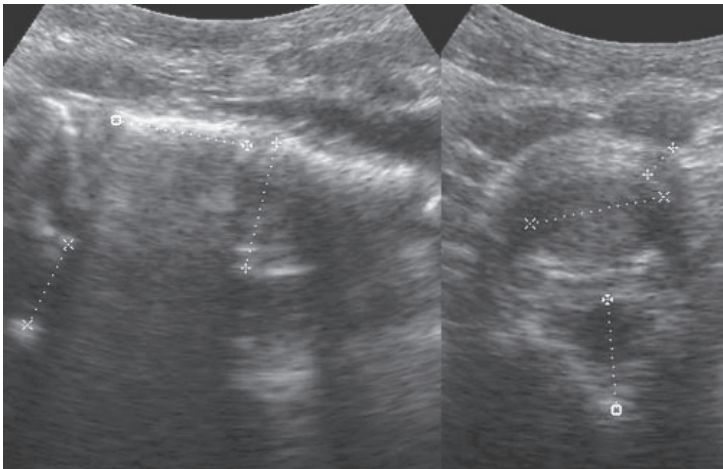


**Fig. 21.** Longitudinal view of lumbar vertebrae (*left*), transverse view of intervertebral discs and spinal canal (*right*)

In the sagittal projection, the height of the vertebral bodies and the thickness of the intervertebral discs are determined. The latter is measured between the most prominent bone contours of the endplate of vertebral bodies at the level of the anterior and posterior sections of the intervertebral fissure, which varies within 7–9 mm.

In the sagittal plane, a smooth, slightly convex contour of the arch is revealed through the front surfaces of the vertebral bodies in the static position due to the lumbar lordosis. In this case, there should be no stupiform protrusions in both the anterior and posterior parts of the bodies adjacent to the vertebral canal, which are visualized through discs.

After identifying the bodies of the vertebrae and intervertebral discs with an anatomical guide, one of the well-visualized discs is then selected, the plane is compared with the sensor axis, which rotates 90 degrees to the horizontal plane and with slight up and down movements while maintaining pressure on the abdominal wall, an axial section of the discs and vertebral Channel. The criterion for qualitative visualization will be a clear image of the spinal canal. In this case, the scanning plane for L3–L4 and L4–L5 disks is practically horizontal, for L3–S1 because of lordosis it is inclined caudally, for drives L1–L2 and L2–L3, for the same reason, it is slightly inclined cranially.

An axial ultrasound tomogram divides the fibrous ring around the periphery of the disk in the form of a circular fibrillar structure of medium echogenicity. The thickness of the fibrous ring in the posterior part of the disc, measured median, as well as in the right and left paramedian regions with horizontal scanning varies within 7–9 mm. The fibrous ring in the unmodified disk has somewhat increased echogenicity, the border between it and the fibrous ring differentiates only in young patients (Fig. 22).

The posterior segment of the fibrous ring and the posterior contour of the disc are formed by the posterior longitudinal ligament, a thin layer of epidural fiber and the dura mater. In the center of the intervertebral disc is a pulpous nucleus, which in young people has a hypo- and anechogenous homogeneous structure, is clearly delineated with a fibrous ring. On the upper disc nucleus pulposus typically superimposed area distal gain for echo attached to the front surface of the disc, just left of midline abdominal aorta of the strip higher echogenicity. With age, the echogenicity of the pulpous nucleus rises, the boundary between the nucleus and the fibrous ring does not differentiate. The posterior border of the intervertebral disc is defined as a clear, slightly concave hyperechoic line between the cartilaginous structure

of the disc and cerebrospinal fluid in the vertebral canal. Normally the anteroposterior size of the discs is 30–34 mm, width – 38–42 mm. The cross-sectional area of the vertebral canal varies between 2–3 cm<sup>2</sup>.

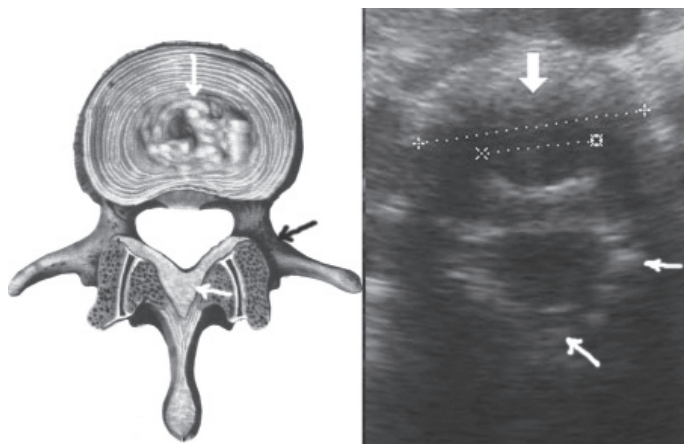


**Fig. 22.** Axial anatomical and ultrasound section at the level of the intervertebral disc and spinal canal. The fibrous ring – the hyperechoic peripheral zone of the disc and the pulpous nucleus – the central hypo-anechogenous zone of the disc (upper arrow) are clearly delineated. The lateral arrow shows the radicular canal, the lower one – the yellow bundle

In the cavity of the vertebral canal filled with CSF, closer to the posterior plate of the dura mater, a mid-echogenic structure corresponding to the horse's tail is visualized. At the level of the upper lumbar segments in the posterior sections of the vertebral canal, the roots of the cauda equina are in the form of structures of medium echogenicity. On both sides of the spinal canal there are channels of spinal nerves (lateral), which terminate at the level of the intervertebral foramen. The lateral projection of the spinal nerve roots channels investigated segments visualized as hyperechoic two horizontal lines not in contact with their front and rear boundaries (Fig. 23). In the posterior segment of the canal, the posterior leaf of the dura is visualized as a horizontal concave hyperechoic line with a yellow ligament of the middle echogenicity attached to it. For image ligamentum flavum are usually visible bone contour of the wish-bone, but depending on the scanning plane and the structural features of spinous processes and arches can be visualized mezhduzhkovoe and interspinous space located therein cords that in such cases, create an illusion of thickening ligamentum flavum with unaltered dimensions dural sac.

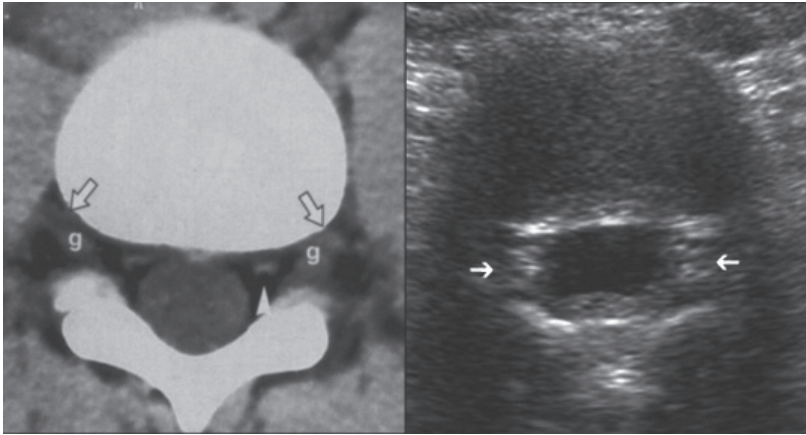


**Fig. 23.** Computer (*left*) and ultrasound tomograms of the intervertebral disc, vertebral canal and canal of the spinal nerves with a clear visualization of the nerve roots (*arrows*)

On axial scans for identification of pathological changes determined sagittal (anteroposterior) the size of the spinal canal, dural sac (between the forward channel circuit and the rear leaf dura or front edge of the ligamentum flavum), measures the lateral channels in the most narrow spaces between the disk surface and the front loop Arches and the thickness of the yellow ligament. Normally the anteroposterior size of the spinal canal is 18–21 mm, the dural sac is 12–17 mm. Anteroposterior size of lateral canals is determined in the narrowest sections of them symmetrically on the right and on the left and is 8–10 mm. The thickness of the yellow ligament is less than 5 mm.

It should be borne in mind that all the given sizes vary to a greater or lesser degree depending on the constitutional features of the patients. Among these parameters the most stable are the height of the disc, the width of its fibrous ring and the dimensions of the lateral canals, the difference between the sizes in patients usually does not exceed 2 mm. The sagittal size of the spinal canal, measured by ultrasonography, is less than in the radiographic study, since the latter can not visualize the posterior longitudinal and yellow ligaments. Anteroposterior size of the spinal canal (cerebrospinal fluid) in patients varies within the range of 12–18 mm. Reducing it at one of the levels by 3 mm or more in comparison with a number of levels located indicates a small stenosis of the spinal canal. In most clas-

sifications, the sign of absolute stenosis is a decrease in the anteroposterior size of the vertebral canal less than 12 mm.

In the longitudinal section, a sample with the maximum possible extension is carried out with the sensor position unchanged. It is carried out in the lying position, by placing the patient under his back dense bead height of 12–15 cm. More important is the front score line connecting the contours of the vertebral bodies at sagittal scan, which allows to see step-deformation formed adjacent vertebral bodies, which are caused ante- and Retroolistheses of vertebral bodies. With ultrasound, it is possible to estimate the magnitude of such displacements, although the final diagnosis of spondylolisthesis remains the prerogative of X-ray spondylography. The crucial role of ultrasound in the survey given to such patients evaluating the size of the dural sac on the bias level as spinal stenosis with spondylolisthesis is a serious complication that makes the clinical picture and requires in some cases surgical correction. Carrying out the functional load improves the visualization of the spinal canal and allows obtaining more accurate information on the shape and size of the hernias, especially located at the upper and lower edges of the disc.

### *Ultrasound from the posterior access*

The study from the posterior access is carried out in the longitudinal (sagittal) and transverse (axial) sections in the patient's position lying on the stomach or sitting. Studies from the rear access are performed by convective and linear sensors in the frequency mode 3.5–7.5 MHz.

In the longitudinal section, the best way to identify the level of the spine is to use a linear sensor with a working aperture of 4–5 cm. The sensor is located above the spinous process of any thoracic vertebra (approximately at the Th9-Th11 level) and slowly moves downward. When moving from the 12th thoracic vertebra to the 1st lumbar on the monitor screen, the relatively short spinal process of the thoracic vertebra is replaced by a longer process of the lumbar spine. Behind the spinous processes, acoustic shadows are visualized, between which a vertebral canal is visible (Fig. 24).

On axial ultrasound tomograms, a spinous process, a vertebral canal, a posterior contour of the intervertebral disc, and a channel to the left or right of the center of the spinal nerves, articular and transverse processes (Fig. 25) are visualized from top to bottom.

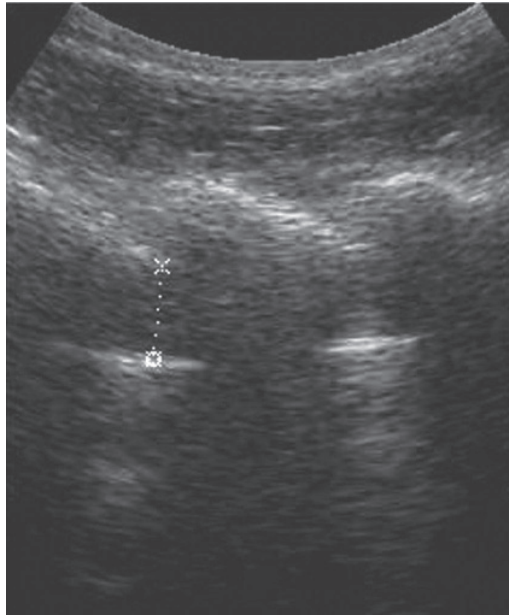


**Fig. 24.** Posterior access, longitudinal section. Visualization of the spinal canal

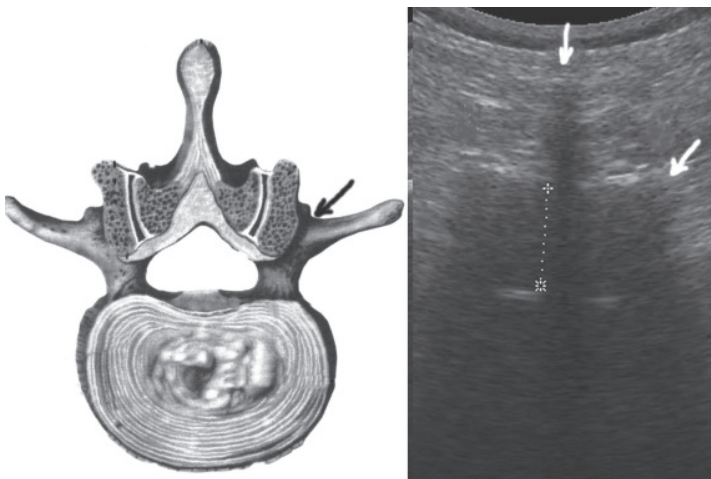


**Fig. 25.** Posterior access. Anatomical and ultrasonic transverse section through the interstitial space. The central arrow shows a spinous process, lateral – transverse process. Determination of the anteroposterior size of the spinal canal

One of the main advantages of the study from the rear access is the visualization of the intervertebral foramen – what can not be done from the front access. The sensor installed in the sagittal plane moves consecutively to the right and to the left. In this case, depending on its inclination in the horizontal plane, it is possible to visualize both the transverse and articular process. The intermediate position between them allows for better visualization of the intervertebral foramen. Holes are found between bone and soft tissue structures in the form of hypoechoic spaces between the two (top and bottom) hyperechoic lines that make up their borders from the side of the disc and the arch. The anteroposterior opening size is determined, which is normal with obligatory symmetry usually 1–2 mm wider than the corresponding lateral canal in the forward scan, since the scanning plane in this case is not perpendicular to its anterior and posterior borders. Access makes it possible to diagnose narrowing of the orifices, which can be caused by posterolateral and foraminal hernias of discs, and osteophytes of the anterior surfaces of articular processes in spondyloarthrosis.

Intermediate between the sagittal and frontal sections, the position with an easy displacement of the sensor up and down allows you to examine the arcuate joint. In doing so, one can examine part of the joint surface, which is normally even and slightly curved. Hyaline cartilage has a reduced echogenicity and a thickness of about 2 mm. Behind the hyaline cartilage, the subchondral bone plate is defined as a thin hyperechoic curved line.

Ultrasound tomography in the axial plane can be performed above the posterior surface of the sacrum, over its arches, where the continuity of the spinous process becomes the sacrum of the sacrum, this also helps to obtain information about the anomalies of the posterior sacral vertebrae.

Evaluation of the epidural venous plexus significantly increases the information content of the study, it requires devices with an energy Doppler regime and high sensitivity to the detection of low-velocity currents (velocities in the range 2.0–5.0 mm / s are estimated). Epidural veins are visualized in the axial plane of the spinal canal in the form of single low intensity color echoes located throughout the contour of the epidural space (Fig. 26). The most stable echoes from the main venous trunks are determined along the anterior contour of the dural sac and in the lateral sections of its posterior contour. Visualizations occasionally have radicular veins placed along the roots in the lateral canals (Fig. 27, 28).

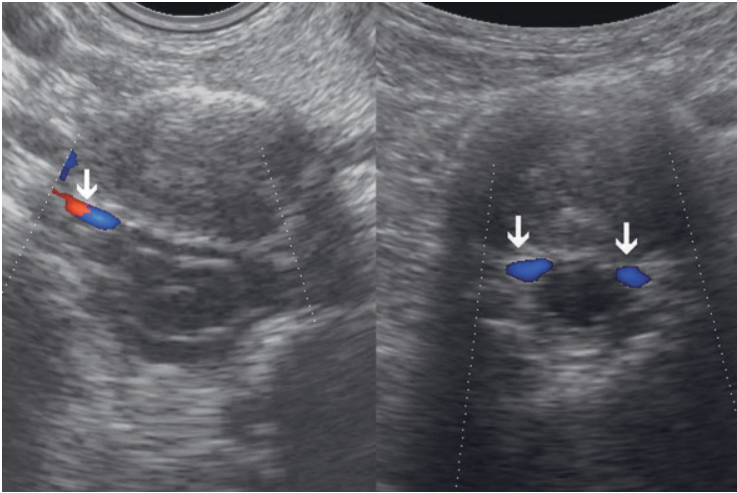


**Fig. 26.** Registration of blood flow from the epidural veins (arrows)

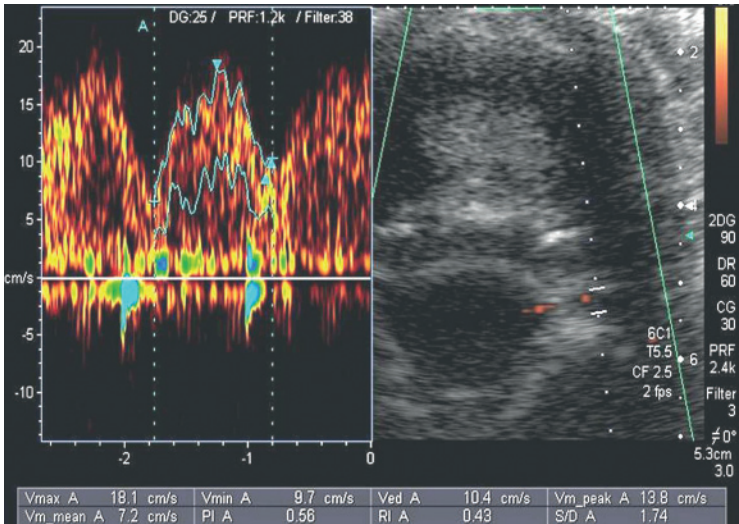


**Fig. 27.** Registration of blood flow from the left radicular vein at the level L3–L4 in triplex mode

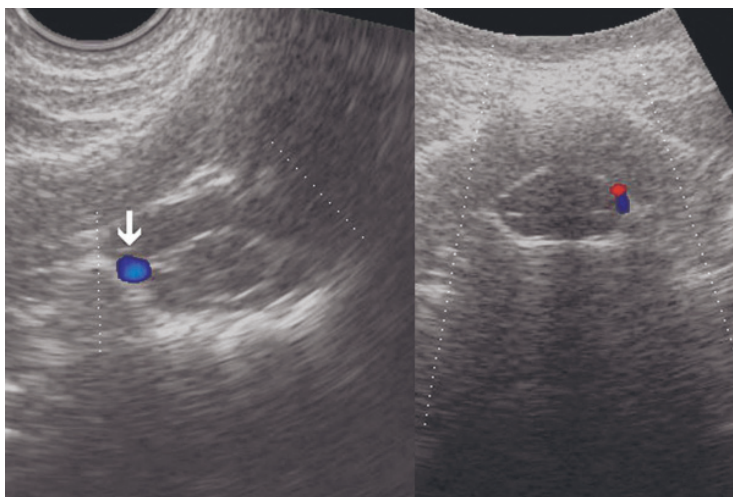


**Fig. 28.** Registration of blood flow from the root veins at the level C1–C2 from rear access in triplex mode

## **Chapter 2**

# **Ultrasonography in the diagnosis of causes of vertebral pain**

The topical diagnosis and determination of the mechanism of pain of vertebrogenic origin remain the actual problems of medicine. This is due to the difficulty in differential diagnosis, the high incidence of occurrence, the severity of clinical manifestations of the spinal column pathology and their consequences, and the anatomical features of the structure of the vertebrae. From the clinical point of view, the solution to the problem of vertebrogenic pain involves a number of aspects: the definition of the source of pain, the establishment of its mechanisms and paths for its elimination.

Most elements of the human vertebral column contain nerve endings, the irritation of which can be a source of pain. Free nerve endings that perform the function of pain receptors are found in capsules of the apophysic (facet) joints, posterior longitudinal, yellow, interosseous bundles, solid cerebellum, epidural fatty tissue, periodontal vertebrae, arteriolar and vein walls, paravertebral muscle vessels, outer third of the fibrous ring of intervertebral disc. Any of the listed above structures may be involved in the pathological process.

Among the causes of vertebrogenic pains, degenerative-dystrophic changes in the vertebral motor segment are significant. They also lead to the development of protrusion and hernia of the intervertebral disc, stenosis of the vertebral canal, instability of the vertebral motor segment, spondylolisthesis. The intensity and localization of the pain depend on the mechanism of irritation (irrigation) of the sinuvertebral nerve receptors in the zone of the changed intervertebral disc. In one and the same patient with chronic changes in the vertebral motor segment, the immediate cause of pain may be different in each particular case. With the advent and further development of MRI and ultrasound, the ability to evaluate soft tissue structures, in particular, the vertebral motor segment, was expanded. It is known that degenerative changes in the intervertebral disc are observed more often than the damage to the vertebral bodies. Ultrasonography allows to evaluate the condition of all elements of the vertebral motor segment.

There are several mechanisms of occurrence of irritative syndrome:

1) mechanically compressive, when the protrusion and hernia of the disk or the crack directly affect the nerve root; 2) mechanically-disfacial, when irritation of the neural endings occurs when the fixation of the structures of the vertebral motor segment or displacements of the vertebrae is weakened; 3) dyschemical, when irritation of afferent endings is caused by a violation of microcirculation in the tissues adjacent to the affected disk; 4) aseptic-inflammatory, when the irritation of the nerve fibers is due to inflammatory changes (epiduritis) in the structures of the vertebral motor segment.

Comparison of clinical symptoms and ultrasonography results in patients with vertebrogenic pain made it possible to detect a certain correlation between them. For example, among people with cervical gland, frequent ultrasound findings are a moderate heterogeneity of the pulp nucleus, an increase in its echogenicity, especially at the boundary of the fibrous ring, the compression and fracture of the latter. In patients with spondylogenic radiculosis, a disc hernia with the development of deformation and stenosis of the central vertebral column, as well as the root canals at the level of the affected intervertebral disc is often detected.

Long-term traumatising of the fibers of the fibrous ring at a levels of excessive physical load leads to its breakage and promotes the output of the pathological process beyond the disc.

With the involvement of surrounding structures, which causes the most pronounced clinical symptoms. The break can occur at any point Circles of the disk, however, the weakest parts of the fibrous ring are the posterior, where there are feeding vessels between the fibers in the process of intrauterine development.

There are several variants of the shape and direction of the rupture of the fibrous ring – from the simple radial to the complex course between the fibers, which sometimes flows into the vertebral canal almost at the edge of the disc, in this connection, the hernia of the disk may have an atypical arrangement. One of the mobile fragments of the pulp cornea under the action of an axial load on the spine exits through the formed hole, forming a herniated disc. Dropping a fragment in the front or side of the disk does not lead to a conflict between it and the structures that play a significant role in the development of clinical manifestations, therefore such episodes are usually asymptomatic, hernias discs with such a localization – diagnostic findings. In the posterior parts of the disc, the dropped fragment usually ruptures a thin leaf of the posterior longitudinal ligament, without effort, into the epidural fiber, located adjacent to the veins of the epidural plexus, the solid cerebellum

and the roots of the spinal cord. Such breaks always combine with neurological symptoms of varying degrees of severity (Fig. 1–14).

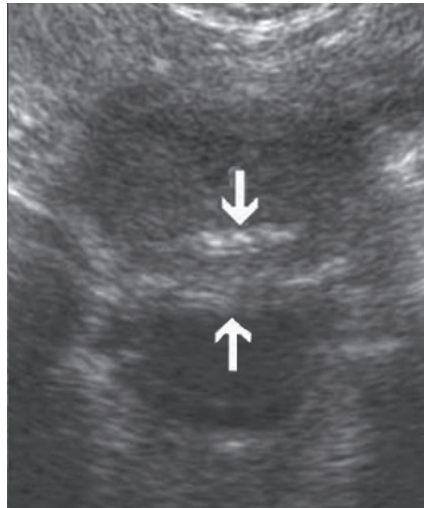


**Fig. 1.** Echogram of intervertebral C4–C5 disc in a patient with cervicogenic pain. The *upper arrow* shows the least pronounced calcification of the pulp nucleus, and the lower one – the deformation of the front dural space due to circular protrusion

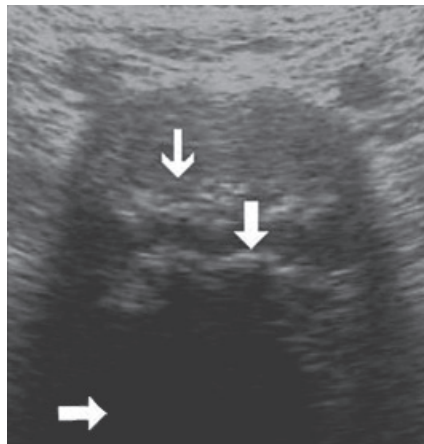


**Fig. 2.** The patient has clinical manifestations of the shoulder and upper chest radiculitis. Expressed fibrosis of the C6–C7 disc with a large calcification of the pulp nucleus and the fibrous ring (*upper arrows*) with the presence of a dorsal acoustic shadow covering the image of the vertebral canal (*lower arrow*)

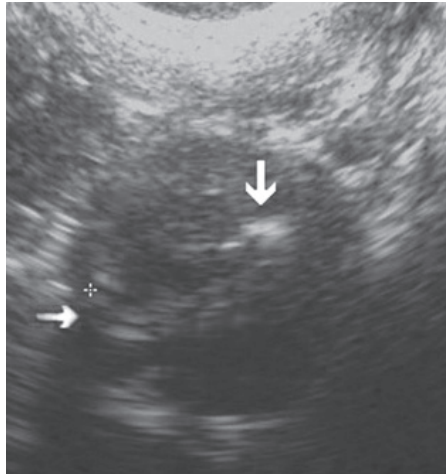


**Fig. 3.** Echogram of C2–C3 intervertebral disc in a patient with prolonged neck pain, irradiation in the right shoulder, restriction of withdrawal and reduction of strength in the arm. The upper arrow shows focal calcification of the pulp nucleus, the right – paramedian-foraminium hernia. Significant deformation of the front dural space and right root canal

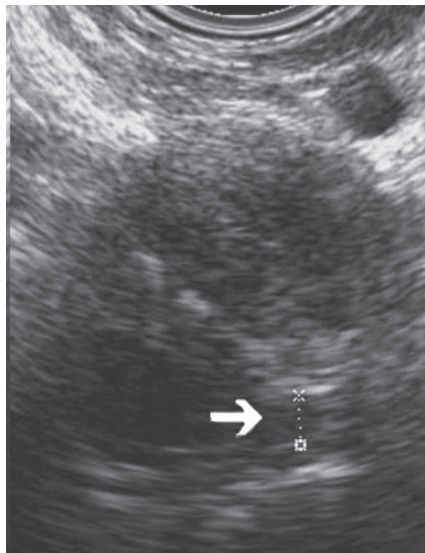


**Fig. 4.** A similar clinical picture with left-sided localization. The arrow shows a foraminal hernia with a stenosis of the root canal

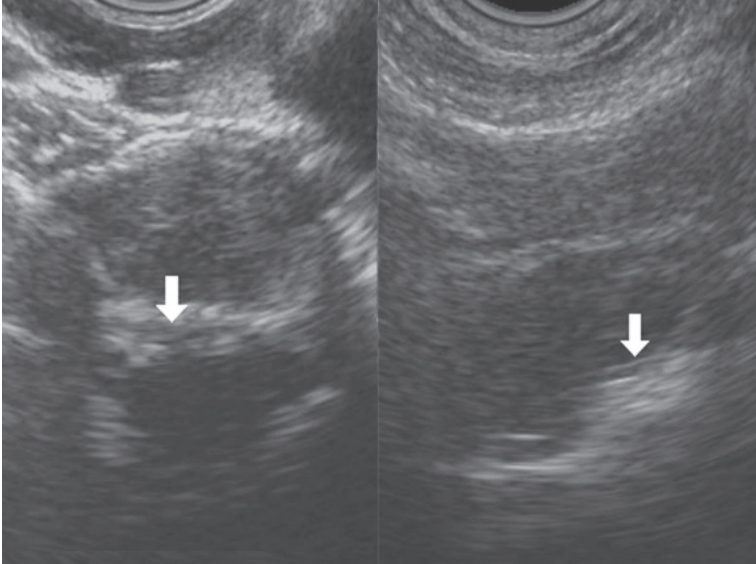


**Fig. 5.** Visualization of the median paramedial hernia of the C4–C5 intervertebral disc in a patient with a cervicogenic pain from the anterolateral (*left arrow*) and posterolateral access (*right arrow*)

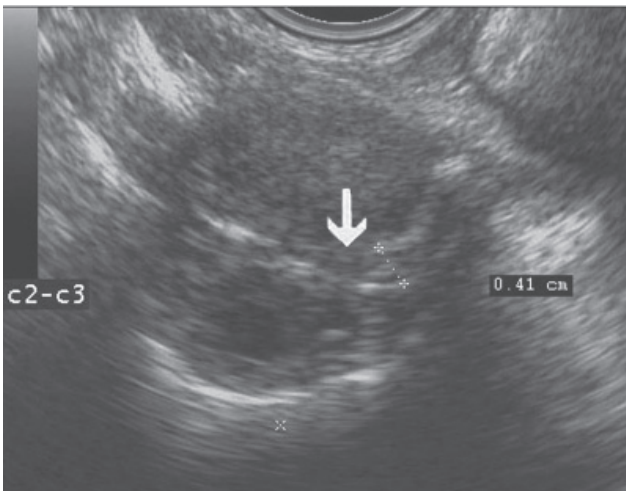


**Fig. 6.** Echogram of intervertebral C2–C3 disc in patient with cervicogenic pain. The *arrow* shows a newly emerging hernia with a rupture of the fibrous ring and a stenosis of the root canal on the left

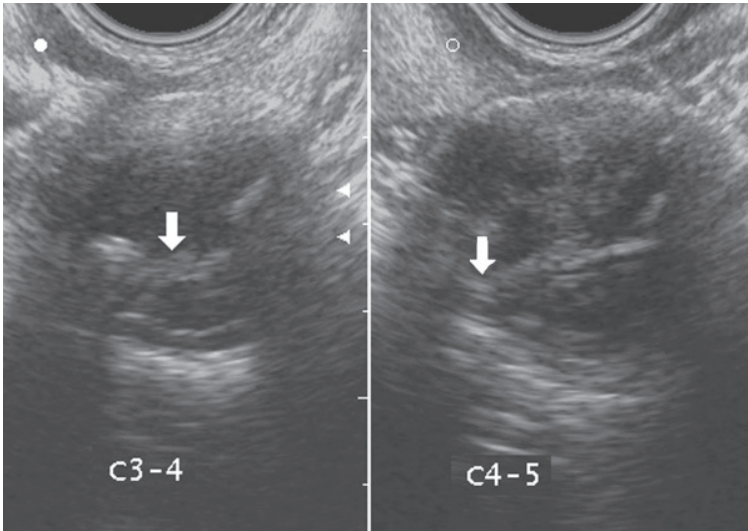


**Fig. 7.** Patient demonstrates a long-lasting pain in the collar area with spread to the right arm. Visualization of median hernia of C3–C4 intervertebral disc with spinal stenosis (*left arrow*), right paramedian hernia C4–C5 with root canal stenosis (*right arrow*)

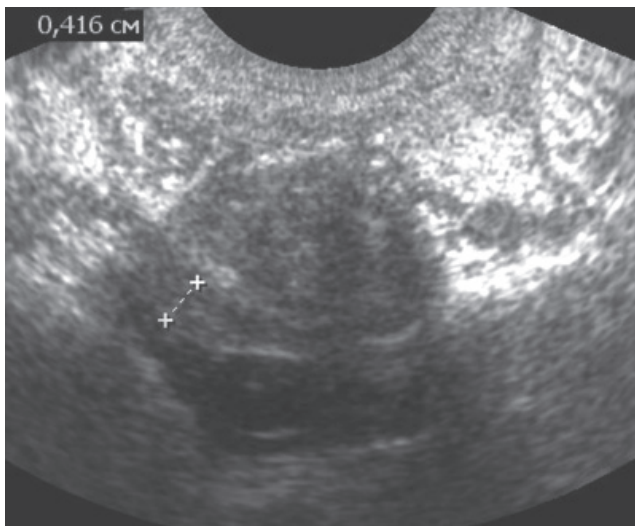


**Fig. 8.** Large right-sided paramedian-foraminal hernia with smooth contour of intervertebral disc C4–C5 with moderate stenosis of the nerve root canal

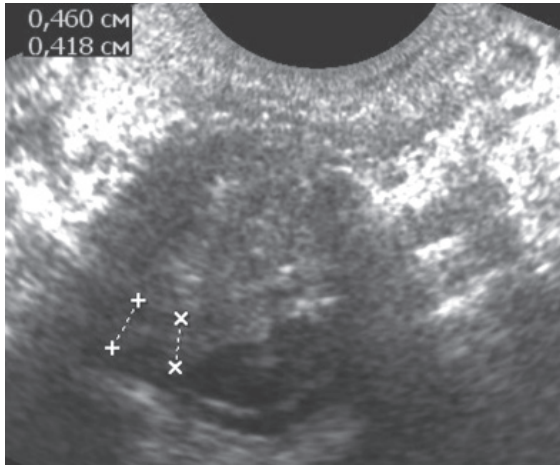


**Fig. 9.** Large right-sided, predominantly paramedial, hernia with uneven contour of intervertebral disc C5–C6 with pronounced stenosis of the root canal

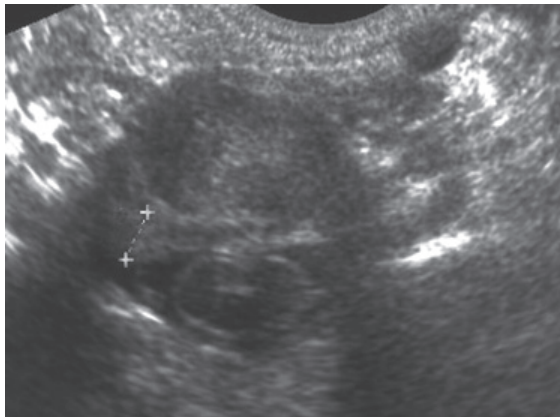


**Fig. 10.** Combination of large right-sided paramedial hernia and median prothrustia C4–C5 with pronounced stenosis of the nerve root canal and compression of the front dural space.

In the presence of a satisfactory ultrasound window, it is not difficult to detect fibrosis, hernia and disk protrusion, vertebral canal *stenosis*, *spondylosis*, *spondylolisthesis*, hypertrophy of the yellow ligament, the expansion of epidural veins, the scar and adhesion process in the epidural space, the instability of the vertebral-motor segment, the reactive epiduritis, which develop at the various stages of degenerative-dystrophic process in the vertebral-motor segment.

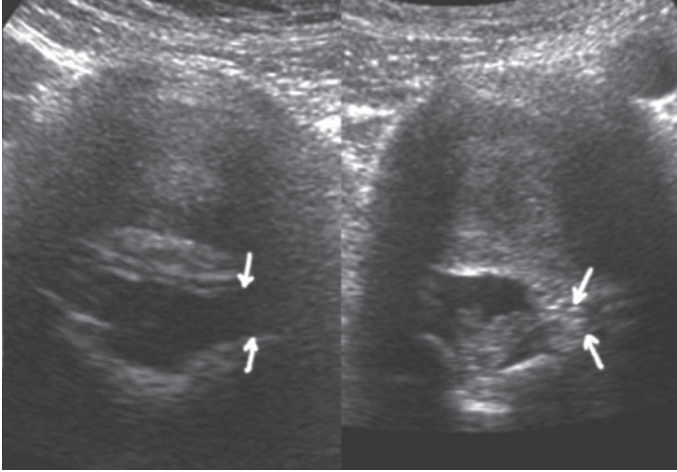


**Fig. 11.** Echogram of intervertebral disc in a patient with pain in the left upper lumbar region. At the L2–L3 level, the root canals are symmetrical (*left arrows*), at the level L1–L2, a left-side paramedial protrusion with a stenosis of the root canal (*right arrows*)

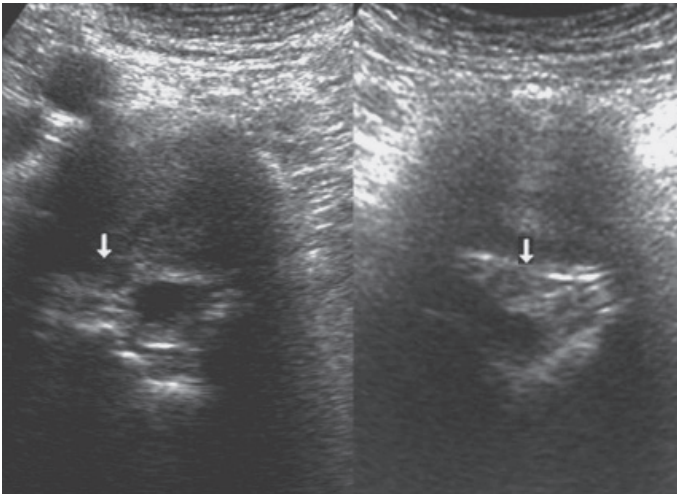


**Fig. 12.** Echograms of intervertebral discs L3–L4 and L4–L5 in a patient with lumbar pain and irradiation in the right side of the pelvis and left leg. At the L3–L4 level, a large paramedial hernia with stenosis of the root canal (*left arrow*) is determined, at the level L4–L5 – median paramedial hernia with stenosis of the central vertebral canal (*right arrow*)

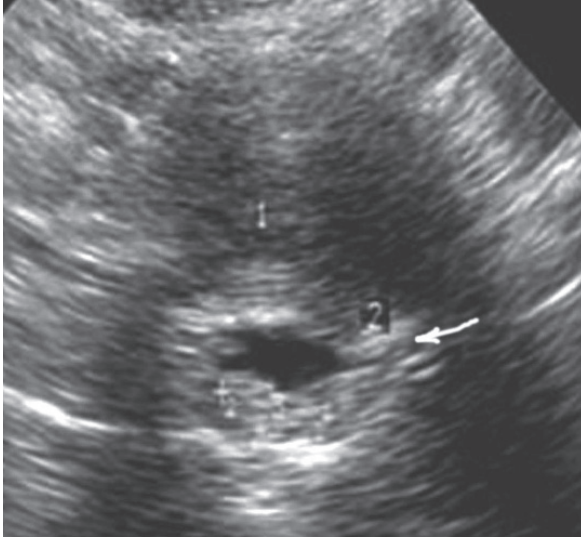


**Fig. 13.** Echogram of intervertebral disc in a patient with pain in the left upper lumbar region. At the L1–L2 level, a left-sided paramedial hernia (2) with stenosis of the root canal (*arrow*) is determined.

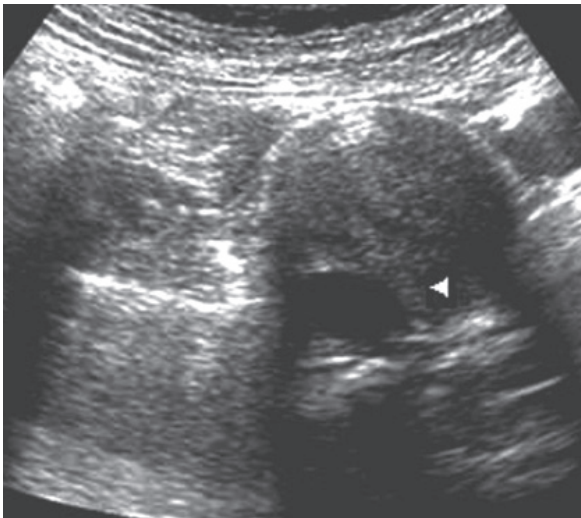


**Fig. 14.** An echogram of an intervertebral disc in a patient with pain in the lumbar region with irradiation on the back surface of the left leg. At the L4–L5 level, a large left-sided paramedial hernia (*arrow*) with stenosis of the root canal is determined.

### *Spinal canal stenosis*

Stenosis of the spinal canal is often observed in patients with a different localization of vertebrogenic pain. By the term “vertebral canal stenosis,” a clinically significant reduction in the boundaries of the vertebral canal is determined. According to the etiologic principle, the dysplastic, degenerative, post-traumatic, and, according to localization, concentric, medial, lateral, and foraminal types of stenosis are distinguished.

The most common causes of spinal stenosis are degenerative changes in the elements that make up the wall, as well as the displacement of the vertebrae. According to the anterior-posterior dimension of the cervical spine, three degrees of gravity of the stenosis can be distinguished: a) weak – 12–16 mm; B) moderate –10–12 mm; C) expressed-less than 10 mm. The division of stenosis variants into the size of the vertebral canal is relative. Clinically, stenosis of the vertebral canal can be manifested with a decrease in its anterior-lateral size or transverse area so much that compression of the spinal cord occurs or irritation of the roots of the spinal nerves.

The size and shape of the spinal canal and the channel of the cerebrospinal nerve depend on the degree of compression of the dural bag and nerve roots. Localization of hernia or protrusion determines the nature of the deformation of the vertebral and lateral channels. Median hernias and protrusions cause the maximum reduction of the anterior posterior size of the dural bag. The contraction of the latter, due to paramedial hernias and protrusions, is less pronounced than the median condition. The least vertebral canal deforms when posterolateral localization of a hernia or protrusion. At circular protrusions of disks, a simultaneous narrowing of the dural bag and lateral canals is observed, which is more often on the lumbar level. Foraminic and anterior hernias do not result in changes in the size of the dural bag and lateral root canals. Indirect signs of foraminal hernias are ruptures of fibrous rings at the level of intervertebral holes (Figs. 15–22).

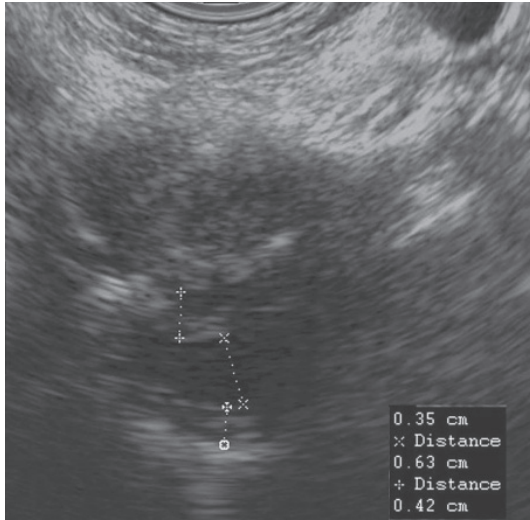


**Fig. 15.** Stenosis of the spinal canal at the level of C4–C5, due to the right paramedial hernia. Prenatal size of the vertebral canal 0.63 cm

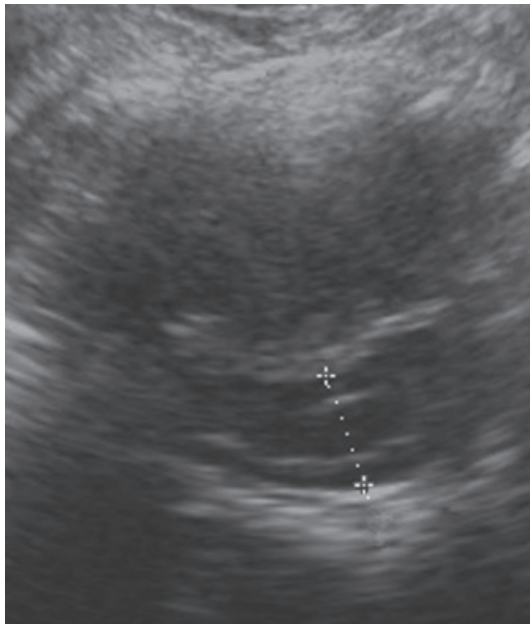


**Fig. 16.** Stenosis of the spinal canal at the level of C4–C5, due to median hernia

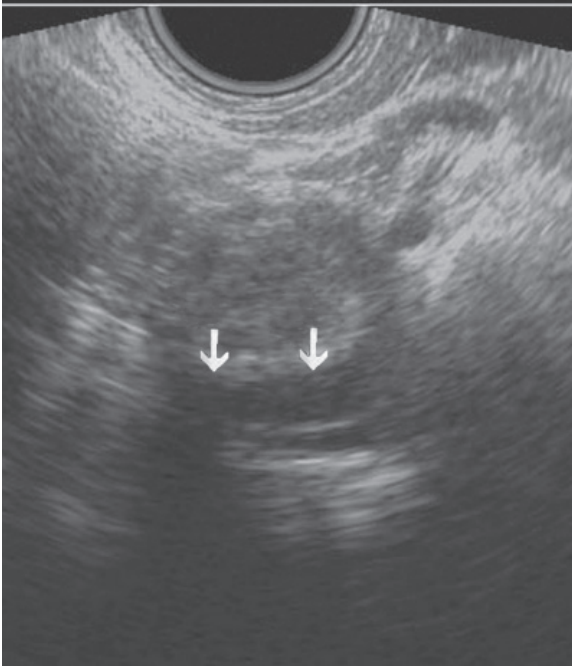


**Fig. 17.** Stenosis of the spinal canal at the level of C5–C6, due to circular hernia

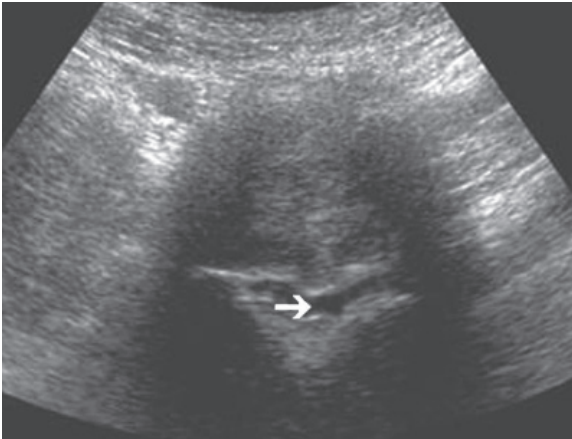


**Fig. 18.** The expressed stenosis of the vertebral canal at the level of L4–L5 is due to circular hernia

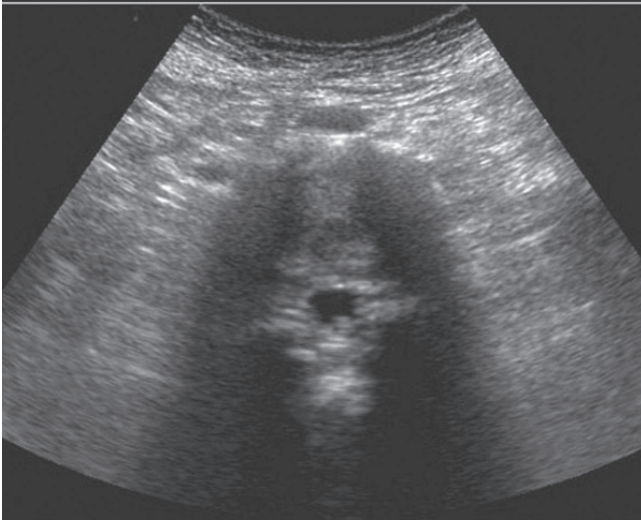


**Fig. 19.** The expressed stenosis of the vertebral canal at the level of L3–L4 is due to the right paramedian hernia, left-sided paramedian protrusion, and hypertrophy of the yellow ligament

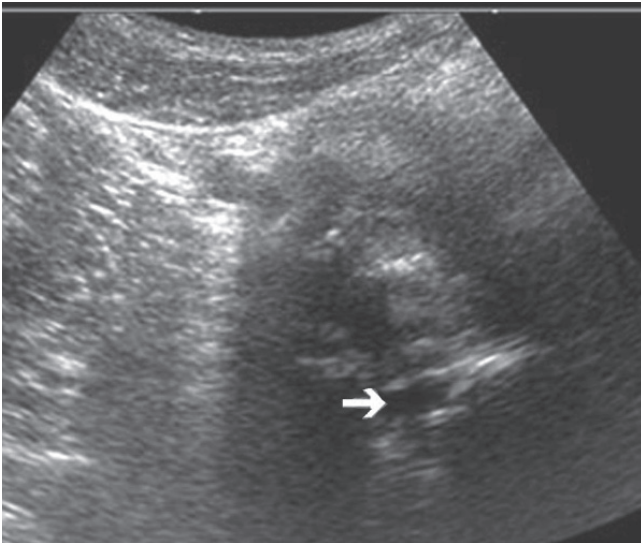


**Fig. 20.** The expressed stenosis of the central vertebral and root canal L5–S1 is due to circular hernia

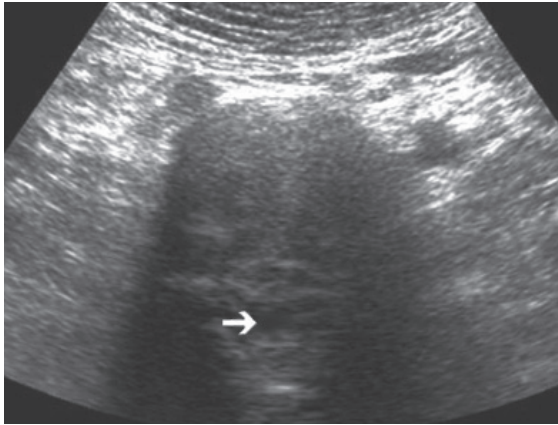


**Fig. 21.** The expressed stenosis of the vertebral canal at the level of L4–L5 is due to circular hernia and hypertrophy of the yellow ligament

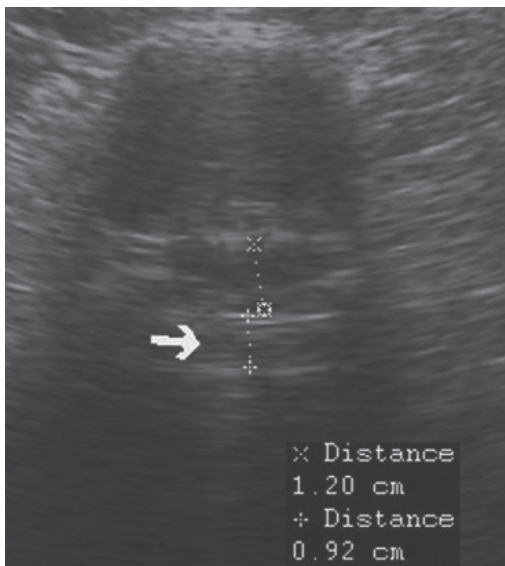


**Fig. 22.** Stenosis of the vertebral canal is due to hypertrophy of the yellow bundle (*arrow*)

The development of hernia is always accompanied by an inflammatory process in the epidural fiber – epidurite. The phenomena of this disease can develop as at the time of the formation of the rupture of the fibrous ring, as well as when the hernia disappears. They distinguish between reactive and

scar epiduritis. On the echogram, it manifests itself by the splitting of the boundary of the disk and the spinal canal with the visualization of hypo- and hyperechoic structures and displacement of the image of the front of the solid cerebellum in the direction of the vertebral canal and its contents.

The reactive epiduritis develops at a very small sized hernial “focus”. The protrusion of the posterior contour of the disc does not exceed 3 mm. In such cases, a microscopic dropout of a pulp nucleus fragment usually occurs, which does not extend beyond the posterior longitudinal ligament (some authors call these hernias an extrusion).

Stubborn epiduritis is characterized by small splitting elements that form the posterior contour of the disc, without a clear hernial “Focus”, but with a sharp increase in the echogenicity of the back contour

And epidural space. Such changes are formed with frequent exacerbation and, accordingly, conservative treatment of the inflammatory process or after surgical removal of the hernia. The presence of a hernia is usually indicated by the adjacent rupture of the fibrous ring. Signs of scar epiduritis can also be expressed in the presence of characteristic hernia disc criteria, usually in the region of its posterior contour. At the same time, they indicate a long and ineffective therapy, which did not lead to resorption of the hernia node (Fig. 23–25).

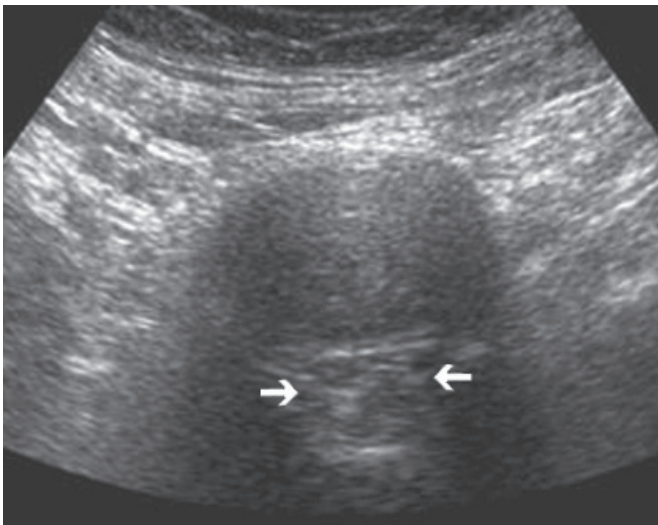


**Fig. 23.** Paramedial hernia L4–L5, epidurite (*arrows*)

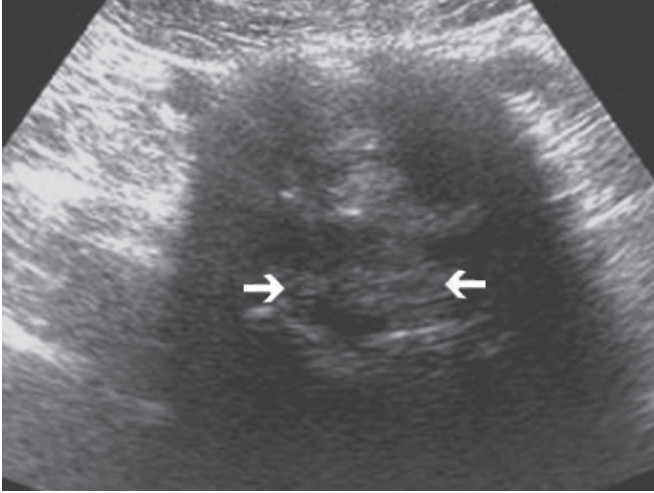


**Fig. 24.** Deformed degenerative changes in the intervertebral disc L5–S1, circular hernia, epidurite (*arrows*)

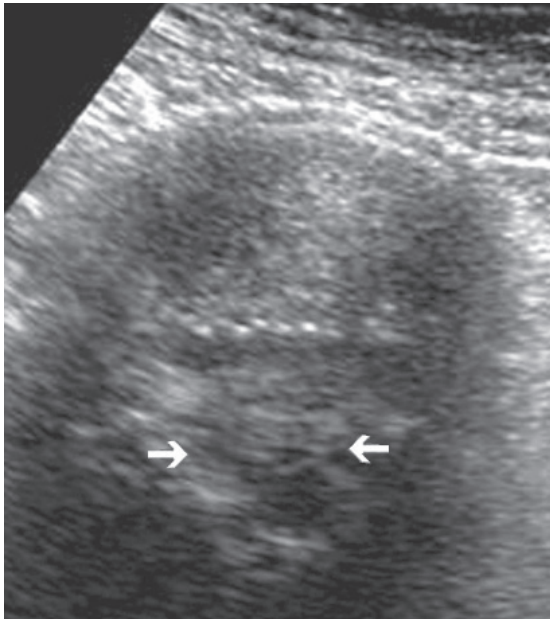


**Fig. 25.** Significant degenerative changes in the intervertebral disc L4–L5, circular hernia, epiduritis (*arrows*)

### ***Degenerative-dystrophic changes in the ligament-articular apparatus***

The fibrous degeneration of the pulp nucleus and the destruction of the fibrous ring with the formation of a hernia are accompanied by pronounced degenerative changes in the ligament apparatus, the development of deforming arthrosis of articular joint with a rude reorganization of their synovial articular surfaces. In parallel, compensatory changes occur in the bodies of the vertebrae leading to the development of *deforming spondylosis* of varying degrees of severity. Due to the formation of coarse regional osteophytes, the bone surfaces of the vertebrae and the area of their contact widen. The formation of bone joints between osteophytes facilitates stabilization of the motor segment at different levels and limitation of mobility due to fibrous changes in the disk. With ultrasound

**The study of bone changes** most often manifests itself in the form of *osteophytes* of different size and shape along the anterior contour of the vertebrae, bone create “bridges” between them.

During the ultrasound examination, it is important to determine the ratio of vertebrae. Normally, in sagittal section, the transitions of the front contour of the body of the vertebrae are smooth and interrupted

#### **Intervertebral discs.**

Degenerative-dystrophic changes in the intervertebral motor segment lead to displacement of vertebrae, which can be detected both in static examination and in the performance of functional tests. The displacement of vertebrate bodies relative to each other in the sagittal plane, detected by scanning from the front access, is called *spondylolisthesis*. Offsets of vertebral bodies forward are named as *antelesthesis*, and displacement as *retrolistesis* (Fig. 26).

Pathological changes in articular processes and articular joint are manifested by spondyloarthrosis. The main ultrasonic criteria for spondyloarthrosis are the narrowing of the articular slit of the articular joint, fragmentation of subchondral plates, thickening and perifocal edema of the capsule of the joint, and the presence of marginal osteophytes. Usually clinically significant spondyloarthrosis, capable of causing compression of the roots, is characterized by one-sided changes and significant size of osteophytes. In the cervical department, osteoarthritis arthrosis is often detected, which is detected in the anterior axial section and leads to compression of the vertebral artery on the side of the lesion. At the same time, its diameter decreases and the brightness of the color signal decreases. Spondyloarthrosis can be diagnosed both from the back and front access (Fig. 27).

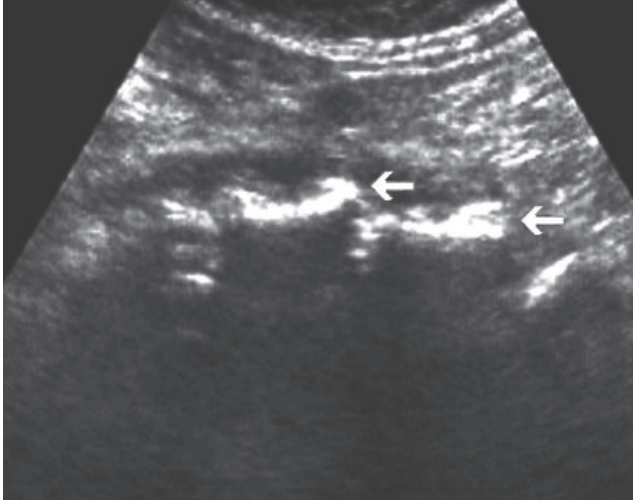


**Fig. 26.** Degeneration of intervertebral discs L3–L4 and L4–L5. Antelies – displacement of bodies of vertebrae forward (arrows)

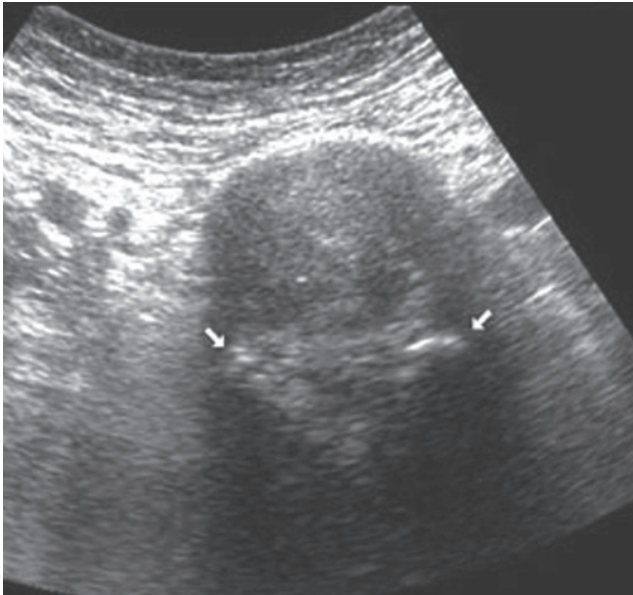


**Fig. 27.** Degeneration of the intervertebral disc L5–S1. Arthrosis of arcuate joints (arrows)

## Chapter 3

# The use of Doppler ultrasound for degenerative changes in intervertebral discs

Doppler ultrasound (Dopplerography) makes possible the study of blood flow in the vertebral artery and epidural veins, which is often violated in unco-vertebral, atlanto-occipital arthrosis, instability of the cervical vertebrae, atlanto-axial instability, and herniated intervertebral discs. Diagnosis of extravasal compression of the vertebral artery is performed in its I–III segments: 1) the first segment occupies a gap from the site of its passage from the corresponding subclavian artery to the entry into the bony canal of the vertebral artery (the blood flow is recorded at C6–C7 level); 2) the second segment is located within the bony canal of the vertebral artery (the blood flow is usually recorded at the level of C3–C4, 3) the third segment corresponds to the atlas's loop, which is located at the level of the mastoid process from the transverse process C2 to the large occipital opening (the blood flow is recorded on the ascending and descending Knees).

The recording of the Doppler spectrum of the vertebral artery is performed sequentially in all three segments on the right and left, followed by a comparison of the obtained data. The maximum peak systolic velocity in the vertebral artery is 30–50 cm/s, the index of peripheral resistance (RI) is 0.60–0.70. Asymmetry of speed indicators in the right and left vertebral arteries is allowed no more than 30 %, the gradient of the decrease in systolic velocity in segment V2 relative to segment V1 is less than 20 %. Research in the V3 segment should be carried out by functional tests (flexion, extension, head turns to the right and left), with a systolic velocity reduction of not more than 10 % acceptable for each sample.

Visualization of the vertebral artery atlant segment is an important element in the diagnosis of cerebral circulation disorders in the vertebrobasilar basin due to its great vulnerability due to frequent anomalies of the osteo-articular apparatus, arthrosis, sublaxations, and also the vessels themselves. The *atlantic* part of the vertebral artery has peculiarities of stroke in different

planes, four times it bends, which makes it impossible to remove this segment on its entire length in one plane of ultrasound scanning.

The third segment of the vertebral artery is best visualized from the rear access. During the study, the patient is in a calm state in the supine position, with support on the forehead. The sensor is placed between the posterior surface of the sternocleidomastoid muscle and the spinous processes of the first and second cervical vertebrae (C1–C2) in such a way that the scanning plane is perpendicular to the longitudinal axis of the vertebral column. The sensor is tilted so that the scanning plane passes through the atlanto-occipital junction and the lateral part of the large occipital foramen. In this position, it is better to see the distal part of the V3 segment of the vertebral artery from the transverse process C1 to the entrance to the cranial cavity, which on its way rounds the lateral mass of the 1st cervical vertebra and passes in the eponymous sulcus. This part of the vessel on the monitor looks like a horseshoe.

After obtaining the longitudinal section of the neck, the sensor is unfolded 90 degrees and parallel to the posterior edge of the sternocleidomastoid muscle immediately below the occipital bone of the skull so that the scanning plane is located parallel to the longitudinal axis of the spinal column. In this position, the proximal segment V3 of the segment of the vertebral artery is seen between the transverse processes C1–C2 of the cervical vertebrae. On the monitor screen, this section of the vessel looks like the letter 'S'. The visualization of the segments of the vertebral artery is shown in Fig. 1–15.

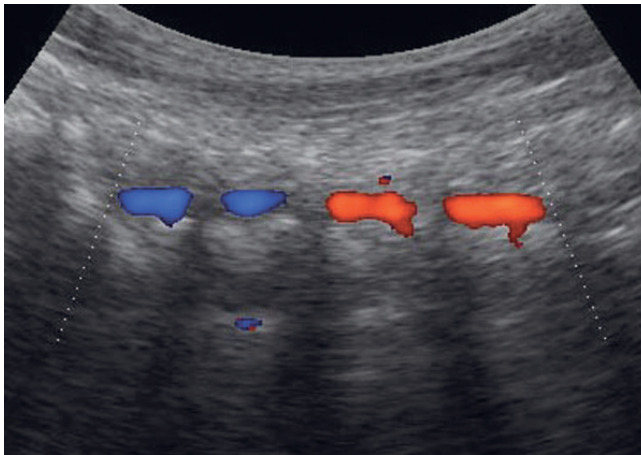


**Fig. 1.** Visualization of the second segment of the vertebral artery in color Doppler mode

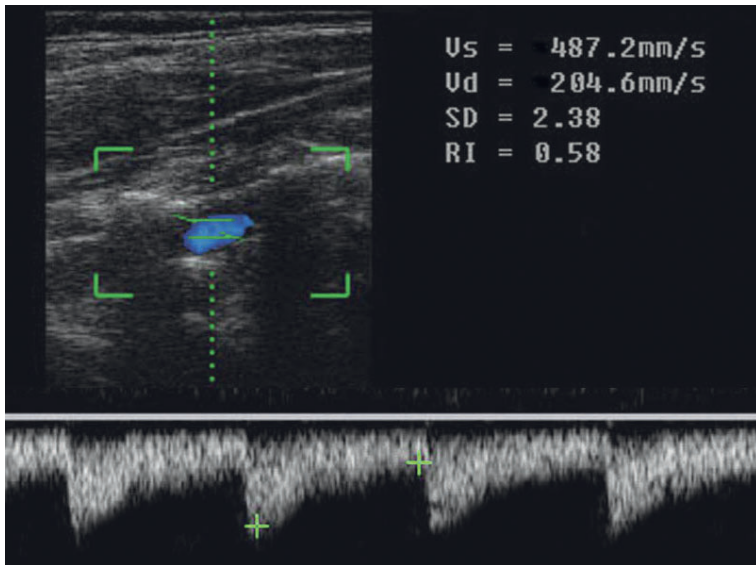


**Fig. 2.** Registration of blood flow in the 2nd segment of the vertebral artery in the color and pulsed doppler mode

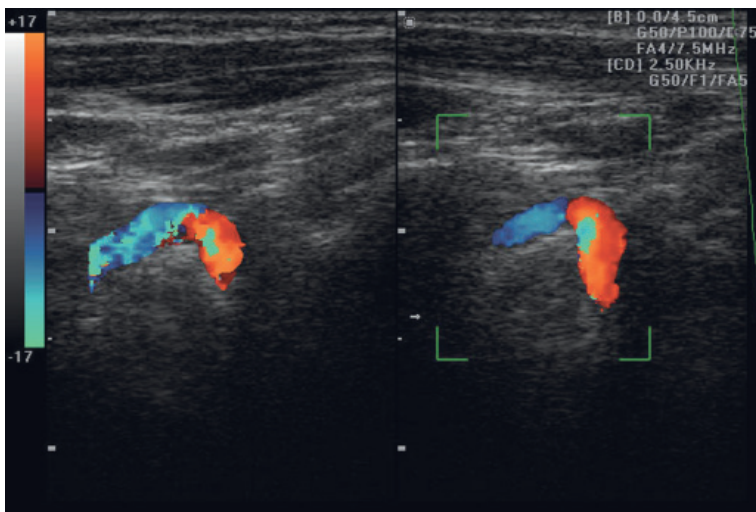


**Fig. 3.** Visualization of the third segment of the vertebral artery in the color Doppler mode

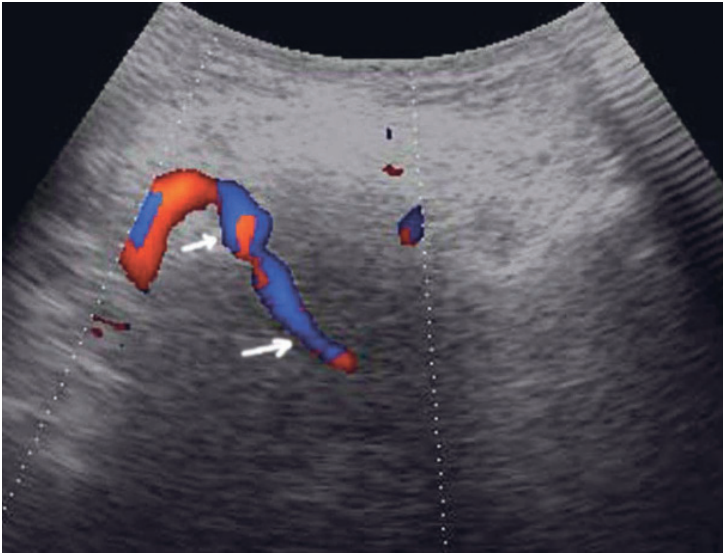


**Fig. 4.** Visualization of the third segment of the vertebral artery in the color Doppler mode (*upper and lower arrows*)

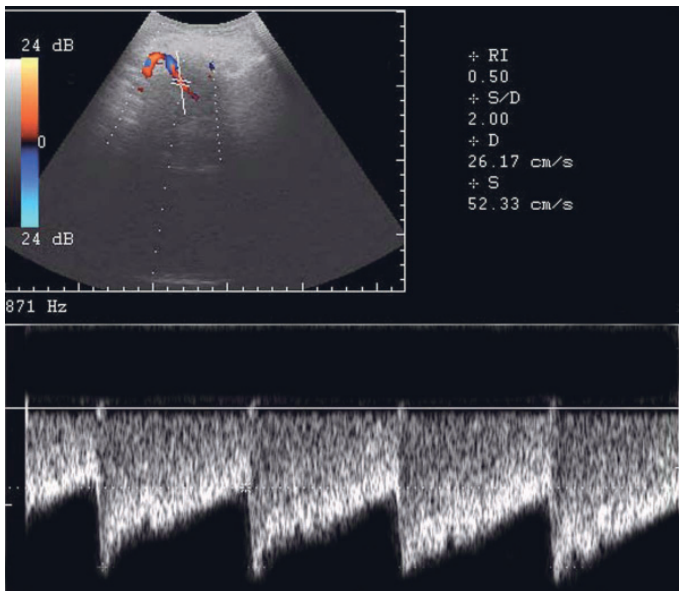


**Fig. 5.** Registration of blood flow from the IV segment of the vertebral artery

- Dopplerometric signs of abnormal blood flow in the vertebral arteries are:
- the asymmetry of the linear velocity of blood flow in the left and right vertebral arteries is more than 20 % with a difference of their diameter not more than 0.5 mm;
  - Vs less than 20 cm/s or more than 60 cm/s, RI – less than 0.50 or more than 0.65;
  - change of Vs by more than 10 cm/s (decrease or acceleration, More often the first), RI – more than 0.05 with functional tests (flexion or extension, turning the head to the right or left);
  - reduction of the diameter of the vertebral artery in segment III by more than 1.0 mm with a functional sample;
  - local tortuosity of the vertebral artery;
  - Absence of visualization of blood flow in the III segment of the vertebral artery on the side of subluxation of the atlant.

In Fig. 6–17 presents echograms for various pathologies of cervical vertebrae with pathological blood flow in the vertebral arteries.

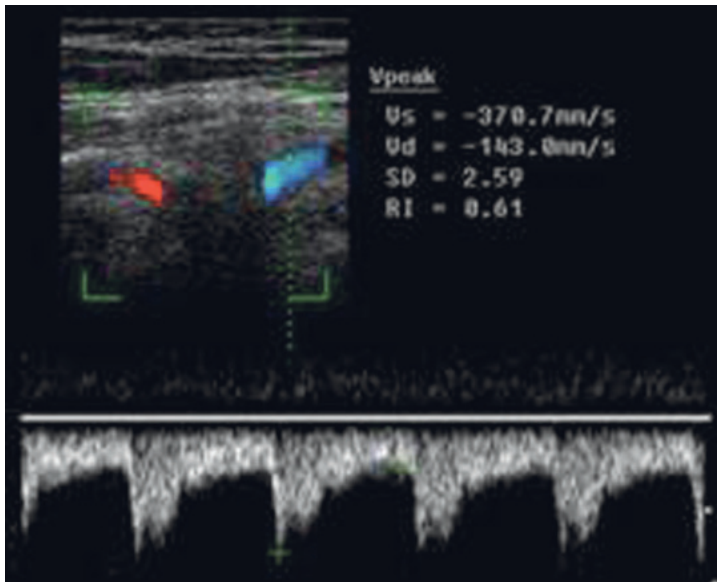


**Fig. 6.** Registration of blood flow in the vertebral artery with C3 retrolisthesis

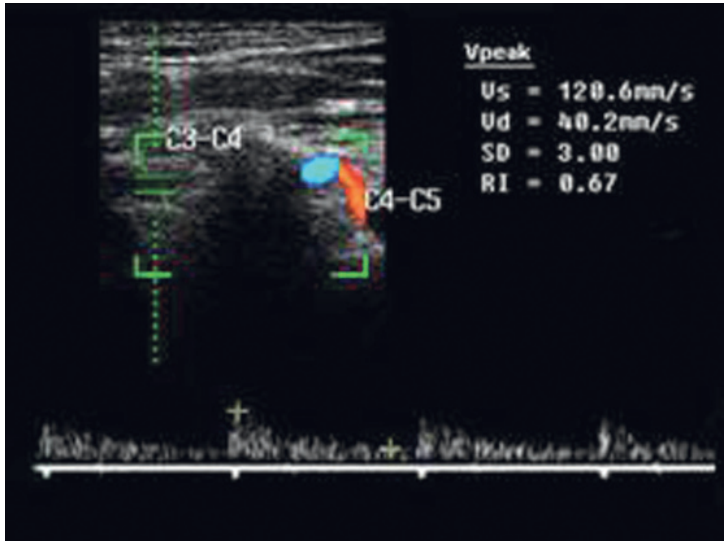


**Fig. 7.** Registration of blood flow in the vertebral artery with C4 antelsthesis. There is a decrease in peak systolic blood flow velocity

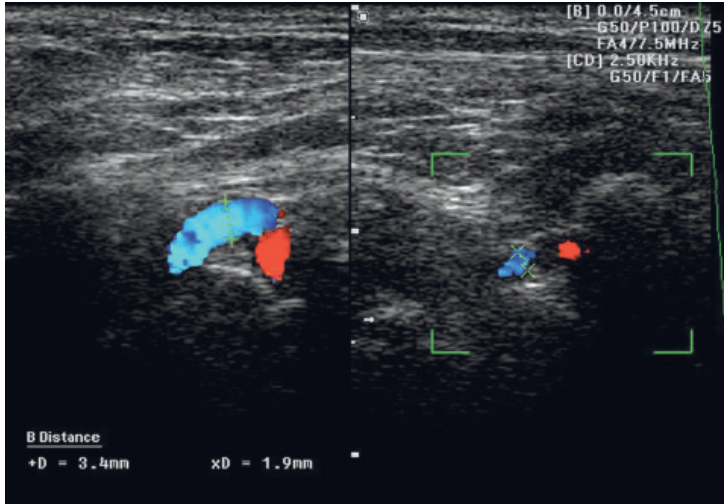


**Fig. 8.** Left-sided compression of the third segment of the vertebral artery with extravasal compression by osteophytes in arthrosis of the atlanto-occipital articulation

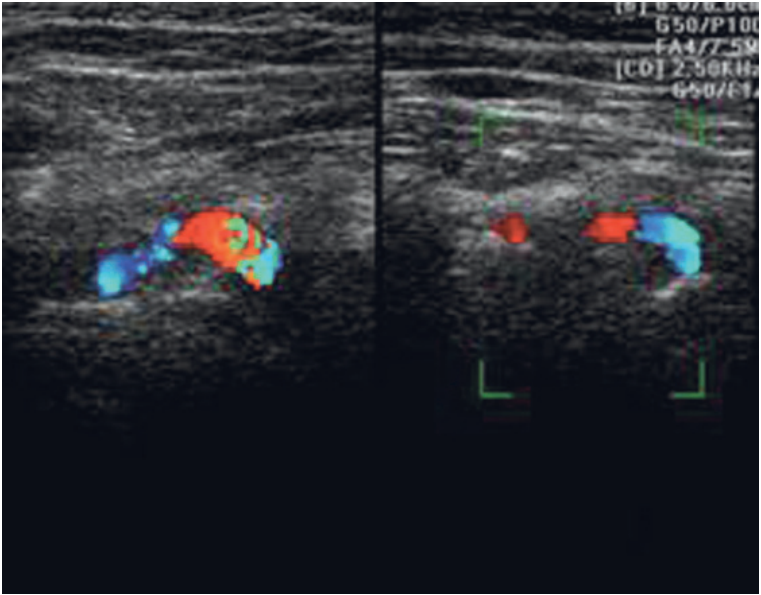


**Fig. 9.** Two-sided compression of the III segment of the vertebral artery with extravasal compression by osteophytes in arthrosis of the atlanto-occipital articulation

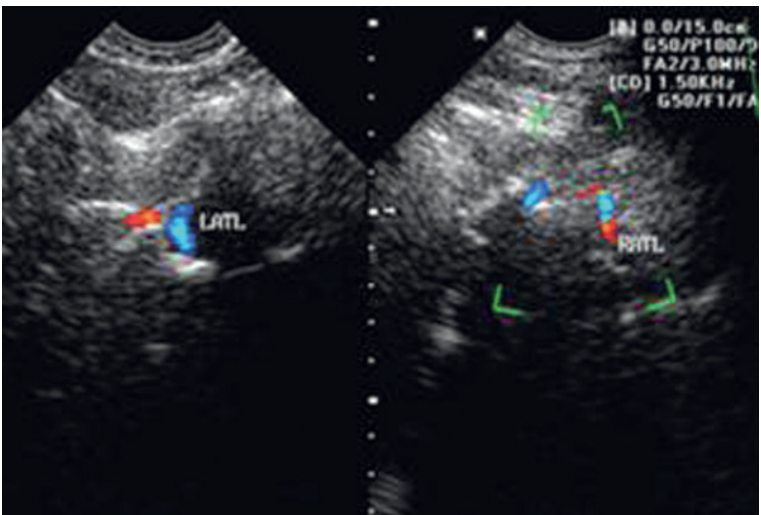


**Fig. 10.** Registration of blood flow in the III segment of the vertebral artery under atlanto-axial instability at rest (*left*) and turn of the head (*right*)

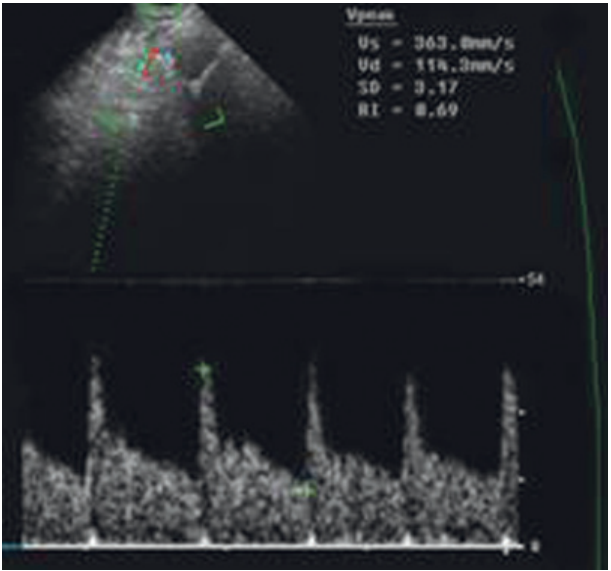


Fig. 11. Registration of blood flow in the III segment of the vertebral artery under atlanto-axial instability in the triplex mode. Reduction of the time of systolic flow with an increase in the index of peripheral resistance

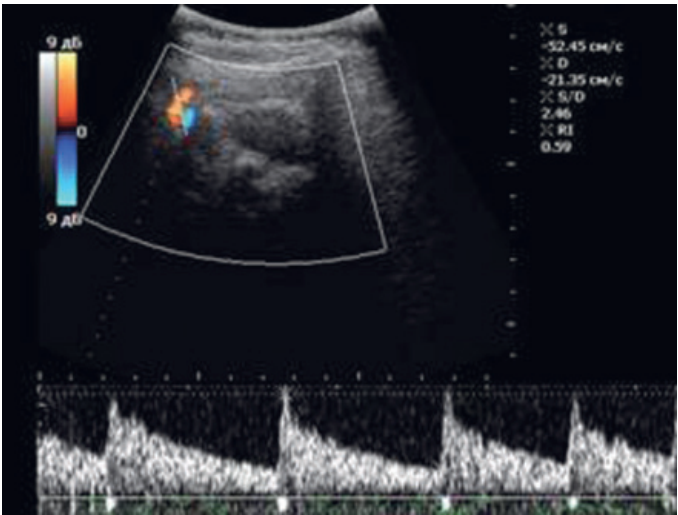
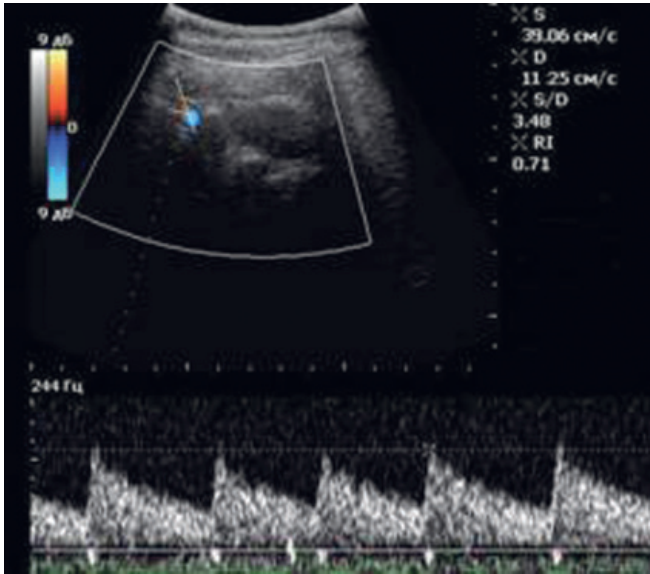
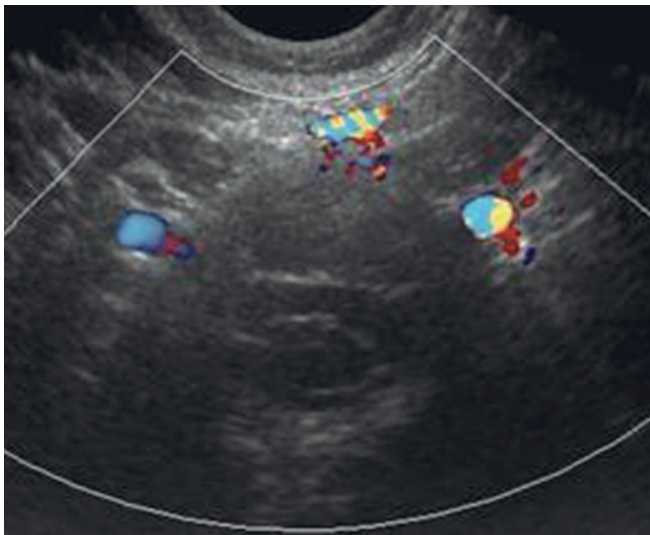


Fig. 12. Registration of blood flow in the III segment of the vertebral artery under Atlanto-axial instability at rest



**Fig. 13.** The same with ipsilateral head flexion. The peak systolic blood flow velocity and peripheral resistance



**Fig. 14.** Simultaneous recording of blood flow in both vertebral arteries at the C2–C3 level with atlanto-axial instability in the flat position of the head

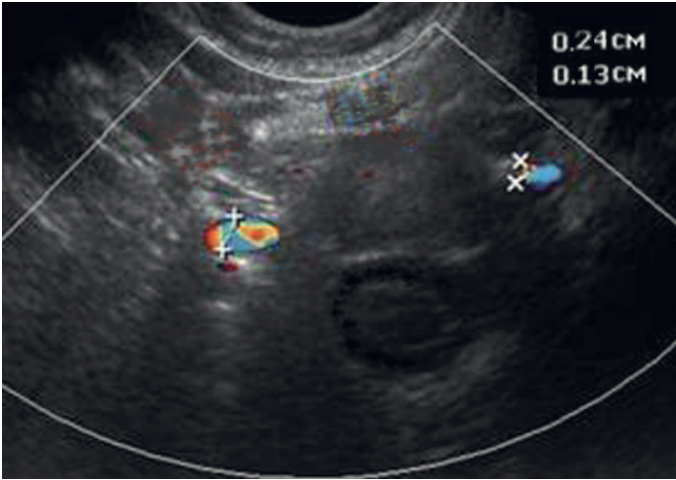


**Fig. 15.** The same when turning the head. Turbulence of blood flow appears

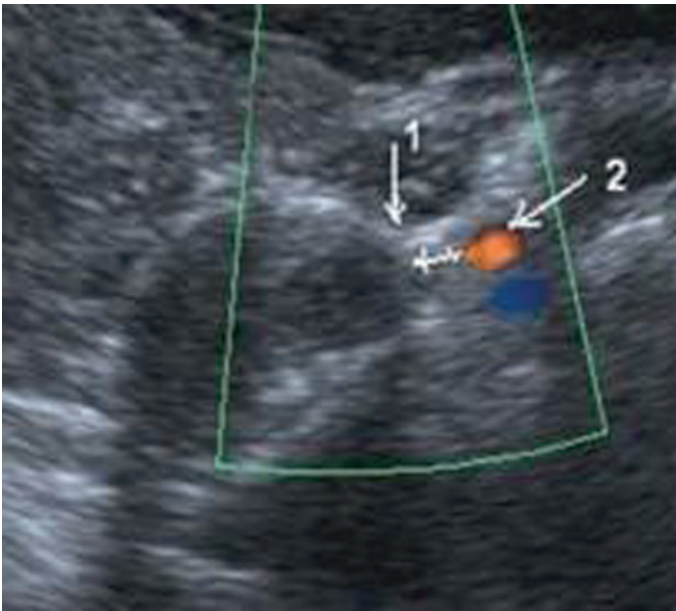


**Fig. 16.** Registration of blood flow in the vertebral artery (2). Luschka's joint is visualized, normally the distance from it to the vertebral artery is more than 2 mm



**Fig. 17.** Registration of blood flow in the vertebral artery with unco-vertebral

Arthrosis. The blood flow is turbulent, unco-vertebral arthrosis is defined, the distance from joint to vertebral artery is lesser than 2 mm

The study of the nature of the blood flow in the epidural veins can contribute to determining the cause of its change. One of the mechanisms for the development of stagnation in the epidural veins is the compression of the vascular plexuses adjacent to the posterior surface of the disc, protrusion or the fallen fragment of the pulpous nucleus. Registration of blood flow in the epidural veins allows to establish the stage of epiduritis development and evaluate the effectiveness of therapeutic measures.

With protrusion of the discs of any localization and intensity, in connection with the preservation of the integrity of the fibrous ring, the epidural blood flow at the disk level does not change (Fig. 18). With median and paramedian hernias, the blood flow at the lesion level is not usually recorded from both sides, weakened at the lower lying level, and with posterolateral hernias it is not determined on the compression side. In all cases, increased blood flow is recorded in the epidural veins and radicular vein at a level above the underlying disc on the side of the lesion. This phenomenon can be explained by the increased inflow of blood from the external venous plexus into the inner. Repeated studies after successful treatment of a herniated intervertebral disc reveal restoration of blood flow in the epidural veins.

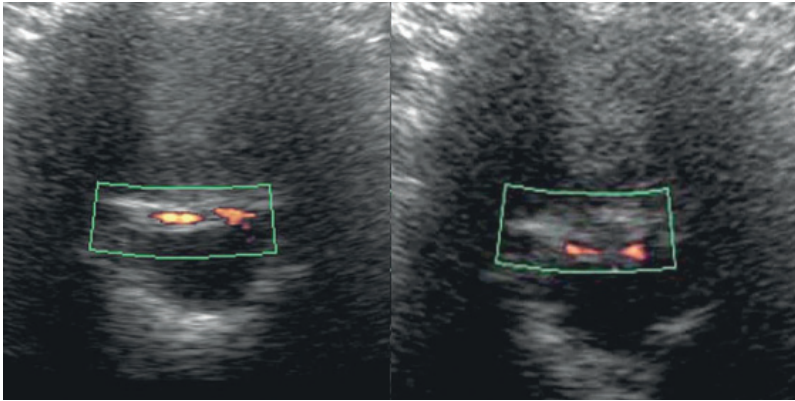


**Fig. 18.** Median protrusion of the disk L4–L5. Blood flow in the epidural veins is not changed

When examining the epidural blood flow at disc levels with the prolonged existence of hernias or their «exile», as well as in the formation of fibrous transformation of the disc during the transition of the process to the fourth period, dopplerography sometimes can reveal the vessels that proliferate into the disc through the hernial gates and microscopic ruptures of the fibrous ring located in the first Case on the border of the fibrous ring with a pulpous nucleus, in the second – along the entire perimeter of the disk. Apparently, this is a sonographic marker of the regular process of final replacement of the specific substance of the disc with fibrous tissue, proceeding both against the background of the herniation, and without it, bypassing the third period of the disease. Even more important is epidural dopplerography in detecting the stenosis of the dural sac caused by the widening of the epidural veins, as well as their involvement in the process of cava-caval flow of blood from the basin of the *inferior vena cava* to the basin of the superior vena cava.

The process of fibrous degeneration is promoted by the germination of the blood vessels into the disc (Fig. 19, 20). It begins in the early periods and occurs either through the hernial gates, or through the microcracks of the fibrous ring. The appearance of a newly formed vascular network in the disc leads to further destruction of the remains of the pulpous substance and its replacement with a connective tissue. On the one hand, these processes to some extent slow the development of hernia, on the other – lead to permanent traumatization of rootlets and the cerebral membrane directly osteophytes of vertebral bodies and arcuate joints, as well as cicatricial-adhesive changes. It should be noted

that degeneration in the discs of different segments occurs non-simultaneously and compression of the roots can be observed in several neighboring segments, on different sides and with varying degrees of severity.

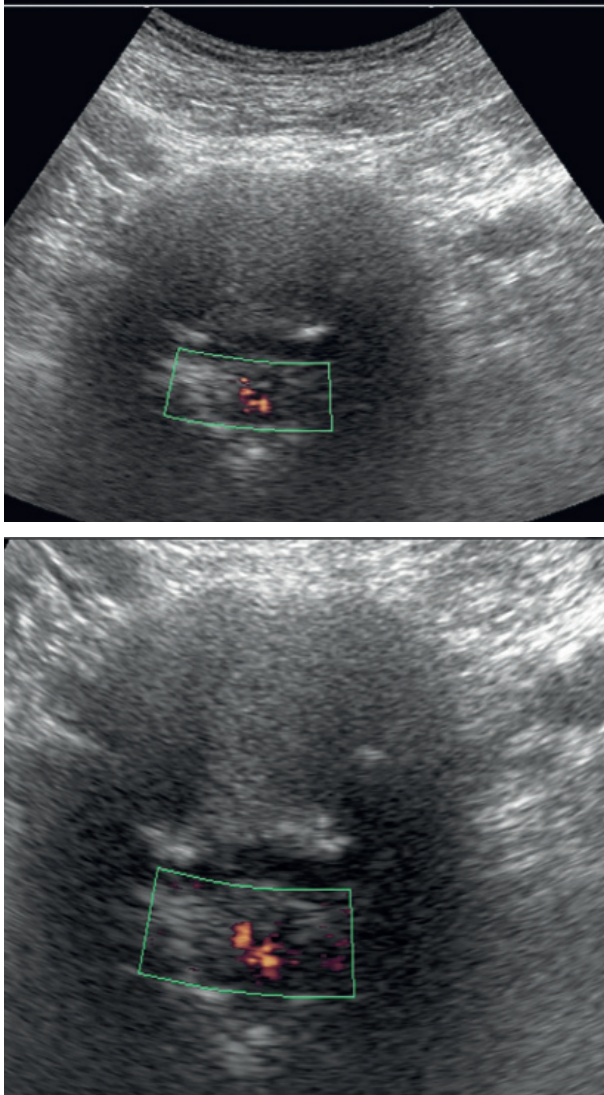


**Fig. 19, 20.** Registration of blood flow in color Doppler mode with vascular germination in the disk

# Chapter 4

## Regional anesthesia of body under US guidance. Ultrasonography for continuous paravertebral block under US guidance

**Introduction.** US-guided continuous thoracic paravertebral block for programmed anesthesia is a procedure of high complexity. Thoracic paravertebral block provides adequate pain relief for a long chest, may be the method of choice in certain groups of patients with chest pain. Ultrasound is an effective method of control of the thoracic paravertebral block in order to prolong pain and minimize the possible complications due evaluation of degenerative changes of the spine. The use of a long line probe allows clear visualization of the paravertebral space at the same time a number of segments, to conduct accurate navigation performance block prevents unnecessary maneuvering needle.

Paravertebral block was implemented U. Sellheim in 1905 as a one-sided to prevent hemodynamic side effects of spinal anesthesia, but was almost forgotten in the middle of the last century. Thoracic paravertebral block provides adequate long-term pain relief, devoid of significant hemodynamic complications, it may be suggested as a method of choice in certain groups of patients with chest pain. The block is very effective for perioperative and chronic pain, but with reduced side effects is comparable to the central nerve block. Paravertebral space puncture is performed using anatomical landmarks (intercostal access), the method of nerve stimulation and US control. There are two difficulties with the classical approach: 1) the distance from the skin to the anatomical landmarks are varied and 2) the lack of control and injection of anesthetic solution.

A number of studies show the high quality of manipulation during the needle under ultrasound guidance in the paravertebral space, with no signs of pleural puncture [4–6].

Today ultrasound monitoring is considered to be «gold standard» of local anesthesia assistance [2]. Sonographical parameters for execution pain medicine procedures under ultrasound guidance [1], visualization of paravertebral space are described in the literature [4,5].

There is convincing evidence that ultrasound navigation can improve the efficiency and safety of a single block [5]. Compared with controls, according to the anatomical landmarks method of two-dimensional US for central venous catheterization was faster and safer for children and adults (Hind et al., 2003). [4] However, the data concerning the paravertebral catheterization under ultrasound guidance is largely contradictory, because further studies are needed to improve the quality programmable paravertebral regional anesthesia.

Knowledge of anatomy is a prerequisite for the use of ultrasound. Paravertebral space is a narrow wedge-shaped gap (5 mm), a limited front parietal pleura, the back-medial-lateral surface of the vertebrae, intervertebral foramen and intervertebral discs, rear lig. costotransversalis. Adequate previous experience in a single paravertebral block on how non-visual control, proficiency ultrasound paravertebral structures are prerequisites for manipulation conduction.

**Methodics of block.** The patient in the sitting position with the neck bent so that his chin touched his chest, palpate the spinous processes indicated by a bullet on the skin, in some cases, in a prone position or on the healthy side.

Infiltration the subcutaneous tissue and muscle paravertebral local anesthetic reduce discomfort to the introduction of the needle. Under US-control with the use of a long linear probe, a needle connected to a syringe with a local anesthetic, is being promoted in the sagittal and multiple cranial direction to a depth of 2–4 cm in contact with the corresponding transverse process vertebrae. In a “blind” procedure needle is in contact with the transverse process, then the direction of the needle is changed in the cranial direction on the upper surface of the bone. Under ultrasound guidance the direction of the needle may be straight on the upper surface of the transverse process. Pushing the needle 1–2 cm below the transverse process. The trajectory of the needle should be installed on avascular, according to Doppler, the site also advisable to aspirate the syringe plunger to identify potential entry needle into the vessel. [14] With the penetration of the needle through the ligament kostotransverzalnuyu a feeling of failure. After that, the needle is promoted 1–2 mm, then – bolus injection of 5 ml solution for infiltration area of spinal nerves. After that, catheter is inserted to a depth depending on the

number of dermatomes to be numb. Mainly catheter is installed to a depth of approximately 5 cm from the end of the needle. The catheter should be carefully inspected for air. For anesthesia five dermatomes need catheter to the appropriate depth and introducing about 15 ml of anesthetic. To perform a mastectomy requires complete block of the C7 level to the level of Th6. The catheter is fixed to the skin, is filled with anesthetic, created specifically for the port to fractional administration.

The indications for paravertebral block is pain management in patients with broken ribs after thoracic surgery, cholecystectomy, axillary approach, interventions on the breast, including anesthesia and immediate postoperative analgesia for mastectomy [8, 9], with herpes zoster [8] with lithotripsy [9], for pleuristhis pain [12]. Continuous thoracic paravertebral block is more appropriate for long-term programmable anesthesia than for surgical anesthesia.

The use of paravertebral block has no negative effects on the fetus and newborn, and in case of any complications of pregnancy and delivery can improve the outcome for the mother and the fetus [3]. Thus, with paravertebral block compared with epidural anesthesia is more rapid expansion of the uterine mouth, and there is no impact on the duration of the second stage of labor.

However, complications due to violation and manipulation techniques because of degenerative diseases of the spine can be substantial. Paravertebral space study using ultrasound to manipulation can detect degenerative changes of the spine. [2] Thus, according to data from the studies [16], it was proposed to improve the diagnosis of degenerative changes of the spine through the development and implementation of integrated ultrasound criteria to increase the efficiency of paravertebral block and optimization of its methods.

**Regional anesthesia anatomy.** Thoracic paravertebral space I sa tapered portion, located on both sides of the spine. Its walls are: the anterolateral – parietal pleura, the vertebral body; medial – intervertebral disk and intervertebral foramen; the top – costo-transversal process and posterior – costo-transversal ligament (Fig. 1). Thoracic paravertebral space is continuous in the ipsilateral side and limited by prevertebral fascia. Therefore, the introduction of anesthetic leads to common anesthesia includes several dermatomes. Anatomical landmarks for paravertebral block [7, 13]:

- spinous process of thoracic vertebrae at concerned dermatome;
- insert the needle at 2.5 cm lateral to the midline;
- the depth of the introduction – at 1 cm below the level of the transverse process;
- for continuous postoperative paravertebral block is advisable to install a catheter for 1–2 segmental levels below the thoracotomy.

**The procedure applies to manipulation of high level accuracy and complexity.**

The mechanism of action involves paravertebral block by direct local anesthetic infiltration in the paravertebral space around spinal nerve, the distribution around intercostal nerve and median spread through the intervertebral foramen. Spinal nerves in the paravertebral space are not surrounded by a dense fascial cover, covered with relatively thin shells that lie directly in the tissue. Therefore, they are relatively easily achieved the anesthetic influence.

*Distribution* of paravertebral block leads to dermatome anesthesia on one side of the body. Prevalence of anesthesia depends on the location of the catheter and the amount of the drug.

**Possible complications.** In violation of manipulation techniques may damage the somatic nerves, getting significant amounts of local anesthetic in the epidural space. [15] When the needle is inserted medial to the risk of epidural or spinal needle insertion with damage spinal structures. When the needle is inserted lateral to 3 cm from the midline risk of pneumothorax is high. When multilevel anesthesia several dermatomes may cause hypotension.

**The medication.** The choice of medication is determined by the sensitivity of the patient. Mainly periodic bolus of local anesthetics are applied. Increase the rate of administrations is rarely adequate. When large bolus injected through a catheter can not reduce pain at 30 min, the catheter should be removed (Fig. 2, 3).

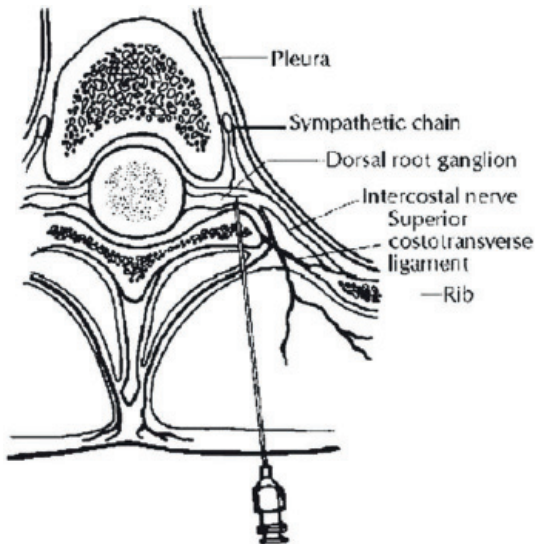


**Fig. 1.** Scheme of paravertebral space injection.



**Fig. 2.** Sonograms placed catheter (sagittal scan 2 cm to the left of the spinous processes)



**Fig. 3.** View of installed catheter. A patient with a fractured left 2–5<sup>th</sup> ribs. Pain syndrome resolved

### *References*

1. Бубнов Р. В., Абдуллаєв Р. Я. Основні сонографічні параметри проведення регіонарної анестезії нижніх кінцівок під ультразвуковим контролем / Лікарська справа. – 2010. № 7–8. – С. 97–107.
2. Абдуллаєв Р. Я., Гапченко В. В., Пономаренко С. О. Ультразвукова діагностика гриж міжхребцевих дисків шийного відділу хребта // УРЖ. – 2006. – № 14. – С. 419–422.
3. Поясничная паравертебральная блокада в обезболивании родов [Текст] / Э. Э. Антипин, Г. И. Мазуров, Д. Н. Уваров // Вестник интенсивной терапии: Научно-практический журнал. – 2008. – № 4. – С. 45–49 .

4. D. Hind, N. Calvert, R. McWilliams, A. Davidson, S. Paisley, C. Beverley et al. Ultrasonic locating devices for central venous cannulation: meta-analysis / *BMJ*, 327 (2003), p. 361.
5. Karmakar Manoj K. Ultrasound-guided thoracic paravertebral block *Techniques in Regional Anesthesia and Pain Management*, Volume 13, Issue 3, July 2009, Pages 142–149.
6. Chelly Jacques E. Paravertebral Blocks *Anesthesiology Clinics*, Volume 30, Issue 1, March 2012, Pages 75–90.
7. Grau T., Leipold R. W., Delorme S., et al. Ultrasound imaging of the thoracic epidural space. *Reg Anaesth Pain Med* 2002; 27: 200–6.
8. Gorp E. J. van, N.M. van Dijk, E. A. Bouman, E. W. Weber, C. N. Paravertebral block, an alternative to general anesthesia for breast-surgery in high-risk patients? *Regional Anesthesia and Pain Medicine* September 2004. – Vol. 29, Page 64.
9. Coveney E, Weltz CR, Greengrass R, et al. Use of paravertebral block anesthesia in the surgical management of breast cancer. *Ann Surg* 1998;227:496–501.
10. Johnson LR, Rocco AG, Ferrante FM: Continuous subpleural-paravertebral block in acute thoracic herpes zoster. *Anesth Analg* 1988; 67:1105–8.
11. Jamieson BD, Mariano ER. Thoracic and lumbar paravertebral blocks for outpatient lithotripsy. *J Clin Anesth.* 2007 Mar;19(2):149–51.
12. Pilar Paniagua, Elena Catala, Juan Manuel Villar Landeira Successful management of pleuritic pain with thoracic paravertebral block *Regional Anesthesia and Pain Medicine* November 2000. – Vol. 25, Issue 6, Pages 651–653.
13. Richardson J, Sabanathan S. Thoracic paravertebral analgesia. *Acta Anaesthesiol Scand* 1995;39:1005–1015.
14. Chul Joong Lee, Yong Chul Kim, Jae Hyuck Shin et al. Intravascular Injection in Lumbar Medial Branch Block: A Prospective Evaluation of 1433 Injections *Anesth Analg* 2008; 106:1274–1278.
15. Frohm et al. Epidural Spread After Continuous Cervical Paravertebral Block: A Case Report *Regional Anesthesia and Pain Medicine* May 2006. – Vol. 31, Issue 3, Pages 279–281.
16. Abdullaev R. Ya., Tamm T. I., Hyzhniak A. A., Golovko T. S. Ultrasonography of paravertebral space for paravertebral block conduction // *Матеріали науково-практичної конференції «Променеві методи дослідження як діагностичний та лікувальний супровід в онкології» Київ: 2012, С. 8–9.*

# Chapter 5

## Spinal dyshammia

### *5.1. Features of the blood circulation of the spinal cord*

Blood supply to the spinal cord is carried out by the 5th-18th radiculomedullar arteries originating in the arterial lines located outside the cranial and spinal cavities: the extracranial part of the vertebral artery, the other proximal branches of the subclavian arteries, the dorsal segmental branches of the aorta and the iliac arteries. Only the oral sections of the spinal cord are provided from the intracranial part of the vertebral artery. In the cervical region, like the Willis circle, a vascular circle (rhombus) of the connecting two vertebral arteries is formed on the anterior surface of the upper cervical and lower barb artery at the point of transition to the main artery and from the two spinal arteries that come down from them, connecting into one anterior spinal artery. This vascular basin, in addition to the upper cervical spine C1–C4, feeds the anterior part of the medulla oblongata, pyramids, part of the lower olive, medial longitudinal fasciculus, the nucleus of the sublingual nerve. Sometimes in the region of C1–C4 there is an additional artery going with the third or fourth spine. The vascular basin of the lower cervical region also forms a branched intraspinal network around the cervical thickening, and its nerve cells are surrounded by a three-dimensional network of capillaries, especially in the deep sections of the anterior horns (Ya. Ya. Popelyansky et al., 1973). Therefore, cervical thickenings are rarely ischemic in the occlusion of the vertebral artery. The entire arterial vascular system of the spinal cord is divided into two basins: upper and lower. The upper vascular basin, represented by the radiculomedullar branches of the subclavian, vertebral and deep cervical arteries, includes the cervicothoracic span from the C1 to the spinal cord segments. He, in his own case, is divided into two divisions: the first includes the upper four cervical segments, the second occupies the site from the C4 to the Th3 segment, they are supplied with the radiculomedullar arteries that flow from the vertebral and deep arteries of the neck.

The lower, vascular, basin, including segments Th4-Th5 and below, in a number of cases, are supplied with one radiculomedullary artery of Adamkiewicz, which penetrates into the spinal canal more often on the left with the Th11-L1 spine. Sometimes Th4-Th8 segments are supplied with the upper extra radiculomedullary artery entering the puncture channel with the Th6 spine. In 20–25 % of cases there is a complementary radiculomedullary artery of Deprozh-Gotteron (“long way” artery) entering the canal with the spine L5 or S1. In Fig. 1, 2 shows the radicular canal and spine nerve root at the cervical and lumbar levels.

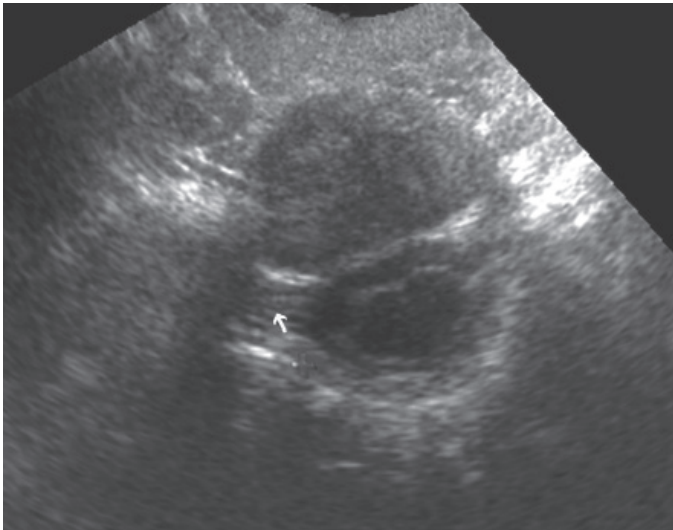


**Fig. 1.** Ultrasonic imaging of the right radicular canal and spinal nerve (*arrow*) at the level of C5–C6

*Radiculomedullary arteries*, reaching the spinal cord, are divided into ascending and descending branches, which, anastomizing with each other, form the anterior and two posterior spinal arteries. The anterior spinal artery, located in the anterior median sulcus of the spinal cord, gives a number of twigs alternately to one side of the spinal cord. The branches of the anterior spinal artery blood supply the anterior 80 % of the diameter of the spinal cord, the anterior and lateral horns, the bases of the horns, the lateral and anterior cords, the central parts of the posterior cord.

The posterior spinal arteries vascularize the apex of the hindbusts, the rear part of the side cord and the back cord, with the Gaull’s bundle having a bilateral blood supply, and Burdach’s bundle only on its side.

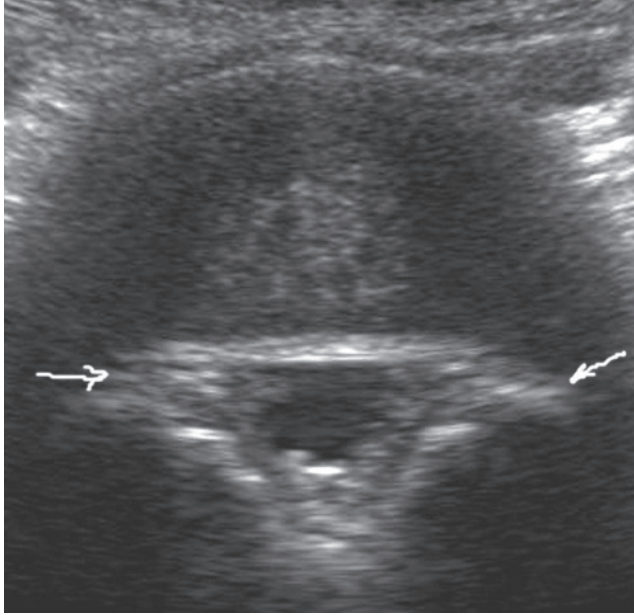


**Fig. 2.** Simultaneous ultrasound imaging of radicular canals and spinal nerves at the level of L4–L5 (*arrows*)

The anterior and posterior spinal arteries anastomose with each other through the perimedullary branches, which run horizontally along the lateral surfaces of the spinal cord and form a vascular crown. From it departs a large number of short branches, immersed in the surface layers of the white matter of the spinal cord. Thus, the diameter of the spinal cord has three zones, supplied with blood by the anterior, posterior and marginal spinal arteries, emerging from the perimedullary vascular crown.

According to the conditions of hemodynamics, in the area of the junction of various arterial basins, critical zones are formed, most vulnerable in the case of circulatory insufficiency, in particular: 1) the area of the base of the horns, Clark's pillars, the posterior adhesion and the anterior part of the side cord; 2) And lateral cord, 3) the area around the central channel.

«Critical zones» are located at the level of the segments C4 – Th4, Th9 – L1 and the cone. The main venous vessels, like the arteries, pass along the spinal cord, connecting at the top with the venous system of the skull. The veins of the spinal cord through the radicular veins are connected to the venous plexuses of the spine, and through them – to the hollow veins.

The number of anterior radicular veins varies from 6 to 40 (an average of 23). At the level of the lower half of the spinal cord, in 90 % of cases, there is a large radicular vein of Adamkiewicz, accompanying one of the roots from Th9 to L1, more often L2, from the left (NN Yakhno, DR Shtulman, 2001). If an obstacle arises in the course of this large vein (compression of the intervertebral disc of a hernia, tumor, etc.), then stagnation of venous blood in the lower half of the spinal cord occurs with a violation of its function.

The posterior radicular veins are also many – from 12 to 42. Like the anterior ones, they fall into a large venous epidural reserve – an internal vertebral plexus. From the latter, through the intervertebral veins, the blood passes into the external plexus of the spine, which connects with the system of the upper and lower hollow veins (Fig. 3–5).

It is important to note the anastomoses between the anterior spinal artery and the vein, which play a definite role in the regulation of the cerebrospinal circulation. With the defeat of the diverting venous vessels, the arterial blood supply reflexively reflexes, which leads to the formation of edema, disruption of cellular metabolism, accumulation of under-oxidized products. As a result, the spinal cord function is upset.

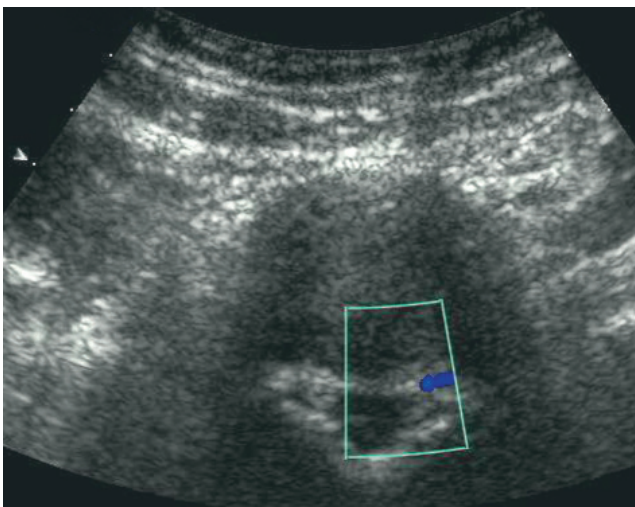


**Fig. 3.** Color Doppler mapping of blood flow in the epidural plexus at the level of L3–L4

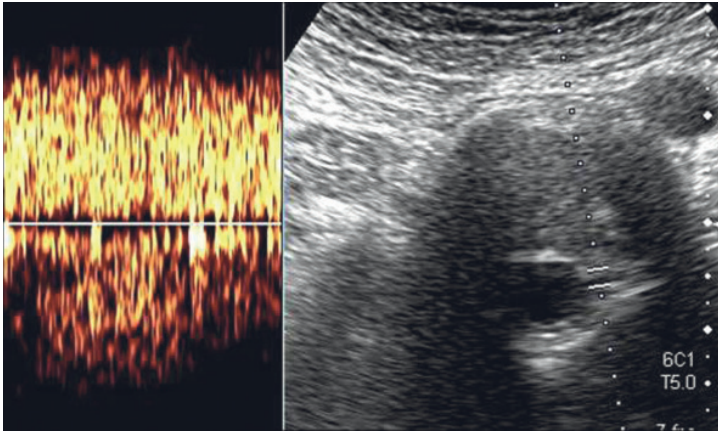


**Fig. 4.** Triplex scanning of blood flow in the left radicular vein at level L5–S1

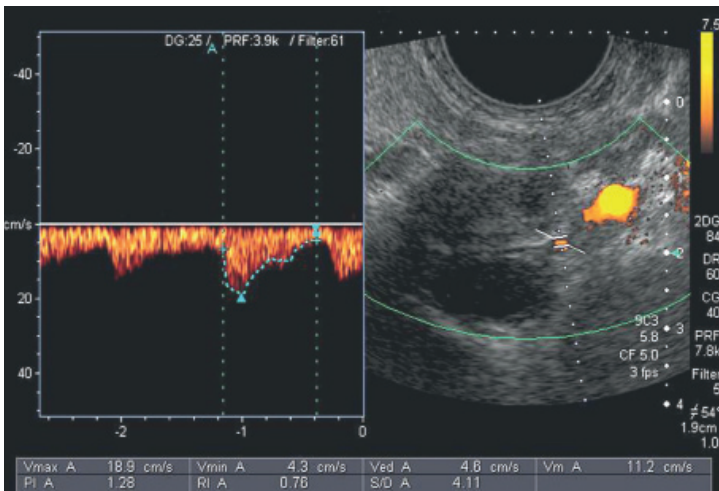


**Fig. 5.** Triplex scanning of blood flow in the left radicular artery at the level of C4–C5

## ***5.2. Anatomical and physiological prerequisites and clinic of spinal cord blood flow disorders***

Myelo-ischemia can be caused both by the inborn vascular pathology in the form of malformations, and acquired. The latter can be aggravated by atherosclerosis of the vascular wall, infectious, toxic, allergic vasculi-

tis. Compression syndromes play a significant role in the development of myelo-ischemia. The first place among them belongs to vertebral pathology, which includes osteochondrosis, spondylarthrosis, hormonal spondylopathy, congenital anomalies, traumatic fractures, spondylolisthesis, tumors. Of great importance are the extramedullary and extravertebral tumors, pregnancy, pseudotumors.

In clinical practice, there are iatrogenic myelo-ischemia due to laminectomy, thoracotomy, laparotomy, operation on the aorta, epidural blockades, lumbar puncture, rough manual therapy. A special place is occupied by congenital and acquired stenosis of the spinal canal (LA Kadyrova et al., 1993). An important role is played by violations of general and regional hemodynamics: myocardial infarction, hypertonic and hypotonic diseases, acute cardiovascular insufficiency, vegetative-vascular dystonia, blood diseases and changes in its physico-chemical properties (AA Skoromets, 1998).

Significant for the clinical analysis is the isolation of three basins of the spinal cord vascularization: the upper C1–C4, the intermediate Th4–Th8, the lower one – from Th9 downwards, including the terminal section of the spinal cord. Accordingly, K. Zulch (1954) distinguishes between “critical zones”, the defeat of which most often leads to the emergence of syndromes of spinal failure: C4, Th3–Th4, Th12–L1.

Disturbances of the spinal circulation are less common than cerebral. This is explained by the fact that the spinal cord is less sensitive to hypoxia and disorders of general hemodynamics, and also that minor spinal symptoms can be masked by a more pronounced cerebral pathology.

Disorders of cerebrospinal circulation can be divided to acute and chronic, and according to the etiopathogenetic factor: compression of the radiculomedullary arteries at the level of the intervertebral foramen or in the epidural space, etc.

### ***Transitory disorders of cerebrospinal circulation***

Transient myelo-ischemia include those in which spinal syndromes occur within 24 hours. The clinic has the following options.

***Unterharnshaidt syncopal seizures.*** FK Ford (1952) associated them with the pathological mobility of the axis and impaired blood circulation in the brainstem in patients with vertebral artery syndrome. F. Unterharnscheidt (1956) described seizures based on the results of

observation of three patients with cervical osteochondrosis, which were provoked by turning the head. Fainting follows pain in the back of the head, a sensation of heat, “bursting” and noise in the head, photopsia and dizziness. Upon coming to consciousness after a fainting (lasting 2–3 minutes), the patients experience a weakness for hours, a headache, they have an objective definition of an organic minisymptomatics. In the opinion of VB Shalkevich, LG Gitkina (1981), with these attacks, loss of tonus and consciousness, as well as emotional-mnemonic disorders are caused by ischemia of the descending reticular formation and limbic structures. Ultrasonography can visualize the atlanto-axial articulation, diagnose subluxation of the atlant, and record blood flow in the compressed vertebral artery (Fig. 6–8).

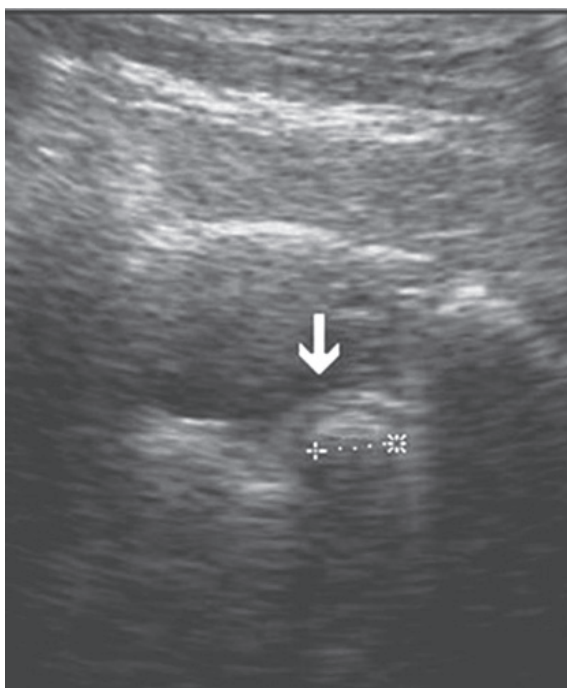


**Fig. 6.** Visualization of atlanto-axial articulation. The arrow shows the central joint (the transverse ligament and tooth C2 are clearly defined), which has the same distance from the lateral masses (hyperechoic structures on the right and left parts of the echogram)

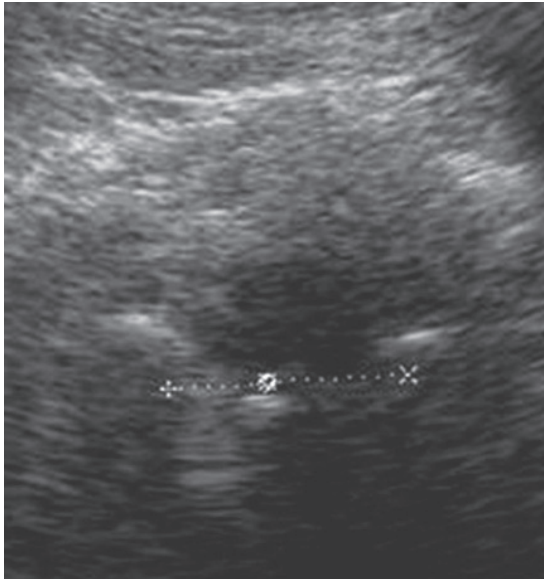


**Fig. 7.** Subluxation of the atlant. The tooth C2 is asymmetrically disposed from the lateral masses

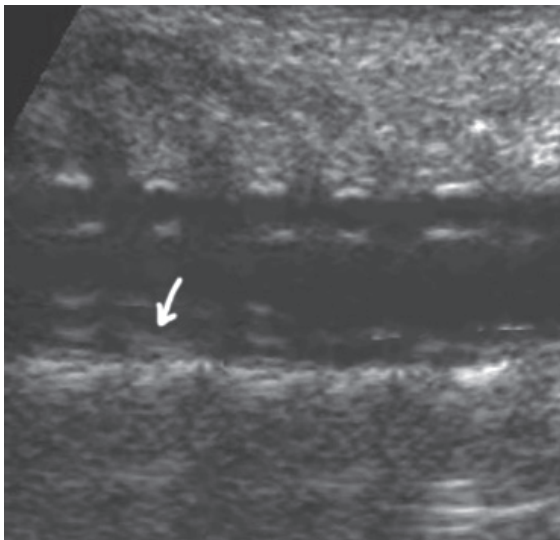


**Fig. 8.** Rotational atlant subluxation. Hemorrhage in the anterior dural space. The arrow shows the hyperechoic mass in the anterior dural space

**Drop attacks.** The patient suddenly has a sharp weakness of the hands and feet with a quick turn of the head to the sides or tipping back, and he suddenly falls. Consciousness does not change, there is pain in the neck and neck. After 2–3 minutes, the strength in the limbs is restored. Proprioceptive reflexes on hands are reduced or absent, on legs – evenly animated, can be determined from both sides by the reflex of Babinsky. After 20–30 minutes the neurological status is normalized. Paracism of tetraparesis is renewed with repeated sharp turns of the head. They arise with cervical osteochondrosis, sometimes in combination with atherosclerosis of the vertebral artery, and are associated with transient ischemia of the cervical segment.

Myogenic intermittent claudication occurs with ischemia in the lower arterial basin of the spinal cord. With prolonged walking, patients develop weakness and numbness in the legs, sometimes imperative urges to urinate and defecate. After a short rest, these phenomena pass, and the patient can continue walking until another attack of weakness and numbness in the legs. In the neurological status, in the period of weakness of the legs, a decrease in knee and achilles reflexes, hypotonia of the gastrocnemius muscles, fascicular twitching in them, sometimes Babitsky's reflex is noted. However, these neurological disorders go away quickly. The pulsation of the arteries of the lower extremities does not change. The patient is forced to stop because of the weakness of the legs, and not because of the sharp pain in them. These criteria are used for differential diagnosis with peripheral intermittent claudication – claudicatio intermitfens Sharko and atherosclerosis or endarteritis of the lower limbs. Sometimes peritoneal gait is formed in patients.

Cudogenous intermittent claudication is a manifestation of transient ischemia of the cauda equina roots, often in the conical segments of the spinal cord. When walking, paresthesia occurs in the distal parts of the legs with spreading to the perineal region, weakness in the legs, incontinence. After a short rest, these phenomena pass. During an attack of intermittent claudication, there are radicular disorders of sensitivity, torpidity of achilles reflexes, easy distal paraparesis.

Coaddogenic and myelogenous intermittent claudication are most often found with congenital or acquired stenosis of the spinal canal.

### ***Chronic failure of cerebrospinal circulation***

Initially, the disease occurs in the form of transient disorders, but subsequently there are signs of persistent, often progressive damage to various structures of the spinal cord.

Sometimes such a clinical picture occurs some time after an ischemic spinal stroke. The clinic is characterized by mixed para- or tetraparesis in conjunction with spotty hyperesthesia, a violation of the pelvic organs. Sometimes the amyotrophic lateral sclerosis develops with a prolonged course and paresis progression.

### ***Acute disorders of cerebrospinal circulation – spinal strokes***

In the past, this pathology was diagnosed as hematomelia – traumatomyelia with foci of necrosis and myelomalacia. Acute ischemia can be caused by intravascular mechanisms, including reflex-spastic, as in cerebral vascular accidents. A significant place in its etiology is also occupied by hyperextension injuries, when the neck and the backbone are overdiagnosed, the yellow and jagged ligaments are infringed, which leads to compression of the vessels of the spinal cord. An important role belongs to the hernia of intervertebral discs. More often during the course of the disease, several stages can be distinguished: 1) precursors; 2) development of a stroke; 3) reverse development; 4) residual phenomena. Precursors of ischemic stroke are paroxysms of transient spinal disorders.

The rate of stroke is different – from a sudden (up to embolism or traumatic compression of the spinal cord supplying the vessels) to several hours and even a day (may be preceded by pain in the spine). Characteristic is the cessation or significant stihanie of this pain after the development of myelo-ischemia (interruption of the passage of pain impulses along sensitive conductors).

The clinic of the spinal stroke is highly polymorphic and depends on the prevalence of ischemia both in the longue and in the width of the spinal cord.

***Preobrazhensky Syndrome*** – blockage of the anterior spinal artery, characterized by acute development of paralysis of the extremities, dissociated with anesthesia, impaired functions of pelvic organs. If ischemia is localized in the cervical segments of the spinal cord, then paralysis develops in the hands – flaccid, in the legs – spastic. Ischemia of the thoracic segments is manifested by lower spastic paraparesis, myelo-ischemia of the lumbosacral localization – lower paraparesis (more often sluggish, less often mixed). The upper boundary of the dissociated paranesthesia helps to orient the prevalence of the ischemic focus along the spinal cord length, and the lower one – according to the Marie-Foix reflex.

***Anterolateral syndrome*** (anterior poliomyelo-ischemia) occurs with limited ischemia within the anterior horns. Depending on how this happens,

we can get information about the fact that the «medial» cells of the spinal cord – flexors and adductors – primarily suffer from anterior activity.

Ischemic syndrome of amyotrophic lateral sclerosis often develops in the upper arterial basin. They are characterized by weakness of the distal sections of the upper limbs, atrophy of the small muscles of the hands, increased proprioceptive reflexes, pathological wrist and stop marks. Fascicular twitching of the muscles of the shoulder girdle is possible. In this syndrome, there is no spread of paretic phenomena to the bulbar muscle group: the tongue, larynx, pharynx. Due to the paresis of the diaphragm and the muscles of the chest, cardiopulmonary insufficiency develops.

***Ischemic syndrome of amyotrophic lateral sclerosis*** develops more often in the upper arterial basin. It is characterized by weakness of the distal parts of the upper limbs, atrophy of the small muscles of the hands, increased proprioceptive reflexes, pathological wrist and stop marks. Fascicular twitching of the muscles of the shoulder girdle is possible. In this syndrome, there is no spread of paretic phenomena to the bulbar muscle group: the tongue, larynx, pharynx. Due to the paresis of the diaphragm and the muscles of the chest, cardiopulmonary insufficiency develops.

The syndrome of a centromedullar infarct is diagnosed with damage to distant arterial drives and ischemia around the central canal. Dissociated segmental sensitivity disorders and limp paresis are detected.

Ischemic Brown-Sacker syndrome develops with ischemia in the basin of only one sulkomissural artery. There is an alternating syndrome: deep types of sensitivity do not suffer, paresis (paralysis) on the side of the focus, a disorder of surface sensitivity – on the opposite side.

The ischemic syndrome of the marginal zone (vasocoron basin) is manifested by spasmodic paresis of the limbs, cerebellar ataxia and mild conductive parahypersthesia. The acute onset of the disease, and subsequently the possibility of intermittent flow resembles the spinal form of multiple sclerosis.

***The syndrome of a centromedullar infarct*** is diagnosed with damage to distant arterial drives and ischemia around the central canal. Dissociated segmental sensitivity disorders and limp paresis are detected.

***Ischemic Brown-Sacker syndrome*** develops with ischemia in the basin of only one sulkomissural artery. There is an alternating syndrome: deep types of sensitivity do not suffer, paresis (paralysis) on the side of the focus, a disorder of surface sensitivity – on the opposite side.

*The ischemic syndrome of the marginal zone (vasocoron basin)* is manifested by spasmodic paresis of the limbs, cerebellar ataxia and mild conductive parahypersthesia. The acute onset of the disease, and subsequently the possibility of intermittent flow resembles the spinal form of multiple sclerosis.

***Syndrome of ischemia of the dorsal zone of the diameter of the spinal cord***

*Williamson syndrome* is associated with a heart attack in the basin of the posterior spinal arteries. Acute ataxia, sluggish paraplegia (paresis), sphincter disorders, segmental hypersthesia, indicating the level of ischemia localization are acute.

*Popelyansky syndrome* (posterior column syndrome) occurs in the presence of changes in the spinal vessels in patients. It manifests itself as symptoms of a rough fall from the side of Burdach's pillar. Clinically expressed by violations of deep sensitivity in the hands, sensitive ataxia when performing palcosovoy test.

The syndrome of occlusion of the anterior cervical radiculomedullar artery (artery of the cervical thickening) is manifested by flaccid paralysis of the upper limbs, spastic lower paraplegia, segmental-conductive anesthesia, impaired function of the pelvic organs according to the central type. It is more common in case of a diver's injury, hyperextension neck syndrome, hernia of intervertebral discs, etc.

Ischemia in the basin of the posterior spinal artery develops into a posterocarcinic syndrome resembling a funicular myelosis clinic (conductive paresthesia of Lershitt, sensitive ataxia, moderate deficiency of the pyramidal system).

Ischemia of the upper thoracic segments of the spinal cord is detected when the blood flow is cut off along the upper additional radiculomedullar artery (accompanies one of the roots from Th1 to Th4), and in its absence this zone suffers by the mechanism of ischemia in the "last ray" or "critical zone" of the adjacent blood circulation between the upper and Lower arterial basins of the spinal cord. Clinically defined lower paraparesis, par-anesthesia with the upper boundary of Th1–Th2, retention of urine, feces. There may be signs of damage to peripheral motoneurons in the form of hypotrafia of small muscles of the hands, hyporeflexia, changes in electrodiagnostics (the phenomenon of "robbery" – pathogenic compensation according to AA Skoromtsu).

**Adamkiewicz artery syndrome.** In the acute phase of stroke, sluggish lower paraparesis (paraplegia), dissociated (less often total) paranesthesia (oscillating) from Th4 to L1, impaired pelvic function (delay, incontinence) are detected in the acute phase of the stroke. Bedsores are often associated. In the future, individual segmental reflexes are restored, pathological stop signs appear, the level of sensitivity disorder decreases: on the background of anesthesia, the areas of enlightenment, the joint-muscular feeling is almost always restored (compensation of blood flow in the basin of the posterior cerebrospinal arteries). The clinical picture varies depending on the size and location of foci of ischemia of the segments of the spinal cord, there may be distal syndromes (peripheral paresis of the hand, paresthesia – a sign of defeat of the cervical thickening). Turning off the artery of Adamkiewicz often leads to ischemia of segments from Th4 to S 5.

Syndrome of the lower additional radiculomedullar artery

**Deproj-Gotteron syndrome.** It often develops due to the compression of herniated discs L4–L5 or L5–S1 without or in combination with an inflammatory process in the epidural space. Clinically, it is manifested by radiculo-ischemia, a paralyzing sciatica syndrome (R. Desproges-Jotteron, 1955) with paresis of muscles innervated by L4-S1 segments (Fig. 9–12). Clinically, this paralysis of the peroneal, tibial and gluteal muscles, and sometimes segmental sensitivity disorders (LA Kadyrova et al, 1993). Often, ischemia develops simultaneously in the segments of the epiconus and the cerebral cone: disorders of the pelvic organs function. Angiotopically, diagnosis is always associated with great difficulties, the reason for this lies in the significant individual variability of radicular arteries, the dynamism of clinical manifestations (the prevalence of ischemia in both the longue and the width of the spinal cord). And here an invaluable service is rendered by dopplerographic research.

**Attacks of a sudden drop.** The patient suddenly feels a sharp break in the head. Consciousness does not change, there is pain in the neck and neck. After 2–3 minutes, the strength in the limbs is restored. Proprioceptive reflexes on hands are reduced or absent, on legs are evenly animated, can be determined from both sides by the Babinsky reflex. After 20–30 minutes the neurological status is normalized. Paracism of tetraparesis is renewed with repeated sharp turns of the head. They arise with cervical osteochondrosis, sometimes in combination with atherosclerosis of the vertebral artery, and are associated with transient ischemia of the cervical segment.

Myogenic intermittent claudication occurs with ischemia in the lower arterial basin of the spinal cord. With prolonged walking, patients develop weakness and numbness in the legs, sometimes imperative urges to urinate and defecate. After a short rest, these phenomena pass, and the patient. In the neurological status, in the period of weakness of the legs, the decrease in the knee and achilles reflexes, the hypotonia of the gastrocnemius muscles, the fascicular twitching in them, sometimes Babitsky's reflex is noted. However, these neurological disorders go away quickly. The pulsation of the arteries of the lower extremities does not change. The patient is forced to stop because of the weakness of the legs. These criteria are used for the differential diagnosis with peripheral intermittent claudication – claudicatio intermittens Sharko and atherosclerosis or endarteritis of the lower limbs. Sometimes peritoneal gait is formed in patients.

Cudogenous intermittent claudication is a manifestation of transient ischemia of the cauda equina roots, often in the conical segments of the spinal cord. When walking, paresthesia occurs in the distal parts of the legs with spreading to the perineal region, weakness in the legs, incontinence. After a short rest, these phenomena pass. During an attack of intermittent claudication, there are radicular disorders of sensitivity, torpidity of achilles reflexes, easy distal paraparesis.

Coaddogenic and myelogenous intermittent claudication are most often found with congenital or acquired stenosis of the spinal canal.

### ***Chronic failure of cerebrospinal circulation***

Initially, the disease occurs in the form of transient disorders, but there are signs of persistent, often progressive damage to various structures of the spinal cord.

Sometimes such a clinical picture occurs some time after an ischemic spinal stroke. The clinic is characterized by mixed para- or tetraparesis in conjunction with spotty hyperesthesia, and a violation of the pelvic organs. Sometimes develops amyotrophic lateral sclerosis

With a prolonged course and jerky progression.

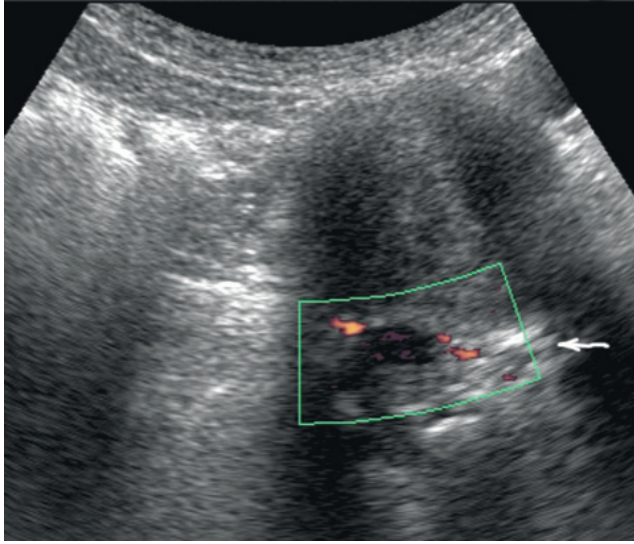


**Fig. 9.** A large left-sided paramedian-posterolateral hernia causes stenosis of the radicular canal with compression of radicular vessels and spinal nerve

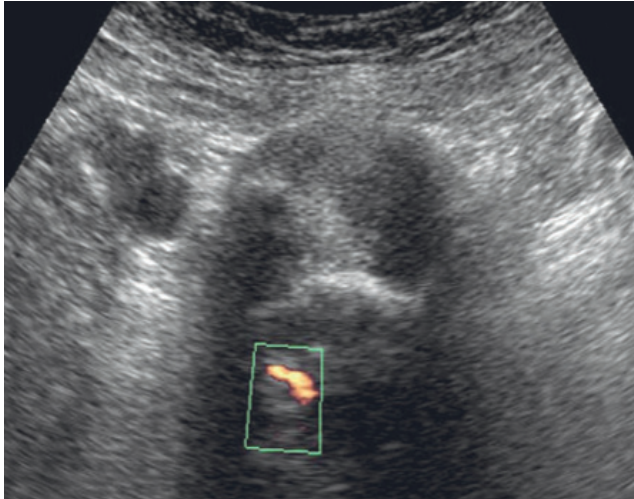


**Fig. 10.** A large right-sided median-paramedian hernia with sequestration causes stenosis of the radicular canal with compression of the spinal nerve. In the regime of energy Doppler mapping, the displacement of the vessels into the central spinal canal is determined

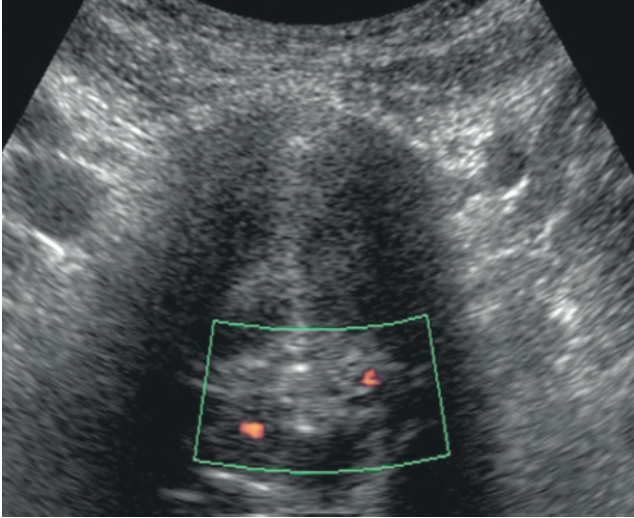


**Fig. 11.** Large median hernia with sequestration causes stenosis of the vertebral canal with compression of the horse's tail. In the regime of energy Doppler mapping, the displacement of the vessels into the central spinal canal is determined

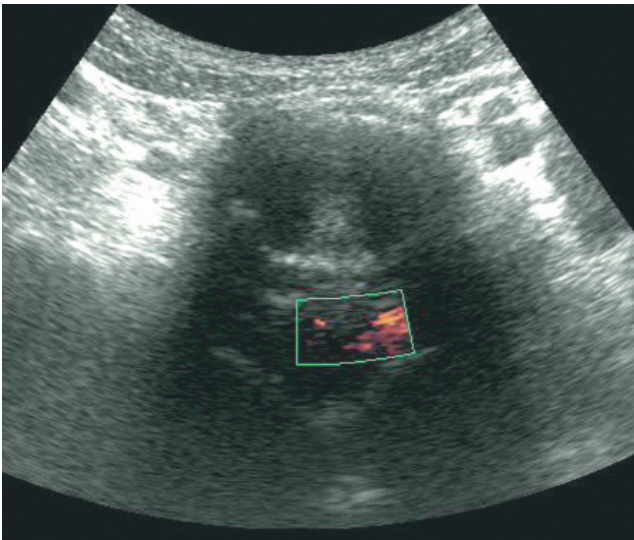


**Fig. 12.** Median hernia with the development of epiduritis causes mild stenosis of the spinal canal. In the regime of energy Doppler mapping, dilatation of the radicular veins on the left

### *5.3. Neurovascular syndromes*

In the study of clinical manifestations of damage to both peripheral nerves and blood vessels providing blood supply to the nervous system, significant progress has been made. Combines the same damage to the nervous and circulatory systems – neurovascular syndromes (NVS) – the neck, shoulders, upper and lower extremities received less attention (L. A. Kadyrova, AI Avramenko, 1993).

Clinical polymorphism NVS reflects the general pathophysiological mechanisms and the unequal etiology and pathogenesis of their specific variants. These include atherosclerosis, low back pain, abnormal mobility in the spinal motion segment, posterior subluxation of the extensor articular processes, Kimmerle anomaly and Powers, fibro-tendon injury, damage to the bones and skin, psychogenic factors. NVS require special consideration in connection with spasm of muscles in response to reflex pulses from a degenerative-dystrophic affected vertebral column. Porazhenie intervertebral disc accompanied by the development ekstenzionnogo, flexion and scoliotic muscle syndromes involving not only the limbs but also the spine. Muscular-tonic changes are facilitated, along with a violation of the functional state of segmental apparatus, innervation of muscles and a disorder of supra-segmental regulation. If the nerves and blood vessels pass close to the muscles in which the spasm has arisen, they can be squeezed. One of the most effective methods for diagnosing NVS is dopplerography.

The syndrome of the anterior staircase (Scalenus syndrome) is described by S. Naffziger (1934). The disease often develops in people who have weights on their shoulders, with a muscle injury, hereditary variations in muscle development. Particular importance is attached to changing the posture in connection with the asymmetric development of the body. I. P. Kipervas also points to the role of apical tuberculosis and pleurisy. The same effects on the muscle from the side of the diaphragm and heart were noted by S. Naffziger (1937), from the gallbladder – Popelyansky et al. (1978). Clinically, the scalenus syndrome is characterized by signs of compression of the neurovascular bundle between the tense front staircase and the 1st rib. The clinical picture is dominated by symptoms of compression of the lower primary trunk of the brachial plexus and the vertebral artery with its autonomic (sympathetic) plexus:

swelling in the supraclavicular fossa, pain and paresthesia in the shoulder belt to spread them on the inner surface of the hand, the prevalence of muscle weakness and atrophy in gipotoneria. There have been a variety of autonomic cardiovascular disorders: cyanosis, or pallor brush, its swelling, reduced skin temperature, reducing voltage pulse at the radial artery. Of particular importance in the diagnosis of the syndrome are pain, thickening and anterior scalene muscle strain, disappearance or weakening of the heart with a deep breath, turning your head, arms abduction. In addition, there may be changes in blood pressure. Scalenus syndrome occurs among patients with cervical osteochondrosis, cervical rib type anomalies, Powers. In this syndrome, there is often a disturbance of blood flow in the thyroid shaft (Fig. 13–15).



**Fig. 13.** Compression and C-shaped bending of the shielded trunk with a scalenus syndrome

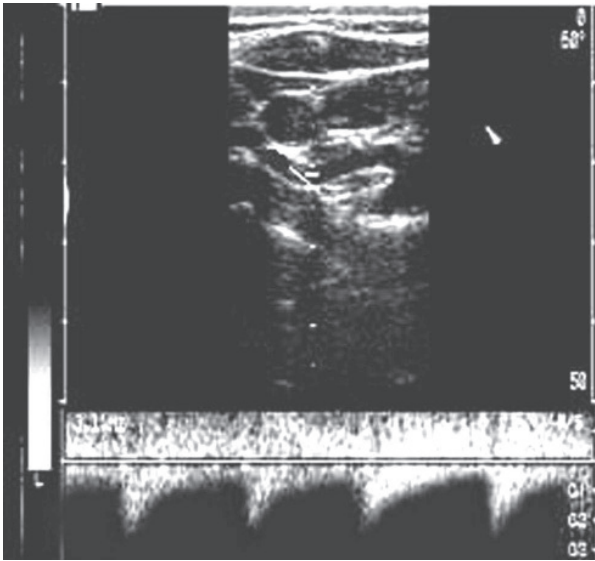


**Fig. 14.** The same. Registration of blood flow at the time of stair muscle tension

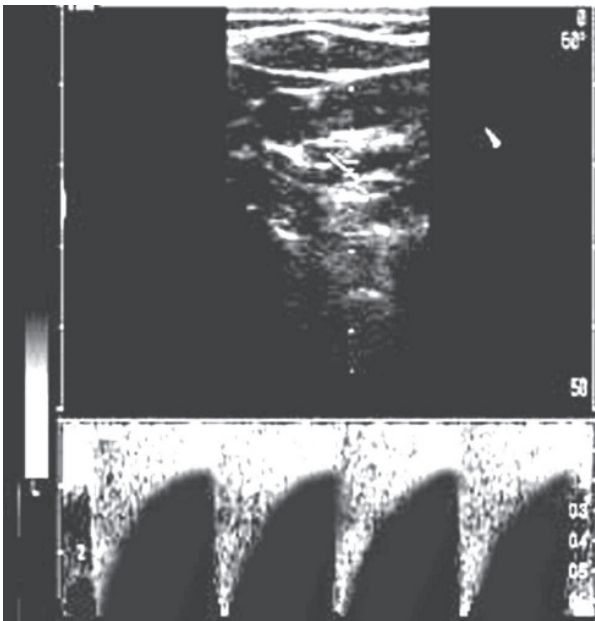


**Fig. 15.** The same. Recording of blood flow after removal of tension in the stair muscle

*The syndrome of a small pectoral muscle* is caused by muscular-tonic, neurodystrophic disorders in this muscle and compression of the neurovascular bundle underneath. Compression of these formations can be caused by abrupt withdrawal of the hand (hyperabduction in anesthesia, immobilization of the humerus, during sleep with the arm thrown back behind the head). A special role in the development of the disease belongs to cervical osteochondrosis (ES Zaslavsky and co-authors, 1976).

Patients experiencing breaking or burning pain in the zone of the muscle – the medioclavicular region at the level of the 3–5th ribs, which can irradiate into the shoulder joint. Sometimes they spread into the hand along the ulnar edge to the brush, and paresthesias are noted in the same area. The last symptoms are caused by the compression of the neurovascular bundle between the corpus spine of the scapula, the 1st rib and the tense small pectoral muscle. Pain in the chest is often intermittent, appearing or intensifying with physical exertion involving the hand (with the weight on the chest). Determine the tenderness in the course of the small pectoral muscle, especially at the point of attachment to the chest (2–5th ribs along the medioclavicular line). Characteristic is the disappearance or change in the pulse when the shoulder is withdrawn, in the position of the hand on the back of the head. If not only the subclavian artery but not the subclavian artery is squeezed, then during suturing and lifting of the hand, a systolic murmur above and below the collarbone is auscultated.

***Shoulder-brush syndrome*** (neurovascular dystrophy of the upper limb). Clinically, this syndrome is manifested by a combination of humeroparous periarthrosis with gross neurovascular and neurodystrophic changes in the brush region. It can be one of the complications of cervical osteochondrosis (O. Steinbrocker, 1948).

The disease develops gradually: first, painful stiffness of the shoulder joint arises, then the damage to the hand. It is also possible to reverse the order of development of pathology.

The leading symptoms are pains of deep, pulling and tightening character in the shoulder, neck and hand regions, painful paresthesias in the hand, hyperesthesia in wide areas in the form of “half-jacket” and “hemitip”. Vegetative disorders are diverse: hyperhidrosis, acrocrosis, thinning of the skin, trophic disorders of nails and hair with redness, limited dense edema of the skin and subcutaneous tissue of the brush with swollen fingers with tightly stretched, dry, flaky, shiny skin.

Dopplerography reveals a spasm of large vessels of the hands on both sides, but more on the sore side, spastico-atic dystopia with a de-

crease in blood filling on the forearm on the side of the pathology, and on the hands, on the contrary, an increase in blood filling, which is probably associated with the appearance of a neurogenic edema. The disease usually lasts 3–6 months, but cases with a duration of up to three years with the development of irreversible contractures of the shoulder and fingers, gross trophic hand disorders are described.

***Costal-clavicular syndrome.*** Along with the cervical rib syndrome, the syndrome of the high 1st rib, or costal-clavicular syndrome, or the upper exit syndrome is clinically considered. This narrowing of the gap between the clavicle and the abnormally high 1st rib with the corresponding pressure of the neuromuscular bundle. It occurs with a fracture of the clavicle, congenital or acquired deformity, abnormally high 1st rib, hypertrophy of subclavian and other muscles. A contributing factor may be the transfer of severity, a significant cervical rotation.

Patients complain of diffuse pain with paresthesia (more often in the legs) starting from the shoulder and with irradiation into the neck, palm and fingers. It is difficult to work with your hands up, control the car, lift weights, sleep on your side or back. Objectively determined hand hypotrophy, puffiness of the hand, lower third of the forearm with a slight cyanosis or mild hyperemia (manifestation of venous or arterial insufficiency), a decrease in tendon reflexes. A positive test for the disappearance of the pulse on the radial artery is possible with the withdrawal and lowering of the shoulder (convergence of the 1st rib with the clavicle, acrocyanosis, numbness of the arm, asymmetry of the arterial pressure).

***Paget-Shreter's syndrome*** initially attracted the attention of surgeons as acute obstruction of the subclavian vein after physical stress. Subsequently, extravasal causes were identified (IP Kipervas, 1985).

The syndrome is characterized by pronounced venous congestion in the hand, developing thrombosis subclavian or axillary vein (venous thrombosis force, compression of these veins edge-coracoid ligament constriction costoclavicular or interscalene intervals at a voltage ladder and the pectoralis minor muscle adhesions and scarring processes, abnormalities of – cervical ribs, elongated transverse processes of the cervical vertebrae).

Clinically manifested by pain, extending from the cervico-brachial region along the entire arm, which is strengthened by turning the head and movements in the shoulder joint, physical exertion, staying in the cold and is accompanied by a feeling of heaviness in the axillary region. There can be a sudden increase in the volume of the limb with increasing edema, cyano-

sis, difficulty in active and passive movements. The skin in the area of the edema is cold, cyanotic, varicose can spread to the upper part of the chest. Venous pressure in phlebtonometry rises from 170 to 300 mm of water. Art. Hyperesthesia is detected in the area from the clavicle to the teat line. Tendon and periosteal reflexes on the arm are first strengthened, and then fade.

***The syndrome of the piriformis muscle*** in certain of its manifestations is known for a long time. So, in gynecological practice it is a peri-formit. At least one third of patients are diagnosed with lumbar osteochondrosis (Kadyrova LA, 1981). Clinically, tonic, dystrophic changes in the muscle area, signs of effects on the nearby sciatic nerve and the lower gluteal artery (Fig. 16, 17). Patients complain of stupid, pulling, tearing, sometimes burning pains in the buttock, in the lumbosacral and hip joints. Pain reduced or even disappear when the patient is in bed, but the increase in standing, walking, squatting on his haunches when and straightening a bent body. Objectively identified: autonomic disorders in the lower leg and foot, malnutrition gluteus, piriformis hypertonicity, often with myokymia palpation. There is soreness at the site of attachment of tendons, muscles and joint capsules to bone protrusion, pain during stretching in a pose Bonn-Bobrovnikova. Almost always violated motor stereotype with compensatory slope of the fixed spine in the sore side. Diagnostic value has a Doppler study of the inferior gluteal artery using a *Bonnet – Bobrovnikova test*, as well as a significant decrease in lumbar ischialgia after infiltration piriformis novocaine solution.

***Popelyansky subpiriformis syndrome of intermittent claudication.*** Intermittent claudication is a paresis of the legs when walking, which disappear when resting. They are not accompanied by impaired sensitivities. Intermittent claudication is diagnosed occlusive disease, painless form – when the spinal cord pathology, pain, intermittent claudication of the cauda equina and described by YY Popelyansky (1978) – intermittent claudication, caused by exposure to diseased piriformis muscle in the inferior gluteal artery. The main manifestations of the latter form are as follows. A patient with vertebrogenic peri-formis syndrome experiences pain intensification after taking a certain number of steps. The pain intensifies paroxysmally and has the character of intolerable, burning, krumpy-like. The patient is forced to bend a painful leg in the knee joint, squat or lie down with a knee bent in the knee. Only resting for a few minutes, until the pain subsides, the patient is able to repeat the attempt to walk, which again ends with a similar paroxysm. The area of pain is the buttock and the back of the thigh. Sometimes the pain starts from the toes. Pear-shaped muscle is painful on palpation.

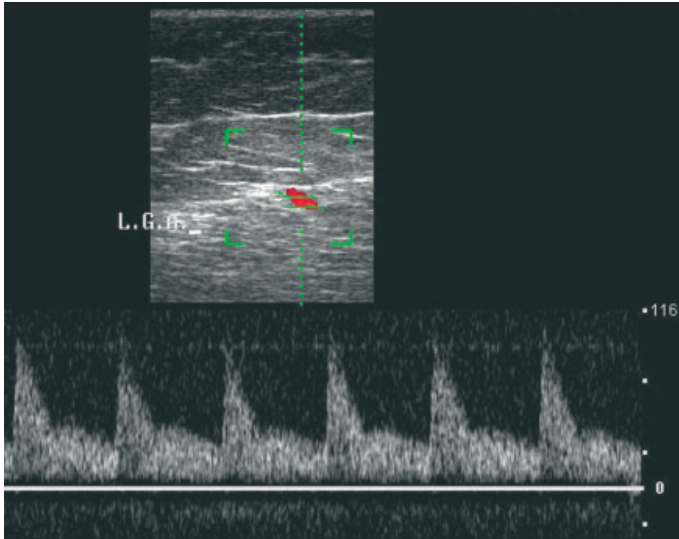


**Fig. 16.** Normal blood flow in the left gluteal artery

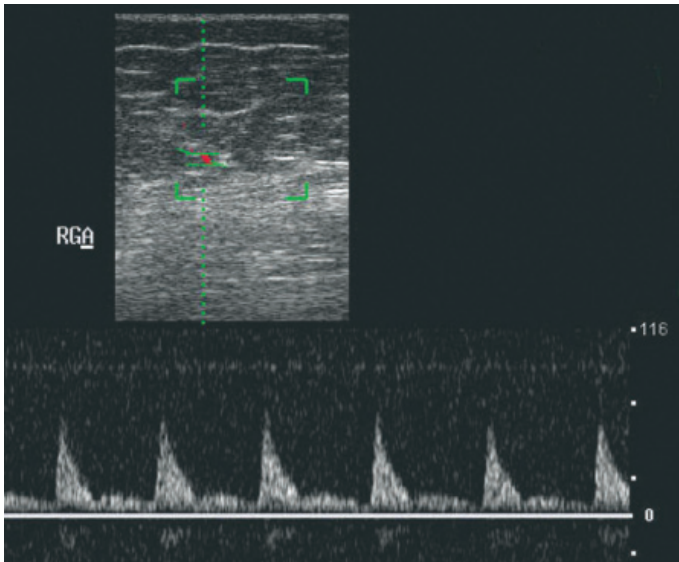


**Fig. 17.** Piriformis-syndrome. Reduced diastolic blood flow in the right gluteal artery

## Chapter 6

# Ultrasonography of peripheral nerves and regional anesthesia

### *Ultrasound imaging of peripheral nerves*

Until recently, there have been formulated principles of visualization of peripheral nerve structures. The first publication of the possibility of peripheral nerve ultrasound Fornage completed in 1988 [1]. Fornage additionally described cellular ('fascicular') pattern of ultrasound nerve visualization, the possibility of identification the nerve relatively to anatomical landmarks, and founded ultrasound of nerves tumors. Prior to this a long time it was considered that the nerves can not be investigated by ultrasound [2]. Only Solbiati et al. [3] reported the sonographic visualization n.laryngeus recurrens a thin hypoechoic tubular structure with a diameter of 1–2 mm on ultrasonography of the thyroid gland. In 1978, La Grange et al. first reported the use of Doppler blood flow detector when the brachial plexus block. [4] This is the first publication on the use of ultrasound for regional anesthesia. In 1994, Kapral et al. [5]. published the first paper on the use of direct sonographic imaging in regional anesthesia (supraclavicular brachial plexus block), with an estimated prevalence of anesthetic. Over the last decade due to the rapid development of health care technologies, including ultrasound we observe at the turn of specialties of anesthesiology and clinical imaging, most of ultrasound, which support high-quality visual information of soft tissues without loss of clinical patient contact. It is creating a new consensus on sonography of nerves and guidance of regional anesthesia on the principles of evidence-based medicine and its constant modification and improvement. Today, sonographic guidance of regional anesthesia receives the status of a 'gold standard', the principles of modern regional anesthesia are formulated [6].

We found the most specific ultrasonographic signs of nerve: round, oval or irregularly shaped cellular structures in cross section (at  $88.0 \pm 4,1$  % sciatic nerve in  $84.0 \pm 4,7$  % of femoral nerve), the detection data sonoelas-

tography structure denser than the surrounding tissue (in  $72 \pm 5,7$  % sciatic nerve in  $74.0 \pm 5,6$  % femoral nerve) and the phenomenon of anisotropy ( $56.0 \pm 6,4$  % of cases sonography sciatic nerve,  $70.0 \pm 5,9$  % femoral nerve) [7]. Ultrasonound guidance of regional anesthesia can provide higher quality of anesthesia than neurostimulator [8].

Today ultrasound becomes n effective method for diagnosis nerve pathology as compressive syndromes [9,10] and different types of neuropathy [11,12].

### *References*

1. Fornage BD. Peripheral nerves of the extremity: imaging with ultrasound. Radiology 1988; 167: 179–82.
2. Hoddick WK, Callen PW, Filly RA, Mahony BS, Edwards MB. Ultrasound evaluation of benign sciatic nerve sheath tumors. J Ultrasound Med 1984; 3:505–507.
3. Solbiati L, De Pra L, Ierace T, Bellotti E, Denchi LE. High-resolution sonography of the recurrent laryngeal nerve: anatomic and pathologic considerations. AJR 1985; 145:989–993.
4. La Grange P, Foster PA, Pretorius LK. Application of the Doppler ultrasound blood-flow detector in supraclavicular brachial plexus block. Br J Anaesth 1978; 50:965–7.
5. Kapral S, Krafft P, Eibenberger K, et al. Ultrasound-guided supraclavicular approach for regional anesthesia of the brachial plexus. Anesth Analg 1994; 78: 507–13.
6. Marhofer et al Ultrasound guidance in regional anaesthesia British Journal of Anaesthesia British Journal of Anaesthesia 2005 94(1):7–17.
7. Bubnov RV, Abdullaiev RIa. Main sonographic parameters of regional anesthesia conduction in the lower extremities under ultrasound guidance]. Lik Sprava. 2010 Oct-Dec;(7–8):97–107. Ukrainian.
8. Bubnov RV, Stokan' AM, Abdullaiev RIa. Comparative study of performance of lower extremities blocks under ultrasonography and nerve stimulator guidance Lik Sprava. 2011 Jan-Mar;(1–2):126–31. Ukrainian.
9. Martinoli C, Bianchi S, Gandolfo N, Valle M, Simonetti S, Derchi LE. US of nerve entrapments in osteofibrous tunnels of the upper and lower limbs. Radiographics. 2000 Oct;20 Spec No: S199–213; discussion S213–7.
10. Stuart R. M., C. Kohl E. S., Bredahl W. H. Sonography of Peripheral Nerve Pathology Am. J. Roentgenol. January 1, 2004 182:1 123–129
11. Bubnov RV Ultrasonography Diagnosis of Peripheral Neuropathy. The Initial Experience. Ultrasound in Medicine & Biology 37 (8), S144-S145.
12. Пат. № 61290 U, Україна. Спосіб діагностики периферичної нейропатії – корисна модель). МПК А61В 8/08 / Бубнов Р. В. – опубл. 11.07.2011, Бюл. № 13, 2011 р.

## *Methodics*

Ultrasound of nerves should be performed using high class ultrasound equipment. More convenient to use are portable ultrasound machines.

*Minimum requirements* for the ultrasonic equipment for the visualization of nerve are:

High-resolution ultrasound (HRUS) – is determined by the technical capabilities of the probe, an efficient Doppler (color and energy), multifocus functions, image optimization techniques – tissue harmonica, etc.; desirable are presets for soft tissue sonography muscle, nerves, nerves puncture.

The study does not require any special training. The study was conducted using an ultrasound machine that works in real time with the use of sensors with an operating frequency of 10–12 MHz (up to 24 MHz).

Recent research points to the need for high-sonography as the deep nerves for clear differentiation of the nerve from the surrounding structures. While using convex probe it is difficult to differentiate the nerve from the tendons, such as the sciatic nerve from the tendon of the long head m.biceps femoris. It is almost impossible to differentiate between neural structures and piriformis muscle in proximal sciatic nerve block when scanning at low frequencies.

The depth of the most nerve ranges from 3 to 7 cm – possible depth of focus adjustment in the high-frequency probes. We believe the optimal frequency of 8–10 MHz, but do not exclude the possibility of using convex probe, especially multifrequency. A few studies indicate that the ideal frequency for the study of the structure of the nerve – 15 MHz. However, it has a very low depth of scanning (up to 2 cm), which is sufficient for the study of the femoral nerve, even in obese patients with deep-seated nerve.

Peripheral nerve trunks are composed of myelinated and amyelinate nerve fibers and connective tissue membranes. Some fibers are single nerve cells and small ganglia. Between nerve fibers in the nerve trunk is thin layer of connective tissue – epineurium. Bundles of fibers are coated by perineurium. US depicts peripheral nerve tissue as a hypoechoic structure that may be clearly defined in plexus bundles. At the level of the peripheral nerves form multiple separate small bundles surrounded by epi-, perineurium, which, is increased echogenicity, so peripheral nerves acquire cellular structure with transverse scanning – hypoechoic neural tissue, increased echogenicity – connecting. This type of structure is called ‘fascicular pattern’ (Fig. 1), that is typical of the large nerves (femoral, sciatic nerves). After visual verification nerve anatomical landmarks are secondary.

Obtaining images of the nerve in the transverse scan is necessary to distinguish nerve from similar in structure formation – e. g., the muscles at hip level – m.adductor magnus and m.piriformis m.gemellus at a higher level. Nerve has a typical ‘fascicular pattern’ – the structure of a tubular structure, whereas the tendon – a homogeneous structure of increased echogenicity – fibrillar (‘fibrillar pattern’, homogeneous) pattern. This is the main differential features of the nerve from tendon (except anatomical principle). Although the majority of the peripheral nerves has multifascicular structure, to be reliably estimated in all nerves is possible only with high-frequency probes. That is not always the specific pattern is a reliable sign of nerve verification. Therefore additional symptoms may be applied. Nerves do not reveal the transition into the muscle. The limbs should help for the final verification in difficult cases. Relative movement of tendons nerves more passive. Besides tendons often are more hyperechogenic.

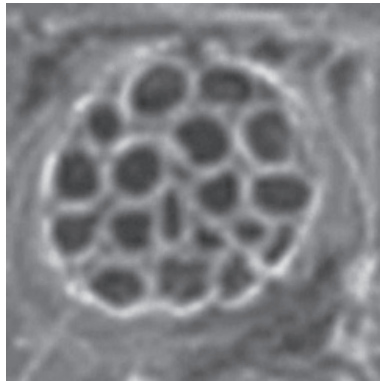


**Fig. 1.** Typical presentation of nerve on ultrasound. ‘Fascicular pattern’ – the nerve of increased echogenicity with hypoechoic spots

### *Visualization of the femoral nerve in the inguinal region*

The femoral nerve is better visualized at the level of the inguinal fold, where it is ventromedial to m. iliopsoas and lateral to the femoral artery, adjacent to the thin fibrous ileoplastic ligament (arc. ileopectineus). To do this, the sensor is positioned conventionally perpendicular to the puarth ligament, then tilted 30–40 degrees inward, depending on the patient’s constitution, according to the anatomical nerve stroke until a typical sonographic scan of its cross section is obtained. It is advisable to first verify the femoral ar-

tery and vein with the help of color Doppler mapping and spectroscopy to differentiate the venous and arterial vessels, and in certain states to assess the blood flow to the extremities. To search for the nerve, systematized ultrasound scanning of the inguinal region and the upper part of the anterior surface of the femur in the transverse and longitudinal sections is performed. With the help of the transducer, the nerve is searched for according to its typical anatomical position and the syntopic arrangement with the surrounding structures. First, the sensor vibrates to obtain the optimum echogram

A lateral scan of the nerve located lateral to the verified artery. The infraginal part of the femoral nerve is visualized directly lateral from the femoral vessels and the medial head of the quadriceps muscle and the ventromedial

Of the distal part m. iliopsoas (Figure 2)., the compression of the nerve with a nearby hematoma can be determined on ultrasound.

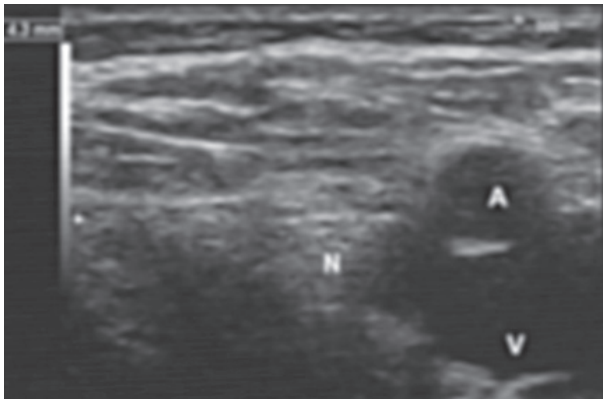


**Fig. 2.** Visualization of the femoral nerve in the inguinal region

### *Ultrasonography of the sciatic nerve*

The sciatic nerve is the largest nerve of the human body. In fact, it consists of two large nerves, united by a common perineural shell: lateral is the common peroneal and medial – tibial. The sciatic nerve is formed from the sacral plexus of segments L4-S2, where the elements of the tibial nerve are connected to L4-S3 by interweaving the fibers of the sacral and lumbar plexus. The sciatic nerve is in behind the peritoneal space of the small pelvis, emerging from its cavity through a large gluteal opening formed by the incisura major gluteal bone and the ligamentum sacrospinous. The nerve passes below the pear-shaped muscle through the podrushovidnoe space of the large

gluteal opening. Here it borders on the pudend nerve and the lower gluteal vessels, surrounded by an appropriate amount of connective tissue and fat.

Scanning of the intraluminal segment of the sciatic nerve concerns sonography of the lumbar and sacral plexus. The sensor is installed at the level of the gluteal fold transversely to the typical location of the sciatic nerve – along the gluteal fold.

The sciatic nerve is located on the side of the tendons of the biceps femoris in its proximal part. The sciatic nerve and the proximal part of the tendon of the biceps femoris muscle can be similar to the nerve in sonography (Figures 3, 4). When ultrasound can determine the compression of the nerve with a number of hematoma located (Figure 5–6). Sonoelastography can improve the efficiency of sciatic nerve imaging.

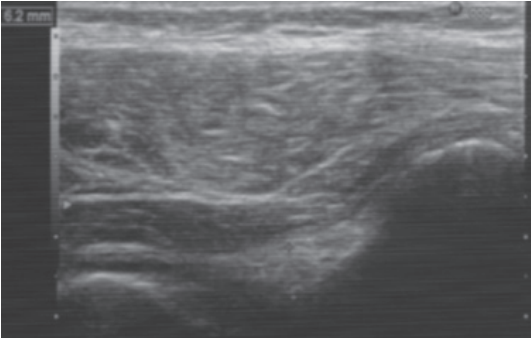


**Fig. 3.** Visualization of the sciatic nerve in the proximal segment under the pear-shaped muscle with a linear sensor

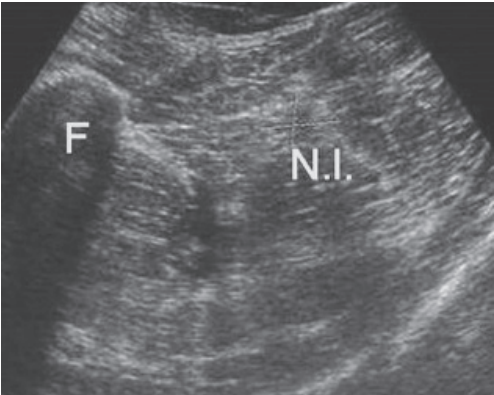


**Fig. 4.** Visualization of the sciatic nerve at the femur level using a convection sensor

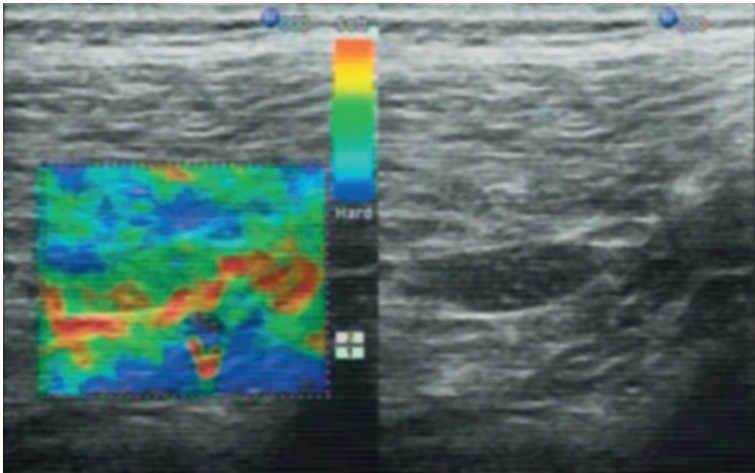
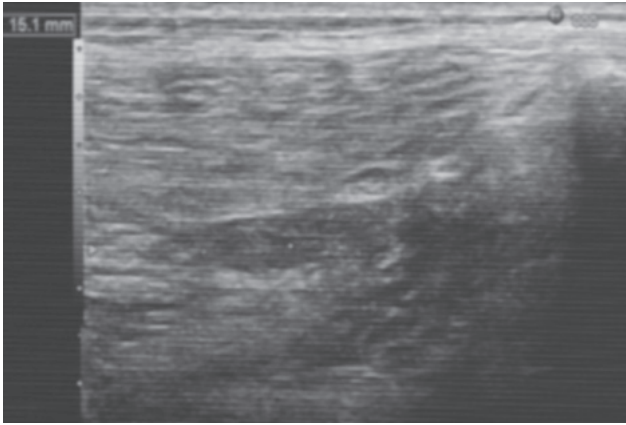


**Fig. 5, 6.** Hypoechoic lesion near the sciatic nerve with lesser density than the nerve according to sonoelastography

### *Nerves of the upper limb*

The innervation of the forearm, wrist and hand is carried out by the ulnar and medial nerves. The medial nerve follows the neuromuscular bundle on the shoulder with the brachial artery and ulnar nerve (Figure 7, 8). In the distal part of the shoulder it is in the aponeurosis of the biceps muscle between the two heads of the round pronator. The forearm is located be-

tween the superficial and deep flexors of the fingers. Climbing upward, the medial nerve enters the carpal tunnel and lies lateral and above the tendons of the flexor of the fingers. Between the tendons of the flexor of the fingers and the tendon of the ulnar flexor of the wrist, the ulnar artery and nerve are located. The ulnar nerve is located lateral to the pisiform, but is medial to the ulnar bone.

The median nerve is often examined when there is a suspicion of carpal tunnel syndrome. It is better to study the nerve at the level of the middle part of the forearm in axial sections. Usually, the nerve is located between the anterior arm muscles, namely the superficial and deep flexor muscles. The nerve has a hyperechoic fascicullar structure. After obtaining the image of the nerve on the axial section, we must move in the distal direction under keeping the image control on the screen of the device, so as not to lose the nerve from view (Figure 9–22). Inside the carpal canal, it adjoins the ulnar nerve.

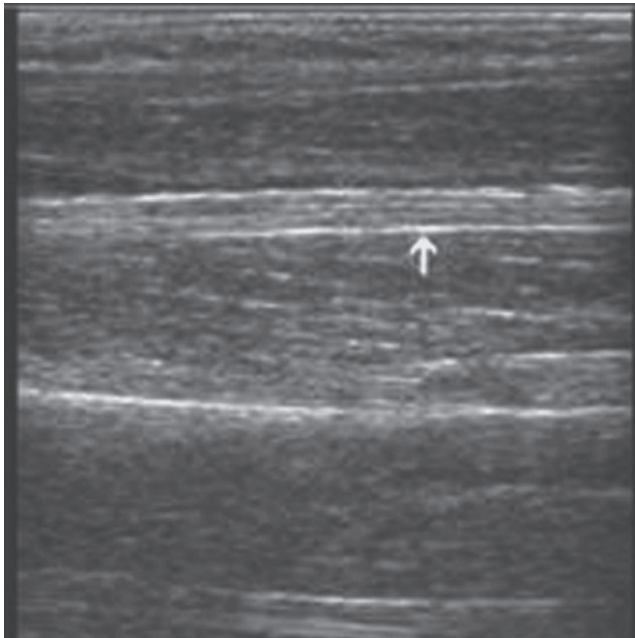


**Fig. 9.** The longitudinal view of the median (*arrow*) of the nerve

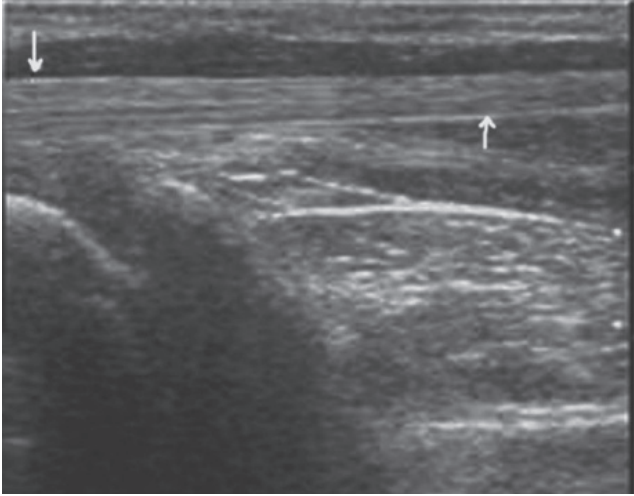


**Fig. 10.** Longitudinal view of the ulnar nerve (*arrow*)

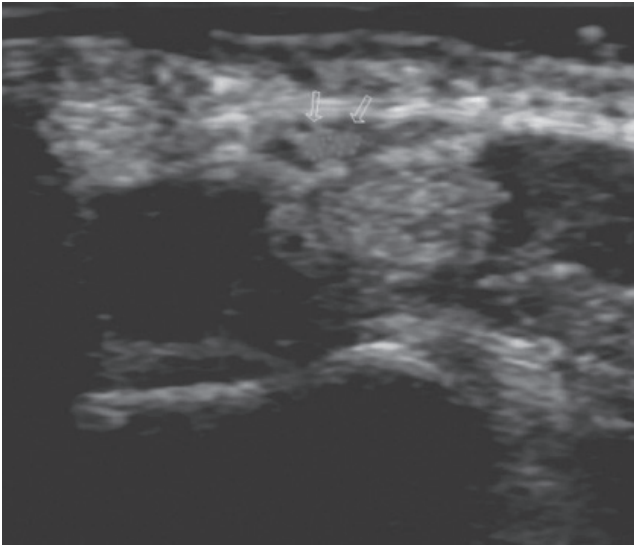


**Fig. 11.** Transverse section of the medial nerve at the wrist (*arrows*)

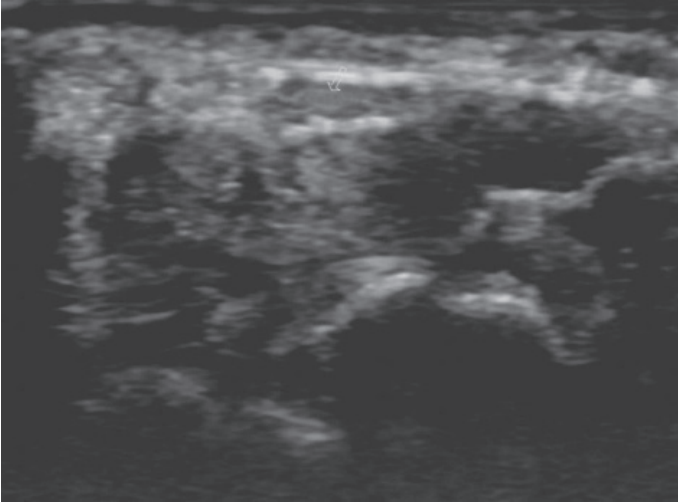


**Fig. 11.** Transverse section of the medial nerve at the wrist (*arrows*)

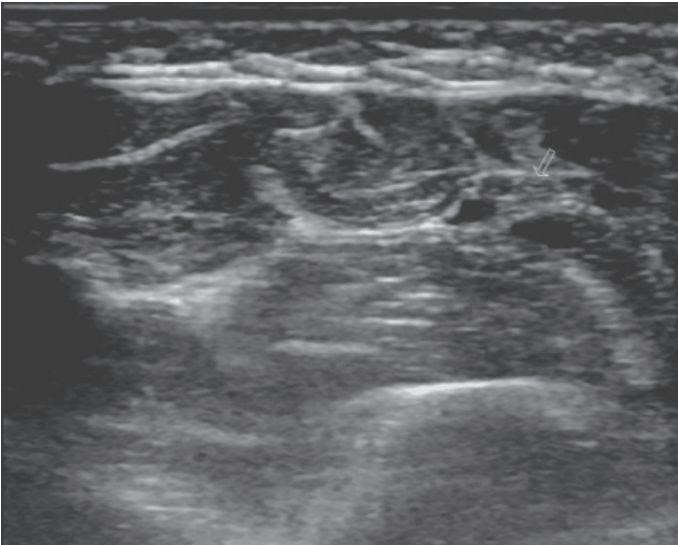


**Fig. 13.** Echogram of transverse cut of the ulnar nerve (*arrow*)

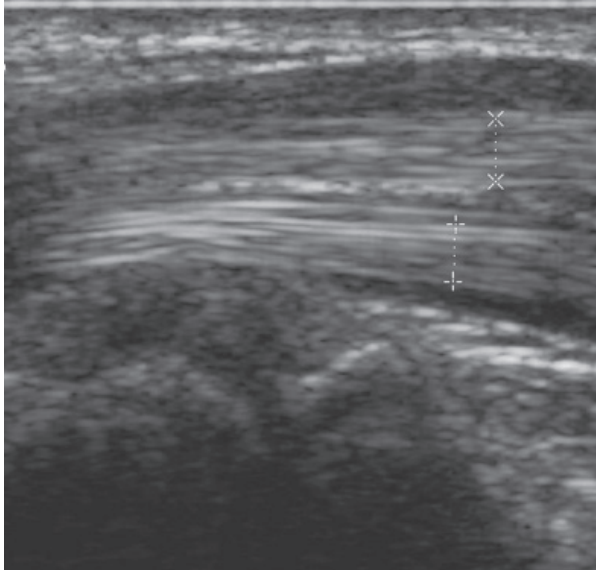


**Fig. 14.** The carpal canal with visualization of the medial and ulnar nerves in the longitudinal section

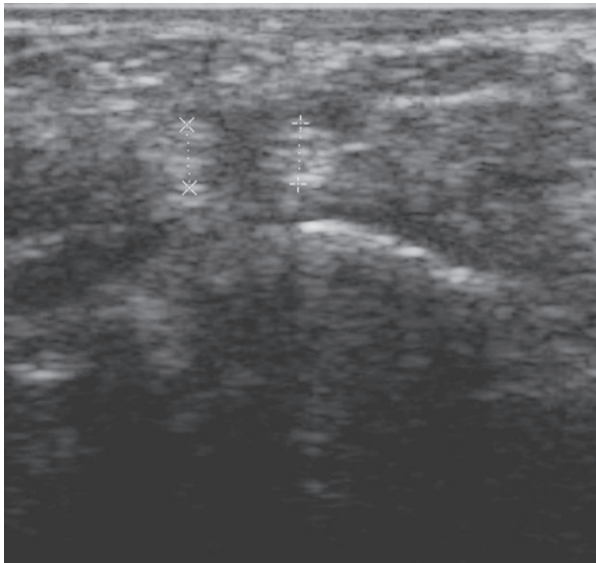


**Fig. 15.** Carpal canal with visualization of the medial and ulnar nerves in the cross section

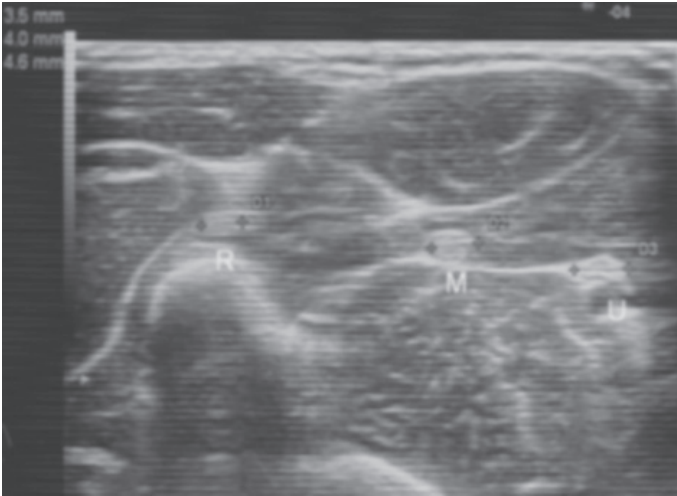


**Fig. 16.** Transverse section of the median nerve in the middle third of the forearm

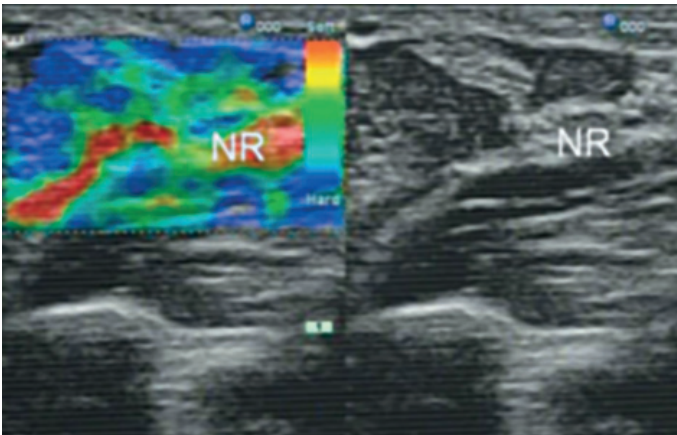


**Fig. 17.** Sonoelastography of the radial nerve, which is denser than surrounding tissues

# Chapter 7

## Trigger Points Dry Needling under Under Ultrasound Guidance for Pain Management. Personalized and Evidence-Based Concept

Most of the pain syndromes in clinical practice have myofascial nature, caused by the formation of myofascial trigger points (MTrP) [1].

The trigger point (TT, myofascial trigger point, MTrP, MTrPs) are hypersensitive areas in skeletal muscle, fascia, tendons and ligaments, painful when pressed and can irradiate a pain in other parts of the body and lead to abnormal sensitivity, autonomic phenomena, such as dizziness, numbness, dysesthesia (Gatterman, 1990). Local anesthetics, the introduction of saline or acupuncture reduces the activity of the trigger point. The trigger point can be in state:

- «active» trigger points that cause pain irradiation during palpation;
- «latent» trigger points –palpation cause only a local hypersensitivity.

Frequency of active MTrP reaches a maximum in middle age. In elderly people revealed a lot of latent trigger points. Women are more likely than men to visit a doctor because of the myofascial pain origin. J. Trevell and D. Simons [2] argue that in normal muscle contains MTrP, they are not compacted strands, they were not painful on palpation, do not give the convulsive reactions and do not reflect the pain of compression. At the same time, according to T. Bates [3], myofascial MTrP is the main source of pain in skeletal muscles in children.

### *Study History*

The term “trigger”, was introduced by Steindler in 1940 [4]. Already in 1816, a British physician, Balfour described as MTrPs as pain inflamed nodules in the muscles. Different terms were used to determine the trigger point: fibrosis miofastsiit, muscular rheumatism, rheumatic myositis, miogelosis,

myalgia, myofascial pain, fibromyalgia [5]. In 1983, Travell and Simons issued a classic two-volume work “myofascial pain and dysfunction”, after its second reissue in 1999, treatment of myofascial pain by acting on the trigger point was put to a modern level of expertise. In 1938, a British rheumatologist Kellgren published a description of specific patterns of reflected pain in the different groups of muscles and ligaments of the spine after injection of hypertonic saline solution.

In 1952, Janet Travell published one of the first of the first articles that recognize the specificity of pain as reflected in the models with more than 30 muscles [6]. Travell (1901–1997) on the right is a pioneer in the treatment of musculoskeletal pain by opredoleniya MTrPs. She introduced the term “myofascial pain syndrome” to describe the pain as a result of trigger points appearance in muscles, tendons, skin, fascia and ligaments. Several subsequent works of Janet Travell devoted to craniomandibular pain [7,8].

### **Hypotheses of pathogenesis**

- The Travell theory of the initial injury;
- Integrated trigger hypothesis;
- Cycle “pain-spasm-pain”;
- Spindle Muscular hypothesis;
- Neuropathy hypothesis;
- The hypothesis of fibrous (scar) tissue;
- Integrated hypothesis Shah (2008) [9].

Activity of trigger point depends on the emotional condition [10].

### **Causes**

- trauma muscle;
- muscle ischemia;
- visceral-somatic reflexes;
- radiculopathy, nerve root compression;
- anxiety;
- other causes.

### ***Trigger points and fibromyalgia***

Until now, evidence-based medicine is widely uses the term fibromyalgia, often also in myofascial pain syndromes [11]. We should distinguish fibromyalgia syndrome (FMS) and Myofascial pain syndrome (MPS), which belong to the group of chronic non-inflammatory pain syndromes af-

fecting the muscles and tendons. Important criteria in the diagnosis of both diseases is the presence of «tender points» and «trigger points». According to the criteria of the American College of Rheumatology, FMS is characterized by the presence of sensitive points and trigger points are usually defined in the MPS.

The term **tender points** is also used. They serve as diagnostic markers for the diagnosis fibromyalgia. Tender Points – extremely sensitive points on the body, painful with compression weighing four kilograms (enough to pale nail). According to the American College of Rheumatology (N. Smyth, M. Yunus, 1990), the FMS is based on two main criteria:

1. The presence of a symmetric generalized pain (extending to the right and left, upper and lower half of the trunk or axial), which lasts for at least the last 3 months.
2. Prevalence by palpation of at least 11 out of 18 (9 pairs) specific sensitive points.

These tender places occur symmetrically on both sides of the body:

- at the base of the skull beside the spinal column;
- at the base of the neck in the back;
- on the top of the shoulder toward the back;
- on the breastbone;
- on the outer edge of the forearm about 2 cm below the elbow;
- over the shoulder blade;
- at the top of the hip;
- on the outside of the hip; and
- on the fat pad over the knee.

The main difference is that the tender points are localized, and trigger points can be found by palpation, which cause reflected pain. Fibromyalgia tender point pain may vary depending on time of day, weather, physical activity, presence of stressful situations and often proves to be more intense after disturbed sleep [12].

In palpation of tender points the node is not determined by, as the trigger point palpation, and no signs of inflammation (redness, swelling, local rise in temperature). The tender points are painful, but when pressed, the pain increased without irradiation. Differences between trigger points and tender points presented on table 1.

Recently conducted research on the specific correlation between the sensitive and active trigger points [15, 16].

**Differential Diagnosis of myofascial pain syndrome (IBS)  
and fibromyalgia syndrome (FMS) [13,14]**

<b>Fibromyalgia Syndrome (FMS)</b>	<b>Myofascial pain syndrome (IBS)</b>
Tender points	Trigger points
Have a specific pain	May be insensitive
Do not cause reflected pain	Cause reflected pain.
Do not cause reflected pain	Cause the reflected pain.
Always multiple	May be single
Have symmetric localization	May occur in any group of muscles

### ***Trigger Point Inactivation***

Trigger point is inactivated only later effect of local twitch response (LTR, LTRs, the local response of spasm), which is caused by either injection or needling strong finger palpation of tense muscles or MTrP, which leads to a brief rupture of motor action potentials, which are available only on constricted fibers. Clinically, there is a slight increase of muscle spasm, after which it decreases [17].

### ***Puncture treatment of the trigger points***

Dry needling (MTrP, TRP-DN) of trigger points, also called intramuscular stimulation (IMS), is an invasive procedure in which a needle (often acupuncture) is introduced in the skin or muscles [18]. TRP-DN – a relatively new technique used in combination with other methods of physical therapy. Local injections are used in different ways for decades. The publications are known from early 1940's [19–21]. Today in the United States Dry Needling the trigger points in the protocols approved by the physiotherapy [22]. There are many parallels between the TRP-DN and acupuncture.

### ***Superficial and Deep Dry Needling***

*Superficial dry needling (SDN)* – the introduction of a needle into the surface tissue to a depth of 5–10 mm directly above the palpable MTrP. In the early 1980 Baldry [23], concerned about the risk of pneumothorax in patients with MTrP in the anterior scalenus muscle. Instead of using TRP-DDN, he introduced the needle into the superficial tissue, just above the MTrP. After

the withdrawal of the needle in a short time, the pain quickly and easily passed. Based on this experience, Baldry popularized the practice of SDN and to inactivate MTrPs in different parts of the body with good empirical results, even in the treatment MTrPs of deeper muscles. He recommended the introduction of an acupuncture needle into the tissue covering every MTrP to a depth of 5–10 mm for 30 seconds.

*Deep dry Needling (DDN)* – is the introduction of a needle directly into deep MTrP, called Local Twitch Response (LTR) and soreness in the course of irradiation, requires manipulation of a needle, a painful procedure, occur pain after the puncture. It is used in cases of compression of nerve roots by deep muscle spasm. DDN has been used for centuries, but the first researcher, who became a strong supporter of its use in modern times was a Czech doctor Karel Lewit. In his classic work, published in 1979 [24], he described the results of treatment of myofascial pain in 241 patients by introducing a needle into the zone of maximum sensitivity, trigger zone, and the pain point (as he termed it), or that of its description, will now called MTrPs. He acknowledged a deep, dry needling this kind leads to considerable pain, but said that its effectiveness depends on the intensity of pain when the needle to a point, and this in turn depends on the accuracy of verification of the trigger point for the puncture.

Chan Gunn [25] thoroughly investigated and popularized the analgesic effect of this type of treatment for myofascial pain syndromes. He called this technique intramuscular stimulation. Deep dry needling is the best way to inactivate the trigger points. The action of the needle with DDN – induction effect of local twitch response. The disadvantages are its low provability and possible complications of the inaccuracy of procedure.

### ***Injecting treatment***

Injections of local anesthetics is not achieved a better effect than the introduction of normal saline [26]. In a comparative study, dry iglokualyvanie was just as effective as injections of local anesthetics like procaine (Novocain), or lidocaine (Xylocaine). Dry needling and the introduction of 0.5 % lidocaine were equally effective in relieving myofascial pain. Postinjection pain develops more often after using the technique of dry needling.

When comparing injection therapy with MTrP TrPDN, many authors believe that the dry needling MTrP provides greater pain relief than injection of lidocaine, but a matter of great postinjection pain. “Typically, these

authors refer to the study of Hong [27], who compared the effectiveness of injections lidocaine with TrP-DN, but this author injection of lidocaine and TrP-DN performed using conventional needles from a syringe, rather than acupuncture needles.

Recently Kamanli et al. [28] updated Hong study in 1994, comparing the results of lidocaine injections, injections of botulinum toxin and TRP-DN. In this study, the researchers also used syringe needles, and they did not take into account the effect of LTRs. In clinical practice, TRP-DN, as a rule, performed acupuncture needle. There is no scientific studies that compare TRP-DN with the use of acupuncture needles with injection treatment MTrP. Based on published scientific studies, the assumption that TrP-DN would cause great pain posleineksionnuyu compared with injections of lidocaine can not be objective, since the latter would not have arisen if acupuncture (fine) needles are used. Studies were conducted to determine the optimum diameter of the needle. It is believed that the use of needle-thick 21–23-gauge – the most effective for preserving the quality of life [29]. Itoh et al. came to the conclusion that the DDN can be more effective in the treatment of low back pain in elderly patients than standard acupuncture (acupuncture) or SDN [30]. Cummings and White concluded: “the nature of the injectable substance is irrelevant to the outcome of treatment, and injections (wet needling) has no therapeutic advantages over dry needling [18].

### ***Visualization of the trigger point***

In 2007, with the help of magnetic resonance elastography were recorded zone of reduced flexibility in the location of the trigger points. This is the only publication of the evidence sample visualization of trigger points. [31]. Minimally invasive manipulation of ultrasound become lately in the conservative orthopedics different parts of the body more important [32]. Ultrasound navigation in minimally invasive interventional orthopedics gives significantly better effects than blind needle insertion based on anatomical landmarks only [33]. There is a pioneer study of attempts to render the trigger points with ultrasound and with the subsequent precise needle insertion under ultrasound navigation [34]. This would avoid complications (damage of blood vessels, nerves, esophagus, etc.) and improve the effectiveness of manipulation. However, before that sonograms of trigger points have not been published.

### ***Comparison with acupuncture***

Dry Needling is not acupuncture. Acupuncture is based on restoring the flow of energy (“qi”) along the meridians in the body. During TrP-DN no direct intent to influence the energy meridians. TrPDN based on modern Western scientific principles and knowledge of anatomy and physiology. Although R. Melzack et al. [35,36] found that 71 % of cases the localization of trigger and acupuncture points (AT) is the same. Most recently, Dorsher [37] compared the anatomic and clinical relationship between the 255 MTrPs described by Travell and Simons, and 386 acupuncture points described in the Shanghai College of Traditional Medicine and other publications on acupuncture. He believes that 92 % of the 255 trigger point correspond acupuncture points and are equal in 79.5 % due to the clinical indications in pain syndromes [38] [38]. Dorsher came to the conclusion that there is considerable overlap between MTrPs and acupuncture points, and claimed that “a high degree of consistency between the treatment of trigger points and acupuncture should contribute to strengthening the integration of acupuncture into contemporary clinical management of pain.” Although these studies prove the feasibility of treatment of TrP-DN as a form of acupuncture, both studies suggest that there are different anatomical localization MTrPs at a time when acupuncture points are anatomical specificity.

### **Challenging Methodology – Trigger Points Dry Needling under Ultrasound Guidance [39,40]**

1. Clinically definition zone of possible trigger point – pain syndrome with of typical referred pain pattern registration.
2. Trigger point palpation. Palpation of a hypersensitive bundle or nodule of muscle fiber of harder than normal consistency. Localization of a trigger point is based on the sense of feel, assisted by patient expressions of pain and by visual and palpable observations of local twitch response.
3. Using additionally other commonly used physical examination tests such as the assessment of intervertebral motion or paravertebral muscle strength testing.
4. When the affected muscle is detected ultrasonography examination is performed for myofascial trigger point visualization using gray-scale, Doppler and sonoelastography (Fig. 1–15).
5. After the visual identification of trigger point, dry needling was performed – acupuncture needles were inserted into MTrP to elicit the LTR effect. The needle is held in tissue until complete disappearance

of the LTR which could be considered similar the phenomenon of the “needle grasp,” which has been attributed to muscle fibers contracting around the needle and holding the needle tightly in place and an increased resistance to further movement of the inserted needle.

6. Ultrasound control after procedure.

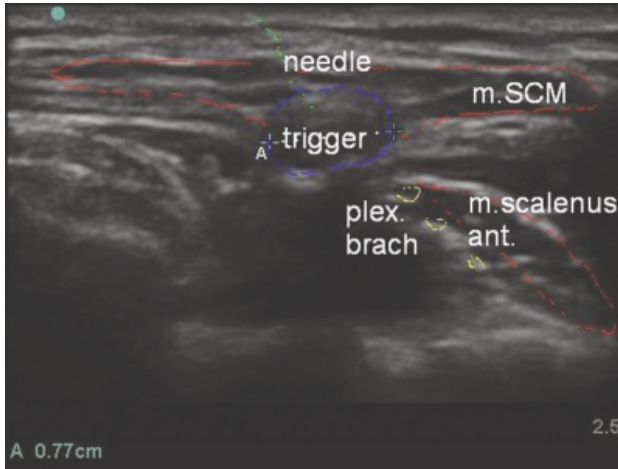


**Fig. 1.** Transverse scan of jugular region. Ultrasound visualization of the trigger points (trigger) and the a needle inserted under ultrasound guidance: Plex. brach – brachial plexus; m.SCM – sternocleidomastoid muscle; m scalenus ant

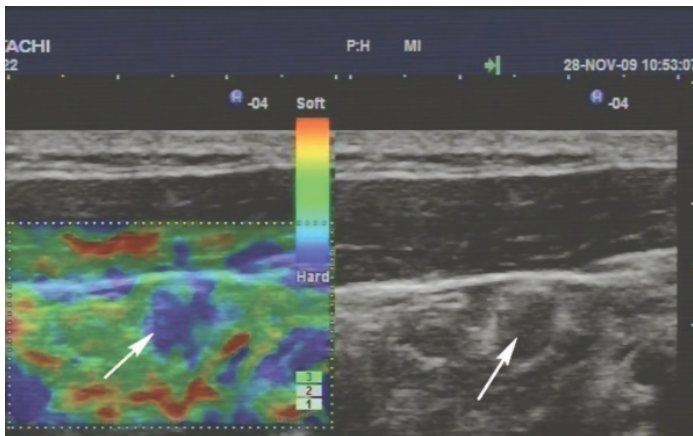


**Fig. 2.** The trigger point in anterior scalene muscle. Sonoelastography application depict blue area 7×6 mm of rigid muscle tissue surrounded by fibrosis

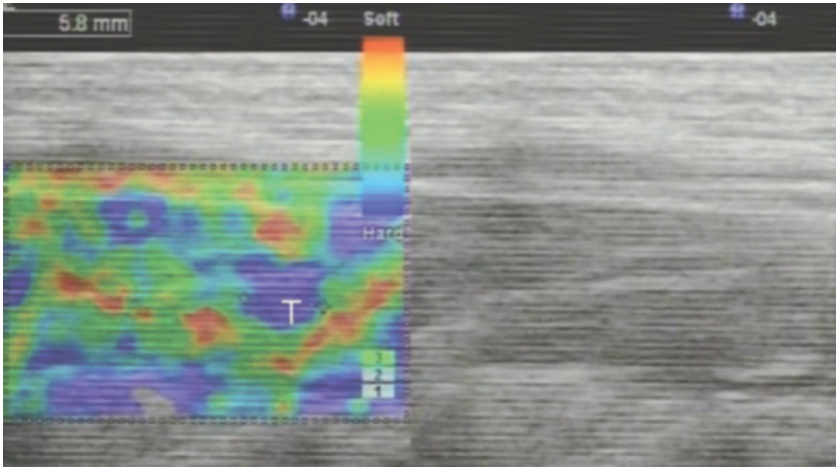


**Fig. 3.** Visualization of trigger points using only sonoelastography – with gray-scale ultrasound trigger zone (T) does not differ from the surrounding tissue. After dry needling LTR effect and typical pain pattern was evoked



**Fig. 4.** Supinator syndrome. Photo and Sonoelastography. Needling trigger of m. supinator and fascial tissue of Frohse arcade

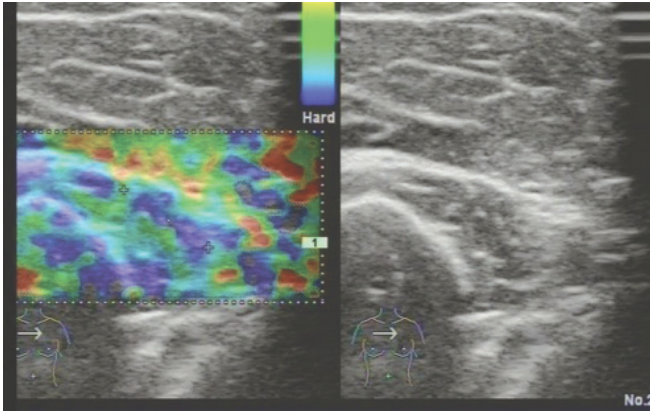


**Fig. 5.** Supinator syndrome. Photo and Sonoelastography. Needling trigger of m. supinator and fascial tissue of Frohse arcade

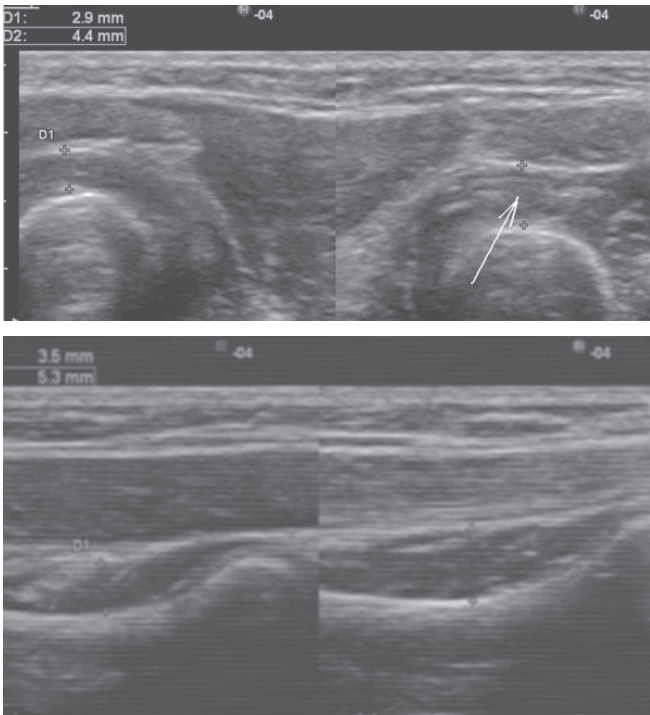


**Fig. 6, 7.** Before treatment – at the forearm area US determined relative thickening of m.supinator (left to 5.5 mm, 9 mm to the right of 4 mm, 7.5 mm).

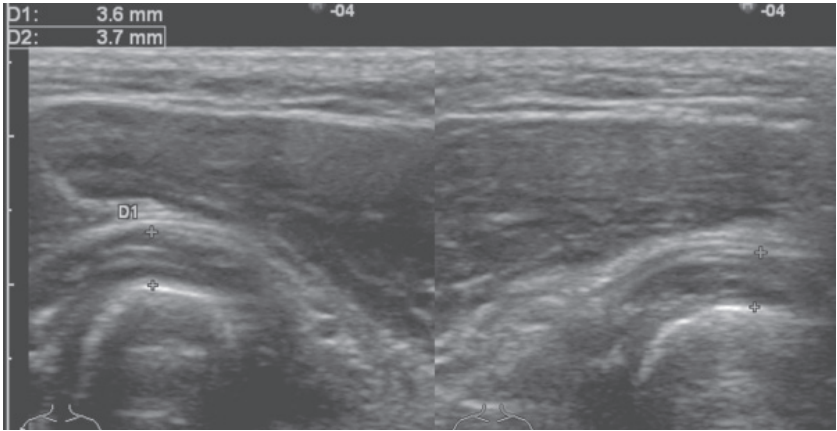


**Fig. 8.** Condition after treatment. After a puncture treatment we notice decrease previously thickened m.supinator (up to 3.8 mm on the left, to the right in the projection of 3.9mm maximum tenderness)



**Fig. 9.** MTrP dry needling under ultrasound guidance in patient with shoulder pain. The secondary trigger points are found in the rhomboid muscle



**Fig. 10.** MTrP dry needling under ultrasound guidance in patient with shoulder pain. The secondary trigger points are found in the rhomboid muscle

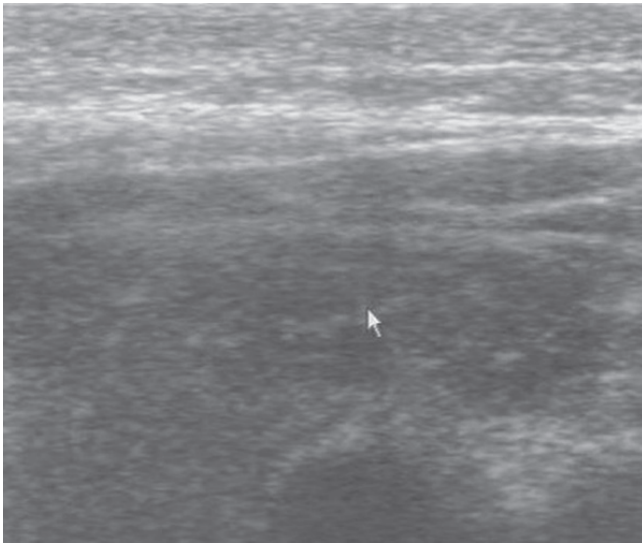


**Fig. 11.** Needle in a trigger point in the projection of capsule of upper-thoracic costovertebral joints and deltoid muscle. Clinically revealed thoracalgia. Pain syndrome was eliminated in two sessions

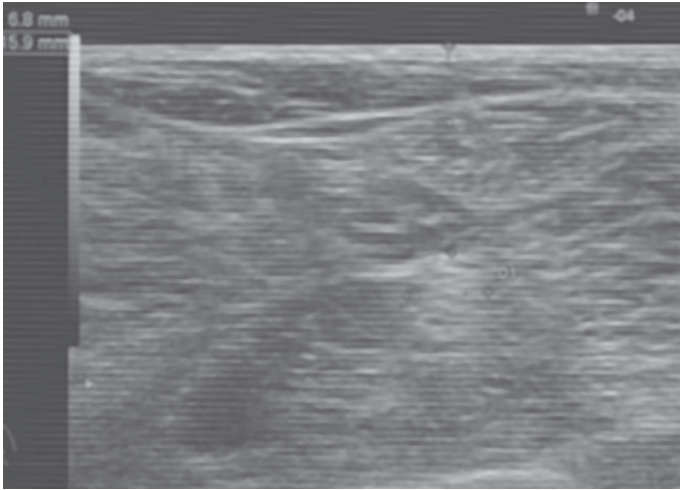


**Fig. 12.** Needle in a trigger point in the projection of capsule of upper-thoracic costo-transversal joints and deltoid muscle. Clinically revealed thoracalgia. Pain syndrome was eliminated in two sessions

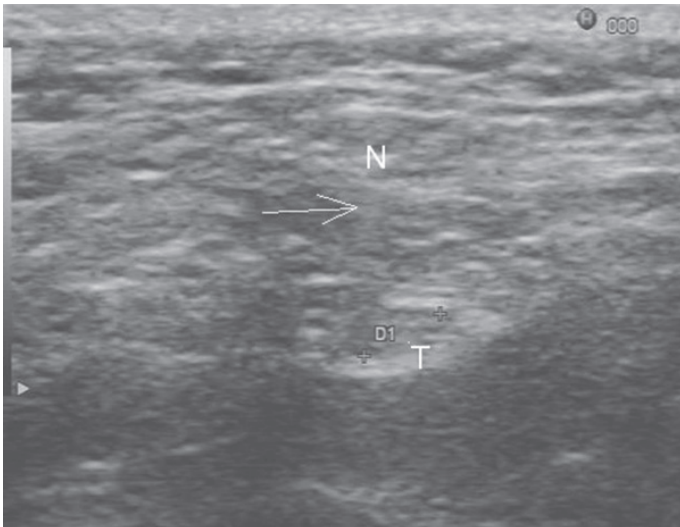


**Fig. 13.** Needle in a latent trigger point (increased echogenicity) of deltoid muscle

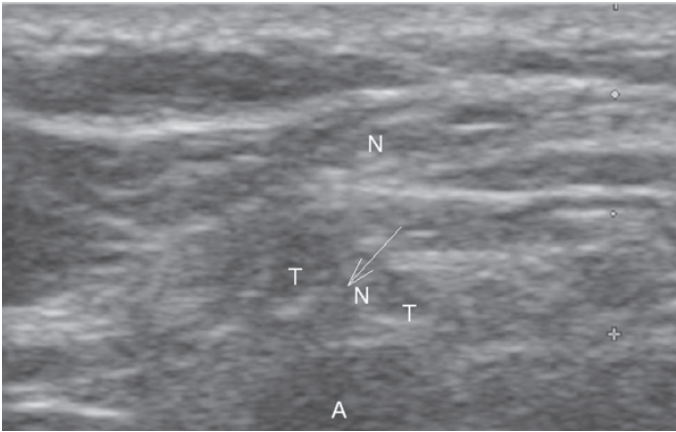


**Fig. 14.** Treatment of acute plexites with dry acupuncture under ultrasound control. The introduction of a needle into the trigger point at the place of attachment m. scalenus ant. Eliminating of tunnel syndrome



**Fig. 15.** The introduction of a needle into the fascial sheath TP of neuro-vascular bundle in the subclavian area. Function hand resumed after 2 sessions

### ***Personalized management of temporomandibular joint dysfunction and craniomandibular pain syndromes [41]***

While ultrasonography application improves the effectiveness and safety of deep dry needling as an optimal method of the trigger points inactivation for myofascial pain treatment it is effective for management temporomandibular joint dysfunction and craniomandibular pain syndromes (Fig. 16–18).

The temporomandibular joint (TMJ) is part of a kinematic chain including the teeth, the opposite TMJ, the muscles of mastication and the upper cervical complex as well as the posterior cervical musculature. In this context temporomandibular joint dysfunction (TMJD) refers to a group of non-specific related disorders of the muscles of mastication and the TMJ, but excludes non musculoskeletal disorders in the orofacial region such as neoplastic, vascular or infectious diseases that produce very similar symptoms. In this regard it is estimated that 85 % to 90 % of the population will develop some symptoms of TMJD in this form at some point during their life.

We believe the use of the deep dry needling without ultrasonic inadequate control as precise puncture of certain muscles can not be performed without a visual ultrasound navigation. Orthopedic occlusion correction should be conducted in the absence of muscle spasm, after inactivation of existing trigger points affecting the TMJ.

#### ***Patterns of muscle involvement in TMJ dysfunction***

Active MTrPs in the upper trapezius, sternocleidomastoid and temporalis muscle are the main causes of the violation of the mobility of craniomandibular area and neck pain syndromes.

It was reported specific reflected the pain patterns in masticatory muscles:

- m. masseter – chewing muscles trismus;
- m. temporalis is TMJ, jaw pain and toothache;
- m. lateralis pterygoideus causes pain, radiating deep in the TMJ, etc.

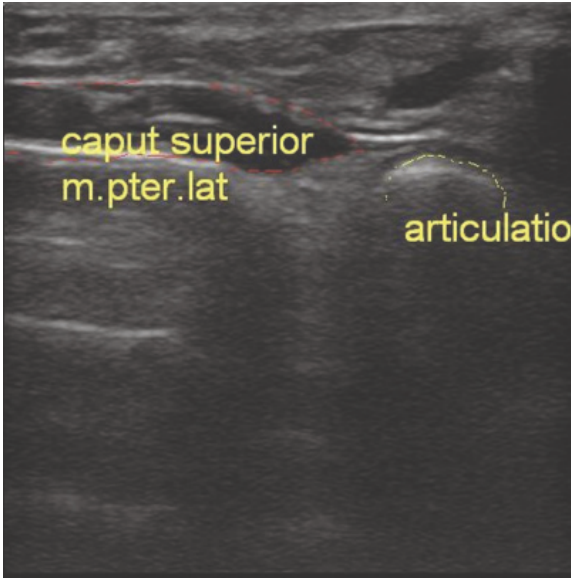


**Fig. 16, 17.** Puncture of the upper portion of the lateral pterygopalatine muscle under ultrasound guidance

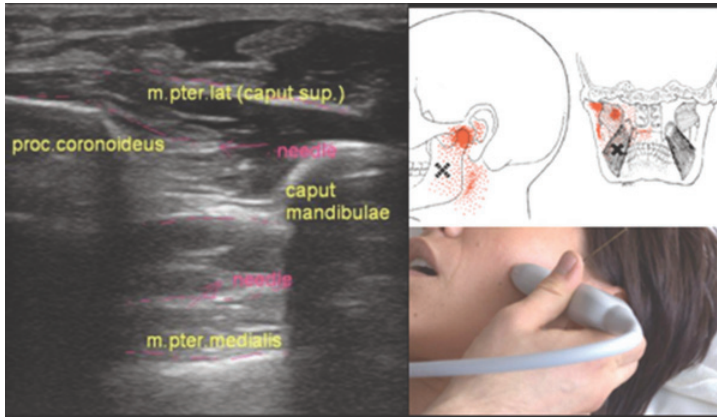


**Fig. 18.** Scheme of the irradiation pattern of the pain (right top), ultrasonogram of needling trigger points in the medial pterygoid muscle (left). Puncture of the lateral pterygoid muscle under ultrasound guidance (right bottom)

### ***Personalized management of local muscle spasticity in different patient groups***

The results of inactivation the TrPs as areas of contracted muscle fibers are reproducible for treatment of other types of local muscle spasticity. Thus we performed study [42], that included recruiting 36 patients, who suffered from local muscle spasticity, that caused movement, postural disorders and pain with different pathology, including hereditary myopathy, Parkinson disease, rheumatic (dermatomyositis, sclerodermia), peripheral neuropathy, poststroke spasticity and trigger points. Patients underwent US guided needle-EMG, biopsy for diagnosis and dry needling for treatment local spasticity. In all patients there were registered changes on ultrasonography [43]. Local spasticity of muscle was visualized as areas of violation the normal fibrillar structure of affected muscles, mostly hypoechoic (Fig. 19). Spontaneous fibrillation was clearly visualized, specific changes of echogenicity and stiffness of affected areas. Functional tests to identify areas with increased susceptibility to spontaneous contractile activity. Sonoelastography identified areas of decreased elasticity in the muscle. Integrated application of neuromuscular US recognized specific patterns and US guided neurophysiologic study and biopsy allows to receive additional information. Dry needling was effective for inactivation trigger points (94 %) and had short effect in 75 % patients with Parkinson disease [42].

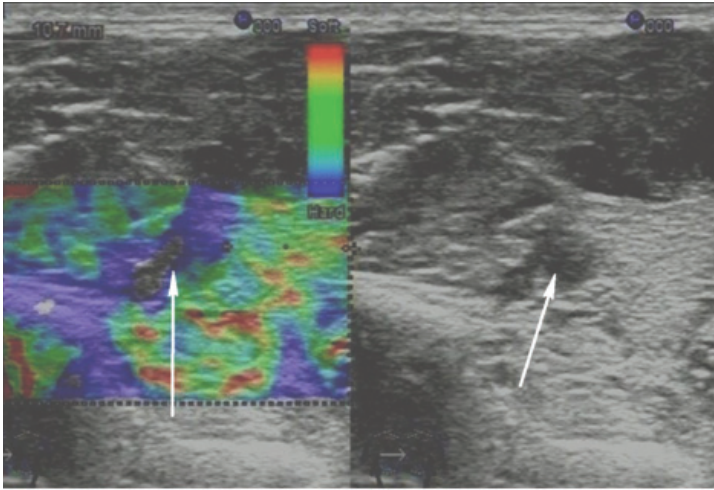


**Fig. 19.** Ultrasound visualization of the affected muscle in patient with hereditary myopathy. The case shows contracted muscle tissue (hypoechoic) vs background of increased echogenicity (bright tissue (*arrow*))

### ***Three dimensional model-guided needling***

Terajima et al. reported about 4-dimensional (4D) analysis of stomatognathic function that combines the 3-dimensional (3D) computed tomography of the cranium and mandible, dental surface imaging with a noncontact 3D laser scanner, and mandibular movement data recorded with a 6 degrees of freedom jaw-movement analyzer [44]. We apply the three-dimensional modeling based on ultrasound data segmentation and conjoining the models [41] with those created from different source data of visual information (CT, MRI, photogrammetry) in a single three-dimensional environment for planning intervention under the ultrasound guidance in real time. The three-dimensional modeling becomes a base of initiation for the model-guided interventions on difficult locations of trigger points (Fig. 20).

Using trigger point dry needling under US guidance the pain was eliminated, the efficient correction of the occlusion, which was previously impossible due to spastic phenomena in muscles, was performed.

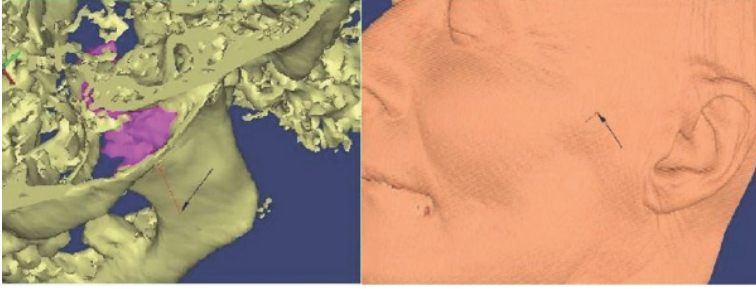


**Fig. 20.** Modeling of needle direction for medial pterygopalatine muscle puncture: left – on the muscle-bone model, right – projection on the skin fine needle inserted (*arrow*)

The correctly performed procedure can be relevant for prevention of posture disorders, pain in cranio-mandibular region and dysfunction of TMJ.

### ***Neurophysiology pain study. Electromyography***

Hubbard and Berkoff studies indicate that monopolar needle electromyograms (EMG) showed sustained spontaneous EMG activity in all TrPs, and was absent in non-TrPs. The authors hypothesize that TrPs are caused by sympathetically activated intrafusal contractions [45]. It was suggested by Gemmell [46], that there is a trend for muscles containing active trigger points to have less electrical activity than muscles containing latent trigger points. We obtained the preliminary results that direct needling EMG under US guidance that showed different spontaneous activity of trigger points (Fig. 21). A needle EMG study from nearby the trigger tissue remained electrically silent. We suppose this depends on the activity of the trigger point and the accuracy of needling to the trigger point. A combination of these approaches gives new opportunities to experimental and clinical studies.



**Fig. 21.** Spontaneous muscle activity in trigger point, needled with US guidance, while LTR effect is evoked

### *References*

1. Gerwin RD, Shannon S, Hong CZ, Hubbard D, Gevirtz R. Interrater reliability in myofascial trigger point examination. *Pain* 1997;69:65–73.
2. Simons DG, Travell JG, Simons LS. *Travell and Simons' myofascial pain and dysfunction; the trigger point manual*. 2 ed. Baltimore: Williams & Wilkins; 1999.
3. Bates T. Myofascial pain. Chapter 14.// In: *Ambulatory Pediatrics II*. – Philadelphia, edited by M. Green, R. G. Haggerty, W. B. Saunders, 1977. – P. 147–148.
4. Steindler A. The interpretation of sciatic radiation and the syndrome of low-back pain. *J Bone Joint Surg Am* 1940;22:28–34.
5. Simons DG. Muscle pain syndromes – part 1. *Am J Phys Med* 1975;54:289–311.
6. Travell JG, Rinzler SH. The myofascial genesis of pain. *Postgrad Med* 1952;11:452–434.
7. Travell J. Identification of myofascial trigger point syndromes: a case of atypical facial neuralgia. *Arch Phys Med Rehabil* 1981;62(3):100–106.
8. Travell J. Temporomandibular joint pain referred from muscles of the head and neck. *J Prosthet Dent* 1960;10:745–763.
9. Shah JP, Danoff JV, Desai MJ, et al. (2008). «Biochemicals associated with pain and inflammation are elevated in sites near to and remote from active myofascial trigger points». *Arch Phys Med Rehabil* 89 (1): 16–23.
10. Bablis Peter, Pollard Henry and Bonello Rod *Neuro Emotional Technique for the treatment of trigger point sensitivity in chronic neck pain sufferers: A controlled clinical trial* *Chiropractic & Osteopathy* 2008, 16:4 doi:10.1186/1746–1340–16–4

11. «Fibromyalgia: diagnosis and treatment». Bandolier (90). August 2001.
12. Brezinschek HP “Mechanisms of muscle pain: significance of trigger points and tender points” (2008 December). *Z Rheumatol* 67 (8): 653–4, 656–7.
13. Alvarez, D.J. and Rockwell, P.G. (2002, February, 15). “Trigger Points: Diagnosis and Management.” *American Family Physician*, 65/No. 4, Retrieved May 25, 2008
14. Fibromyalgia Tender Points Identified By The American College of Rheumatology in 1990. Retrieved May 25, 2008.
15. Ge HY, Nie H, Madeleine P, Danneskiold-Samsøe B, Graven-Nielsen T, Arendt-Nielsen L (2009–12–15). “Contribution of the local and referred pain from active myofascial trigger points in fibromyalgia syndrome”. *Pain* 147 (1–3): 233–40.
16. Brezinschek HP Mechanisms of muscle pain: significance of trigger points and tender points *Z Rheumatol* 67 (8): 653–4, 656–7.
17. Wang F, Audette J. Electrophysiological characteristics of the local twitch response with active myofascial pain of neck compared with a control group with latent trigger points. *Am J Phys Med Rehabil* 2000;79(2):203.
18. Cummings TM, White AR. Needling therapies in the management of myofascial trigger point pain: A systematic review. *Arch Phys Med Rehabil* 2001.
19. Button M. Muscular rheumatism: local injection treatment as a means to rapid restoration of function. *BMJ* 1940 Aug 10:183–5.
20. Howard R. The use of local anaesthesia in the relief of chronic pain. *Med J Aust* 1941 March 8:298–9.
21. Kelly M. The treatment of fibrositis and allied disorders by local anaesthesia. *Med J Aust* 1941 Mar 8:294–8.
22. Jan Dommerholt et al Trigger Point Dry Needling *The Journal of Manual & Manipulative Therapy* Vol. 14 No. 4 (2006), E 70 – E 87.
23. Baldry PE. *Acupuncture, Trigger Points and Musculoskeletal Pain*. Edinburgh, UK: Churchill Livingstone, 2005.
24. Lewit K: The needle effect in the relief of myofascial pain. *Pain* 6:83–90, 1979.
25. Gunn CC. *The Gunn Approach to the treatment of chronic pain*. Edinburgh: Churchill Livingstone; 1998.
26. Hameroff SR, Crago BR, Blitt CD, et al. Comparison of bupivacaine, etidocaine and saline for trigger point therapy. *Anesth Anal* 1981;60:752–5.
27. Hong C-Z. Lidocaine injection versus dry needling to myofascial trigger point: The importance of the local twitch response. *Am J Phys Med Rehabil* 1994;73:256–263.
28. Kamanli A, Kaya A, Ardicoglu O, Ozgocmen S, Zengin FO, Bayik Y. Comparison of lidocaine injection, botulinum toxin injection, and dry needling to trigger points in myofascial pain syndrome. *Rheumatol Int* 2005;25:604–611.
29. Yoon S-H, Rah UW, Sheen SS, Cho KH. Comparison of 3 needle sizes for trigger point injection in myofascial pain syndrome of upper- and middle-trapezius muscle: a randomized controlled trial. *Archives of Physical Medicine and Rehabilitation*, Volume 90, Issue 8, (August 2009) Pages 1332–1339.

30. Itoh K, Katsumi Y, Kitakoji H. Trigger point acupuncture treatment of chronic low back pain in elderly patients: A blinded RCT. *Acupunct Med* 2004;2(4):170–177.
31. Chen Q, Bensamoun S, Basford JR, Thompson JM, An KN Identification and quantification of myofascial taut bands with magnetic resonance elastography *Archives of Physical Medicine and Rehabilitation* 88 (12): 1658–61.
32. T. De Zordo, E. Mur, R. Bellmann-Weiler, M. Sailer-Hück, R. Chhem, G. Feuchtner, W. Jaschke, A. Klauser US guided injections in arthritis *European Journal of Radiology*, Volume 71, Issue 2, Pages 197–203.
33. Kane D, Greaney T, Shanahan M, et al.. The role of ultrasonography in the diagnosis and management of idiopathic plantar fasciitis. *Rheumatology* 2001;40:1002–8.
34. Kenneth P. Botwin et al Ultrasound-Guided Trigger Point Injections in the Cervicothoracic Musculature: A New and Unreported Technique *Pain Physician* 2008; 11:6:885–889.
35. Melzack R., Stillwell D. M., Fox E. I. Trigger points and acupuncture points for pains: correlation and implications. // *Pain*. – 1977. – N 3. – P. 3–23.
36. Melzack R. Relation of Myofascial Trigger points to Acupuncture and Mechanisms of pain // *Arch. phys. med. Rehabil.*, 1981. – Bd. 62. – P. 114–117.
37. Dorsher P. Trigger points and acupuncture points: Anatomic and clinical correlations. *Med Acupunct* 2006;17(3):21–25.
38. Dorsher PT «Myofascial referred-pain data provide physiologic evidence of acupuncture meridians». *J Pain* 10 (7): 723–31.
39. Bubnov RV: The use of trigger point dry needling under ultrasound guidance for the treatment of myofascial pain (technological innovation and literature review). *Lik Sprava* 2010, 5–6:56–64.
40. Bubnov RV. Evidence-based pain management: is the concept of integrative medicine applicable? *EPMA J.* 2012 Oct 22;3(1):13
41. Bubnov RV, Kyselova OG: Three-dimensional modeling for temporomandibular joint dysfunction diagnosis and craniomandibular pain syndromes management. *Acta Biomedical Engineering* 2011, 4: 235–242.
42. Bubnov RV: Ultrasonography for local muscle spasticity management. *Mov Disord* 2012, 27(Suppl 1):336.
43. Bubnov RV: Method of diagnosis of myopathy. 2011, Patent Ukraine 61,291, IPC A61B / 08, issued 07.11.2011 (Bull. N 13).
44. Kraus SL: *Temporomandibular Disorders*. New York: Churchill Livingstone; 1994.
45. Hubbard DR, Berkoff GM: Myofascial trigger points show spontaneous needle EMG activity. *Spine* 1993, 18:1803–1807. PubMed Abstract | Publisher Full Text
46. Gemmell H, Bagust J: Can surface electromyography differentiate muscle activity between upper trapezius muscles with active versus latent trigger points? A cross-sectional study. *Clinical Chiropractic* 2009, 12(2):67–73.

## **Chapter 8**

# **Damage to peripheral nerves in gunshot wounds**

Combat injuries of the spine, spinal cord, peripheral nerves are characterized by persistent disability and constitute about 5 % of neurotrauma. Damage to the peripheral nerves is 11 % in the structure of all injuries received during the hostilities, 15 % of cases are combined with fractures of the bones, 30 % – with injuries of the tendons and vessels of the extremities. During the anti-terrorist operation in the east of Ukraine, gunshot wounds of the spine and spinal cord were received by about 2 % of patients, in 35–37 % of cases, lesions of nerve trunks are combined with injuries of the vessels of the extremities [Ya.L. Zarutskiy, 2014; A. M. Serdyuk, V. I. Tsybalyuk, 2014].

Combat injuries of the spine, spinal cord, peripheral nerve damage include gunshot wounds, explosive lesions, non-fire injuries. By the nature of injury, they are divided into uncomplicated and complicated injuries, isolated wounds. Gunshot wounds are divided into bullet, fragmentation, wounds, arrowheads, balls. Isolate penetrating and non-penetrating wounds of the spine, along the wound channel – through, blind, tangential, paravertebral wounds. There are also injuries of the cervical, thoracic, lumbar, sacral parts of the spine. Combat injuries of peripheral nerves are divided into open and closed injuries. Open fire, cut, chipped, torn, burned wounds, closed ones occur as a type of concussion, bruising, compression, traction and compression-ischemic damage.

Ultrasound examination of the peripheral nervous system was first used to diagnose neural trunk diseases in the late 1990s. Electrophysiological methods of investigation (electromyography and neuromyography) are recognized as the “gold standard” for diagnosing the pathology of the peripheral nervous system, but ultrasound imaging after trauma of inflammatory manifestation of soft tissues allows verifying the anatomical changes of nerve trunks (rupture, scarring) [V. M. Schreiber et al.]. The method allows to reveal the character, localization and the cause of damage to the nerve trunk.

Ultrasound of peripheral nerves can be performed in a mobile hospital, gypsum mobilization of the wounded.

Sensors with a frequency of 7–17 MHz are used for ultrasonography of peripheral trunks, in some cases with a lower frequency of 3–5 MHz. When scanning peripheral nerves determine the anatomical integrity of nerve trunks, the clarity of contours, the structure, the state of surrounding tissues. In case of wounds, the wound channel, the state of the anatomical-topographical zones, the presence of surrounding tissues, foreign bodies (wounding shells, bullets, their skin, metal fragments) are assessed.

When gunshot wounds of the main vessels in most patients, there is a simultaneous damage to the arteries, veins, lymphatic vessels and peripheral nerves (Fig. 1–16).

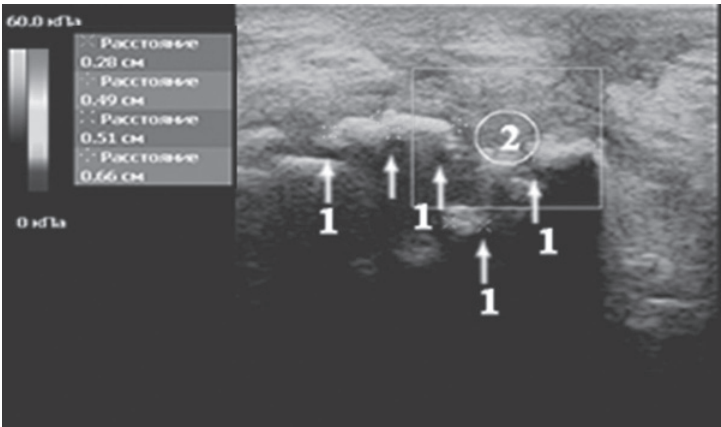


**Fig. 1.** Gunshot and fragmentation wound of the ankle joint. Transverse scanning at the level of the medial malleolus: 1-bone fragments; 2- “dead zone” of visualization of the neurovascular bundle of the medial surface of the ankle joint. Mode of sonoelastography

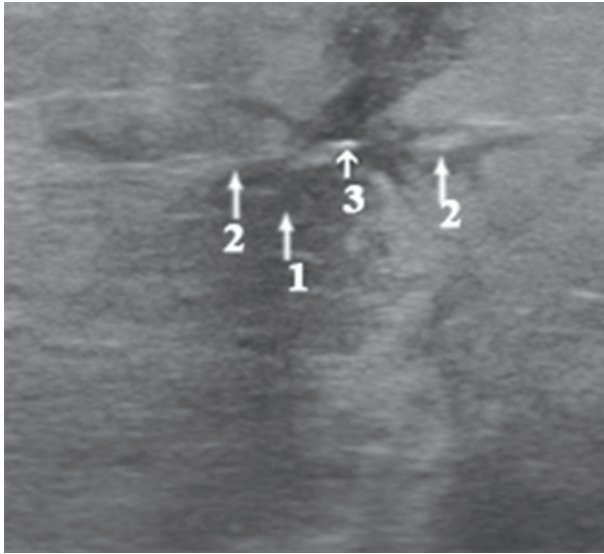


**Fig. 2.** Mino-explosive wound of the lower limb: 1-wound channel; 2-cicatrical degeneration of the peroneal nerve; 3-fragment

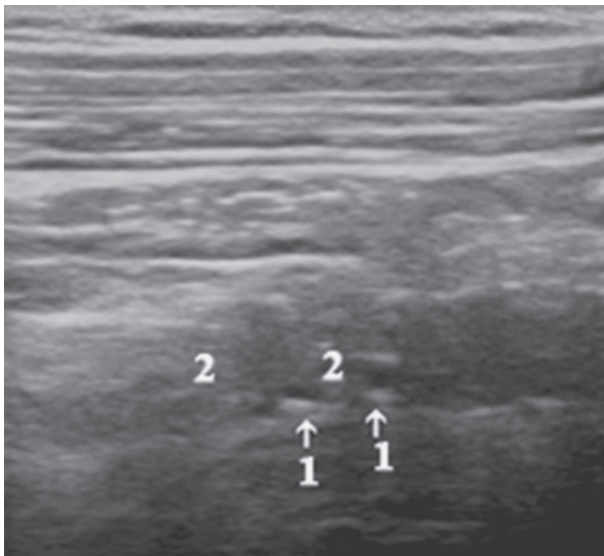


**Fig. 3.** Fragment wound of the thigh: 1 fragments; 2- arteriotrombosis of the superficial femoral artery

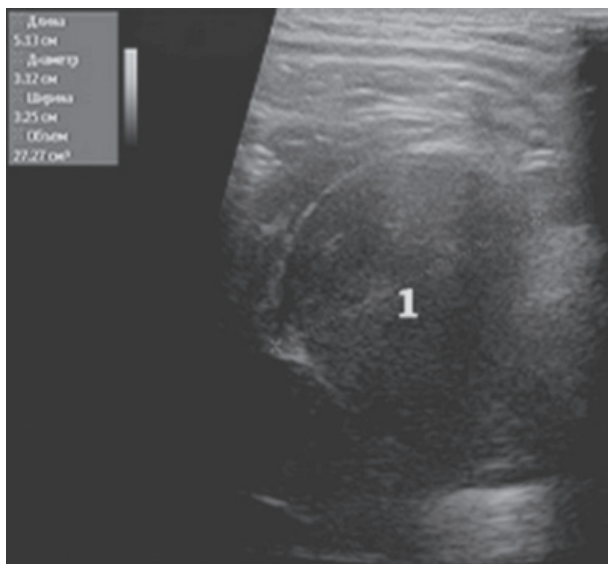


**Fig. 4.** Mine-explosive wound of the upper limb. Post-traumatic hematoma of the axillary region (1)

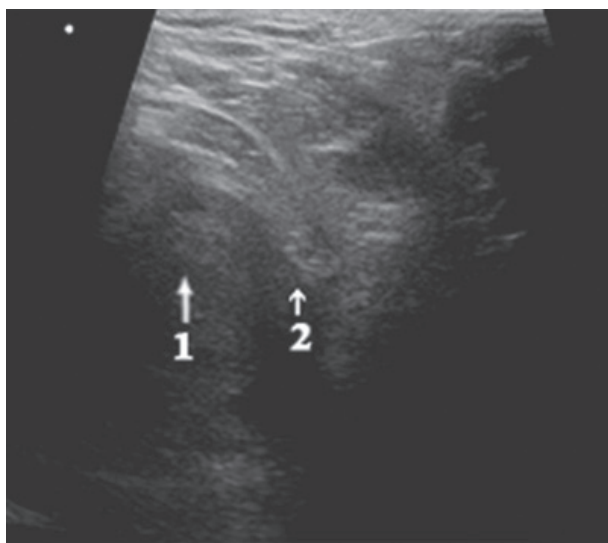


**Fig. 5.** Mine-explosive wound of the upper limb. Transverse scanning of the axillary fossa: 1-posttraumatic hematoma; 2-damage of the brachial plexus

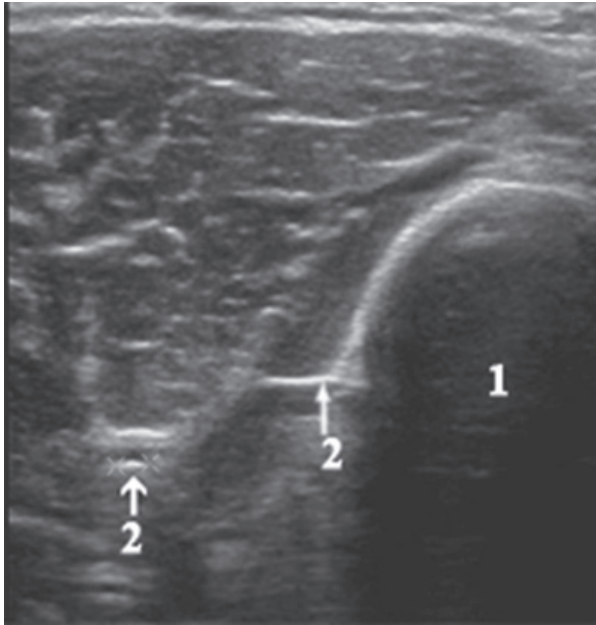


**Fig. 6.** Shoulder injury: 1- humerus head; 2-splinters

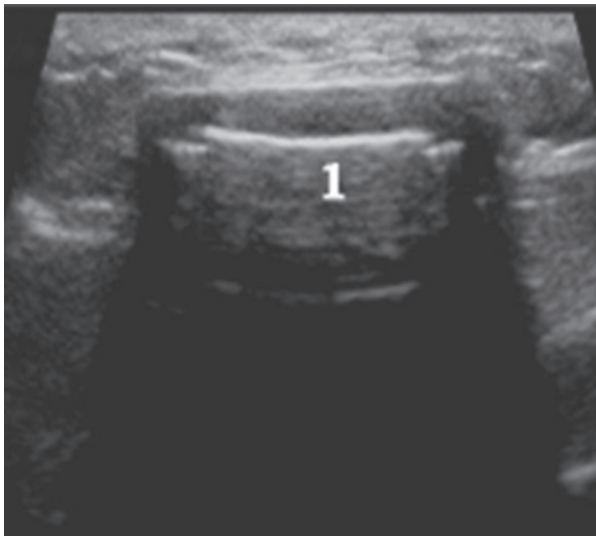


**Fig. 7.** Gunshot wound to the right upper limb. The apparatus by Neissetri (1)

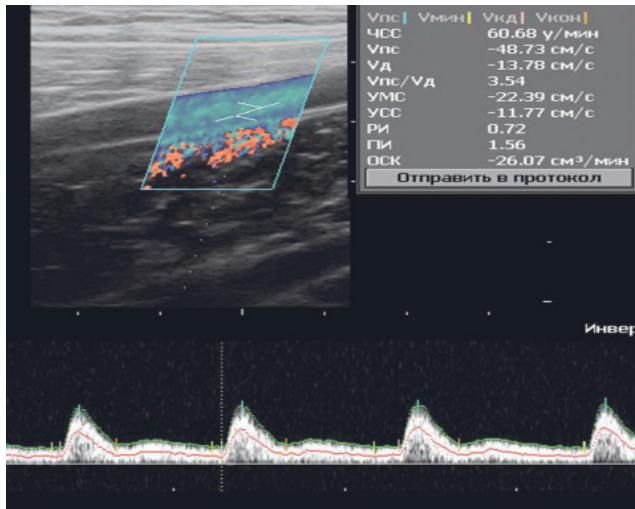


**Fig. 8.** Fragment wound of the upper limb. Infringement of a blood flow of the right humeral artery. Triplex mode

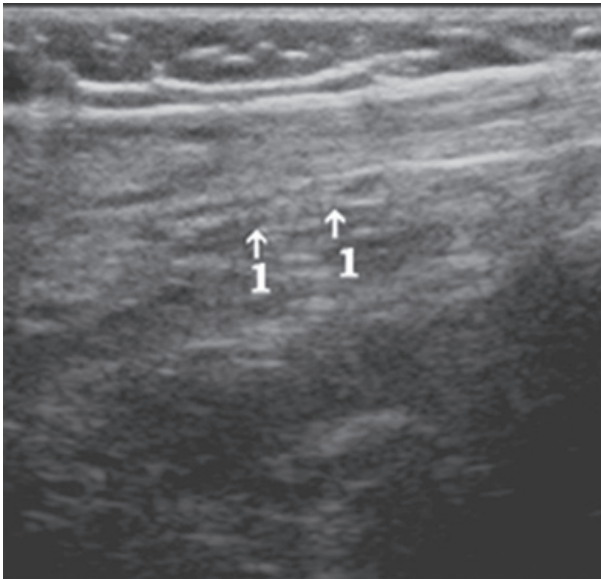


**Fig. 9.** Fragment of a limb wound. Longitudinal scan at the level of the middle third of the shin. Damage to the nerve (violation of its integrity, ehostruktur)

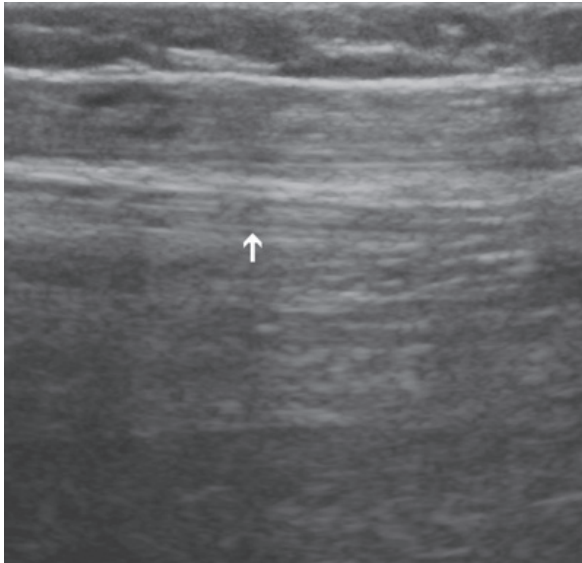


**Fig. 10.** The nerve. Longitudinal scanning of the contralateral middle third of the lower leg of a healthy limb

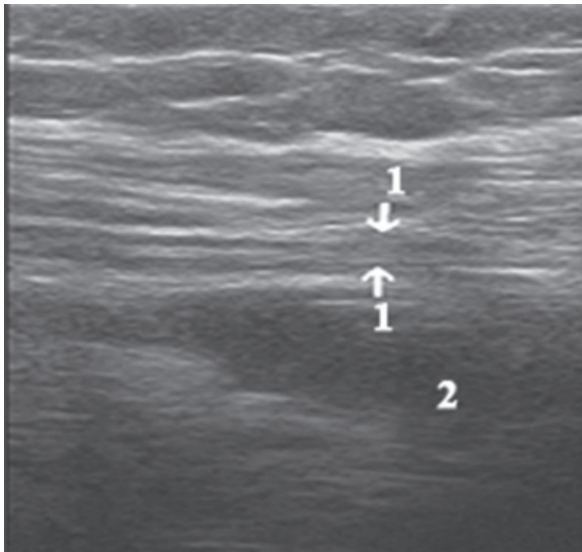


**Fig. 11.** Injury of the posterior surface of the left thigh. Longitudinal scanning of the hamstrings: 1-partial traumatic injury of the sciatic nerve; 2-wound channel

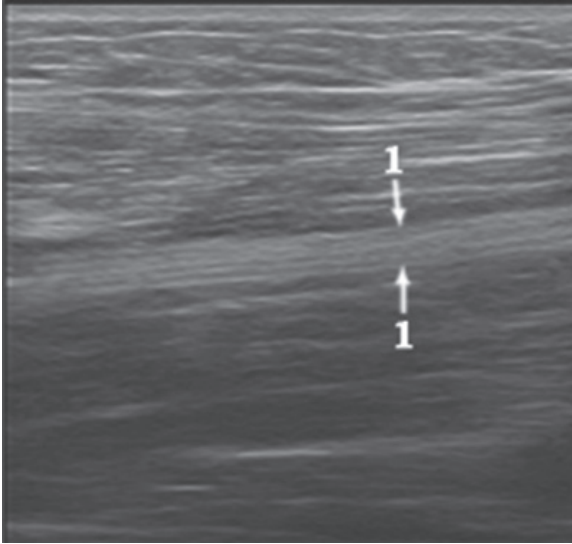


**Fig. 12.** The sciatic nerve. Longitudinal scan of the hamstring of a healthy limb. The unchanged sciatic nerve (1)

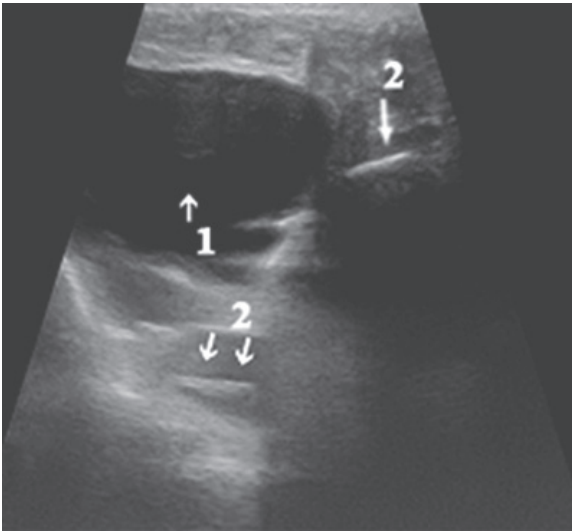


**Fig. 13.** Firing fragmentation wound of the lumbosacral spine L5-S1: 1-posttraumatic hernia; 2-metal fragments of the paravertebral region. Lateral scan of the lumbar spine, back area

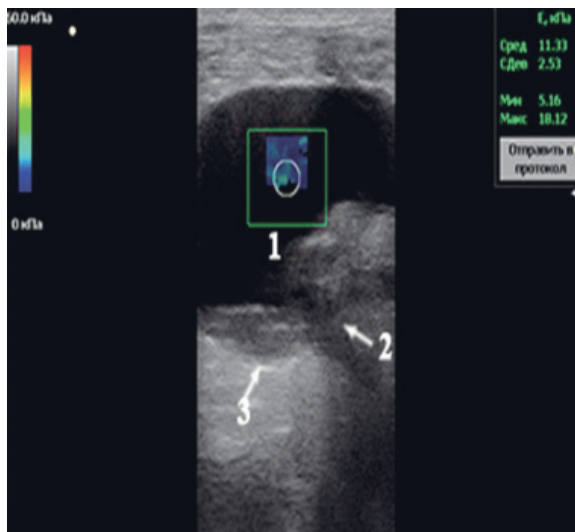


**Fig. 14.** Sonoelastography of a hernia. The blue mapping of posttraumatic hernia corresponds to a liquid homogeneous content (cerebrospinal fluid). Co-orthotactic scanning: 1-posttraumatic hernia; 2-arms of the vertebra; 3-bone fragments



**Fig. 15.** Blind firing fragmentation wound of the middle third of the right tibia: 1-wound canal; 2- swelling of soft tissues

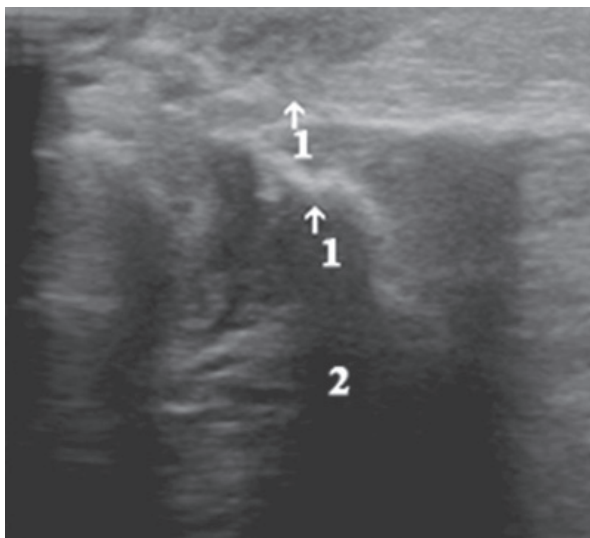


**Fig. 16.** Left hip compartment syndrome. Revision of the neurovascular bundle of the thigh: 1-cicatrical changes of the soft tissues of the inner surface of the thigh; 2-wound channel

The complexity of the study in peripheral nerve trunk injuries consisted in the precise diagnosis of the site of localization and the type of pathological process. Special difficulties in the diagnosis of peripheral nerve damage are caused by closed nerve injuries that occur with dislocations, bone fractures, posttraumatic bruises, compression, which can be accompanied by nerve damage leading to partial or total loss of function. As a result of gunshot wounds, mine explosive and explosive trauma under the action of wounding shells and their derivatives, necrosis zones are formed with demyelination and fragmentation of myelin fibers. When gunshot wounds to the extremities, the anatomical continuity of the peripheral nerves is disturbed.

To diagnose and clarify the severity of peripheral nerve damage, clinical examination and electrophysiological methods of investigation are used in 97 % of cases. However, the reliability of diagnosis of this pathology due to the complexity of the clinical picture is low.

Diagnostic difficulties in traumas of nerves and plexuses consist in the features of their anatomical location and the uniformity of clinical symptoms with various types of lesions.

The method of *magnetic resonance imaging* is used only in some diagnostically complex cases of lesions of the brachial and lumbosacral plexus, sciatic nerve. MRI is highly informative compared to other methods, as it directly visualizes spinal roots, traumatic meningocele, resulting from detachment of roots from the spinal cord of ionizing radiation and the possibility of conducting multiple studies.

**Advantages of ultrasound** over other methods of visualization are: ease of execution and interpretation of data; The level of differentiation of the nerve trunk and its fibrous structure is the highest in comparison with all existing methods of visualization; The absence of ionizing radiation and the possibility of conducting multiple studies.

**The limitations of the ultrasound method are due to several factors:**

- Impossibility of visualization of nerve trunks in the places of passage under the bone structures (subclavian department of the brachial plexus);
- complication of visualization of peripheral nerves with posttraumatic changes in the anatomical-topographical zone, peculiarities of the postoperative wound period;
- a decrease in the quality of visualization with a deep disposition of the nerve trunk after revision of the neurovascular bundles.

# Chapter 9

## Regional anesthesia under ultrasound guidance

### *Blocks of the lower limb*

For regional anesthesia in operations on the lower limbs often use spinal and epidural anesthesia. However, the blocks of somatic branches of the lumbar plexus and sciatic nerve provide adequate anesthesia for surgery on lower extremities. Nerve blocks of the lower limb include mostly sciatic and femoral nerve blocks, and also small branches.

Femoral nerve block is performed as part of regional anesthesia for knee joint and to provide postoperative analgesia.

### *The sciatic nerve block*

The sciatic nerve should be blocked in all operations on the lower extremities. If surgery on the lower limb does not require use of pneumatic tourniquet and goes outside the innervation of the femoral nerve, the sciatic nerve block provides complete anesthesia. The block of the sciatic nerve can be done at the level of the hip joint (proximal block), at the lower third of the thigh (distal block) and in popliteal fossa.

Sciatic nerve – the largest nerve of the human body is formed from the sacral plexus segments L4–S2, where elements of the tibial nerve is formed from the L4–S3 with interlacing fibers sacral and lumbar plexus. Sciatic nerve is located in the retroperitoneal space pelvic obtained from the pelvic cavity through the large sciatic hole that formed incisura major ischium bone and ligamentum sacro-spinous. The nerve passes below the piriform muscle through subpiriformis space large sciatic hole. Here it is bordered by the pudendal nerve and the lower gluteal vessels surrounded by a corresponding amount of connective tissue and fat. It consists of two large nerves with a common perineural sheath: the lateral is the common peroneal and medial – tibial nerve. It is bordered to the pudendal nerve and the inferior gluteal vessels, surrounded by a corresponding amount of connective tissue and fat.

Sciatic nerve can be qualitatively visualized by ultrasound of the gluteal region to the popliteal fossa. The probe is installed at the gluteal fold is installed transversely to the sciatic nerve location. The sciatic nerve appears on US in the proximal femur laterally to the biceps femoris tendon at 2–3 cm laterally to the ischial tuberosity. The diameter of the sciatic nerve – about 5–9 mm. In longitudinal scanning nerve fibers are surrounded by hyperechoic sheath in the transverse cut nerve is oval in shape (Fig. 1). The sciatic nerve and the proximal portion of the tendon of the biceps femoris, may be similar to the nerve on US. Scanning of intrapelvic segment of sciatic nerve periform for assessment of the lumbar and sacral plexus. However, visualization of the sciatic nerve can be complicated for several reasons. A large amount of muscle and adipose tissue around the nerve can degrade ultrasound visualization. Convex probe with a relatively lower frequency ultrasound (5–8 MHz) can sometimes provide a better picture, particularly for through the sciatic (transgluteal) and anterior approaches. Anisotropic display of sciatic nerve is a common cause of its poor visibility.

Block of the sciatic nerve can be performed using a number of methods and approaches. In general, the nerve can be locked in any place on your way with sufficient ultrasound imaging. There are reports of sacral plexus visualization and execution of the block at the formation of the sciatic nerve [3–5].

A wide range of operations on the lower extremity as knee, vessels surgery, amputation, etc., are indications for nerve block, which can be performed in the patient lying flat on his back or on the opposite side. Distal accesses to the sciatic nerve can be used in surgical operations on the ankle and foot. Distal sciatic nerve block can be achieved by applying lateral approach moving the needle in *in plane* scan, or (rear) in *out of plane* scan. It is recommended to begin to implement the distal access sciatic nerve block methodology with the patient lying on his abdomen if possible. In this position the better visualization of the sciatic nerve and easier needle advancement are achieved.

**The femoral nerve block.** The femoral nerve first was studied by ultrasonography in 1991 [6]. Infringuinal part of the femoral nerve is visualized directly laterally from the femoral vessels and the medial head of the quadriceps muscle and ventromedial distal m. iliopsoas [7]. On US femoral nerve has a typical cellular pattern by hypoechoic neural beams and increased echogenicity stroma (epineural and perineural membranes). In distal hip femoral nerve demarcation is unclear, since it is surrounded by tissues of different echogenic properties [8]. Today, femoral nerve block is commonly used in cross-access

scanning (out of plane). This is because the needle is parallel to the long axis of the femoral nerve and a shorter distance from the surface of the skin and easier catheter installation. Some researchers use in plane access with the introduction of a needle in lateromedial direction [9]. Lumbar fascia block under ultrasound guidance is highly effective manipulation [10] and may be a useful alternative to femoral nerve block while it is poorly visualized. However, this method requires a larger volume of local anesthetic than femoral nerve block.

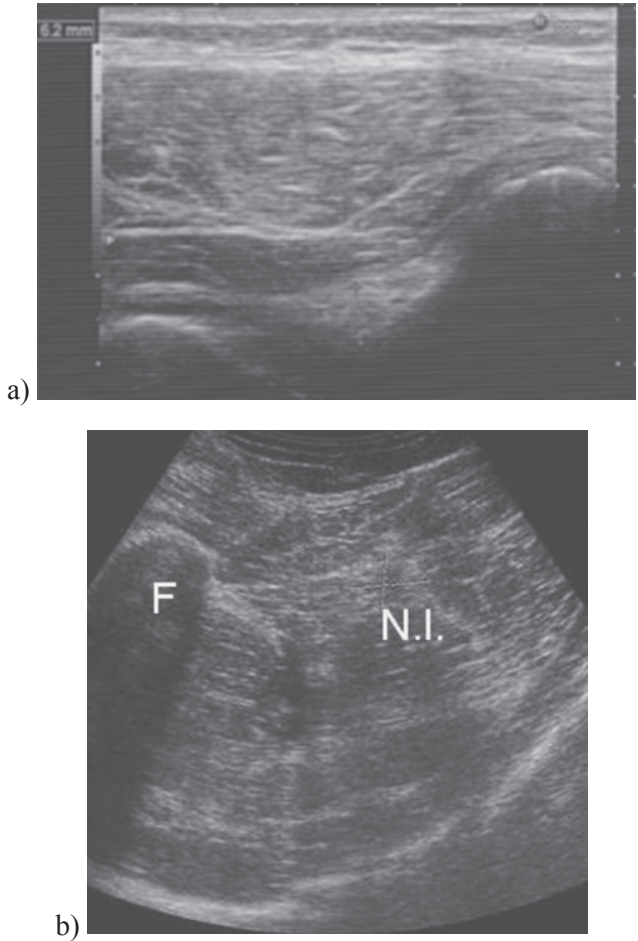


**Fig. 1.** Visualization of the sciatic nerve. a) – visualization of the sciatic nerve in the proximal segment on the piriformis level. b) – sciatic nerve at the middle of the hip. Convex probe application.

### *Visualization of the femoral nerve in the groin*

The femoral nerve is better visualized in groin region, ventro-medially to m. iliopsoas and laterally to the femoral artery, close to the thin fibrous ilio-pubic ligament (arc.ileopectineus). To visualize the nerve, the probe is mounted conventionally perpendicular to inguinal ligament, then tilted by 30–40° inside, depending on the constitution, according to the anatomical course of the nerve, to get a regular sonographic scan of its cross section. Desirable is to verify the femoral artery and vein with color Doppler mapping and spectroscopy for the differentiation of venous and arterial vessels, to assess blood flow to the extremities. To search for nerve ultrasound probe runs systematically in groin and upper part of the front of the thigh in the transverse and longitudinal planes. Motion of probe must be performed to search nerve according to its type of nerve anatomical position of the nerve and syntopic location with surrounding structures. The optimum cross-scan echogram of the femoral nerve is obtained directly lateral to the femoral vessels and the medial quadriceps and ventromedial distal part of m. iliopsoas (Fig. 2).

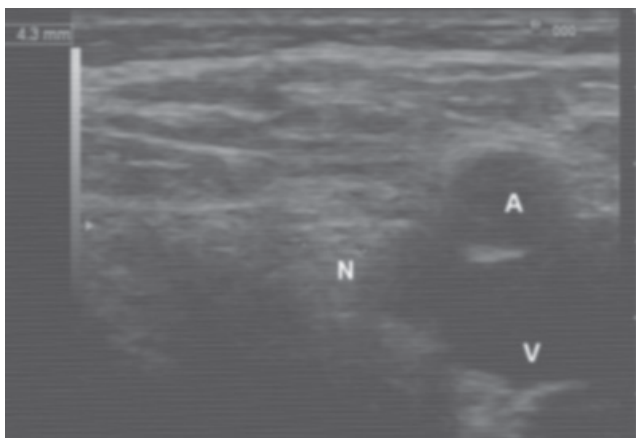


**Fig. 2.** Visualization of the femoral nerve in the groin area for regional anesthesia for ultrasound control. Observed an atypical vascular interposition – femoral vein lies dorsally to artery. Nerve laterally to artery – a typical arrangement

### *Individualized approach*

Different data regarding the level of bifurcation of the sciatic nerve is found in literature [11,12]. Thus, the level of bifurcation within the gluteal area according to Gьvenzer et al. [11] data is 48 %, and according Ugrenovic et al. [12] – only 4 %. Our research indicates that most nerve bifurcations are found in the middle third ( $74.0 \pm 7.9$  %). However frequent cases of bifurcation of the proximal segment ( $13 \pm 6$  %). Instead bifurcation in the «typical» place – the distal third occurs in  $13 \pm 6$  % of cases, the presence of common fascial beam level – only  $52 \pm 9$  % of cases. Atypical location of the sciatic nerve – partial occurrence nerve between piriformis muscle bundles – was found only in  $11.4 \pm 4.1$  % of cases. These differences should be considered when predicting nerve block in the proximal segment. According to our data, the presence of common fascial beam sciatic nerve at the level of the distal femur occurs only in  $52 \pm 9$  % in the middle third – in  $81 \pm 7$  % at the top – 100 %. Puncture below the split beams in nerves requires additional needle manipulation to enter drug separately under each of the «perineural» spaces. Therefore, the units of the proximal segment should choose the place closest to the bifurcation of the common fascial beam. It should get visual confirmation of anesthetic spread around both branches of the sciatic nerve, to carry out the transposition of the needle in the other interfascial, perineural space. When the femoral nerve block should consider passing envelope artery anatomy femoral and intearfscial spaces. As hip triangle passes lateral femoral artery envelope, which often lies between the branches of the femoral nerve in the projection of the puncture site for femoral block (Fig. 3). Therefore, the block should performed above lateral femoral artery envelope, ie at the level of the inguinal crease or slightly above, and clearly identify the artery during puncture. Puncture should be performed optimally in the projection of the lumbar fascia, the need to puncture a broad and lumbar fascia and fascial own bundle block. The specific features of form and branching nerve puncture should be performed to identify the location of the main trunk.

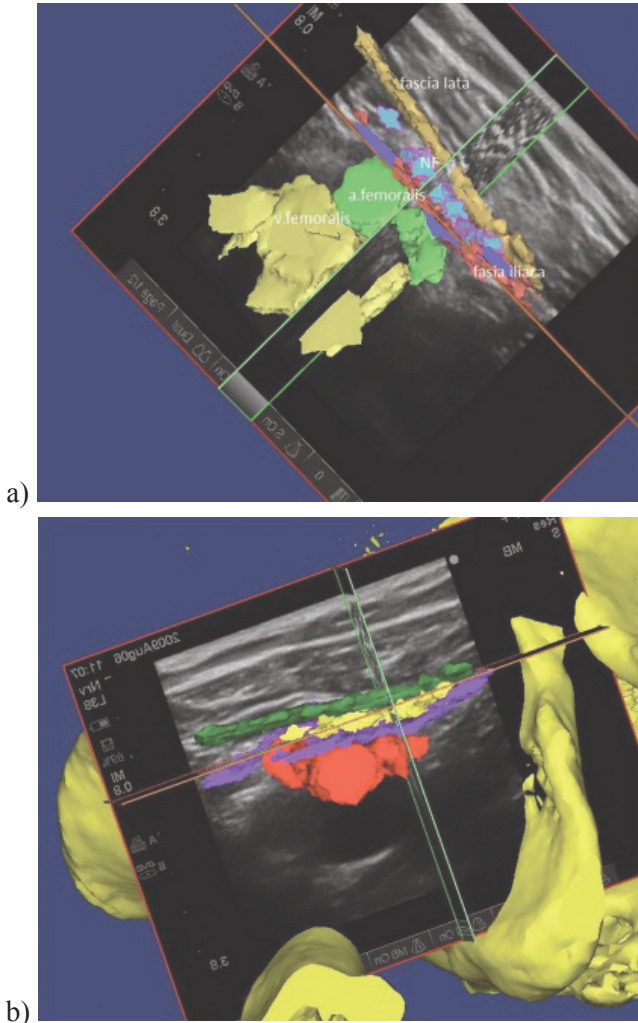


**Fig. 3 a), b).** Visualizing the location of the nerve, blood vessels and fascial sheets on the integrated model based on ultrasound and CT data

**Saphenous nerve blocks**, lateral femoral cutaneous nerve, posterior femoral cutaneous, gastrocnemius (n.suralis), superficial peroneal nerve are effective methods of anesthesia for various surgeries. These blocks mainly have almost no complications and may be good complement of the main blocks of the lower extremities.

**Selective blocks**, such popliteal nerve still are not studied, preliminary clinical experience with the blocks is described. Execution using only anatomical landmarks, without ultrasound imaging can not be effective (Fig. 4).

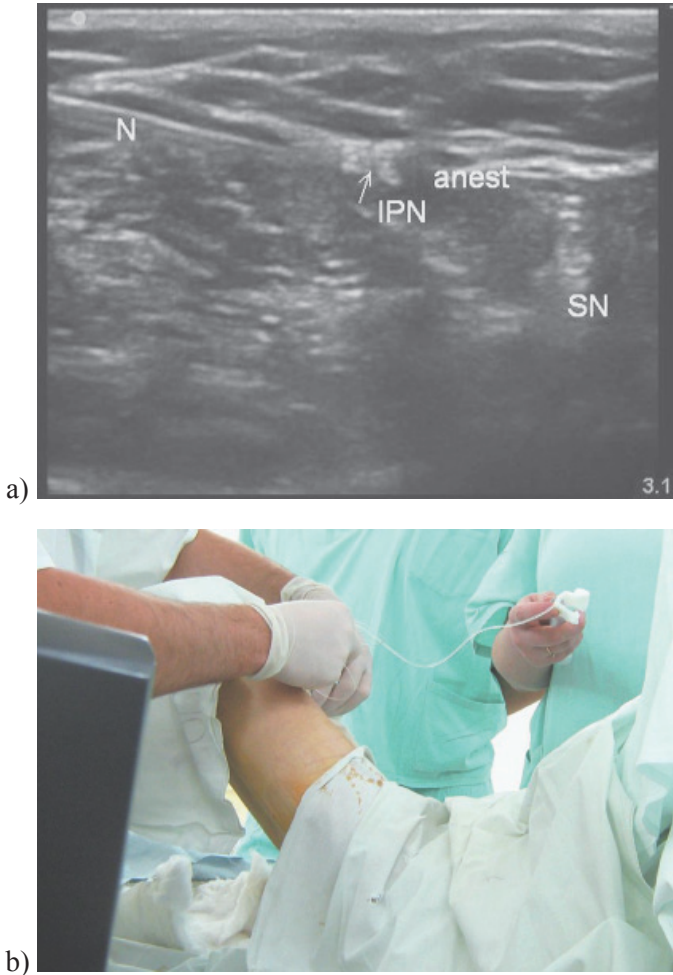


**Fig. 4.** Saphenous nerve block under ultrasound guidance: a) – IPN – popliteal nerve; SN – saphenous nerve; – N – needle; Anest – anesthetic solution. b) – General view. Block in the distal thigh with «in plane» access (needle is parallel to the probe)

## References

1. Graif M., Seton A., Nerubai J. [et al.]. Sciatic Nerve: Sonographic Evaluation and Anatomic-Pathologic Considerations [Text] // Radiology. – 1991. –181. – P. 405–408.
2. Silvestri E., Martinoli C., Derchi L. E. [et al.] Echotexture of peripheral nerves: tendons [Text] / Radiology. – 1995. – Vol. 197. – P. 291–296.].
3. Гьвензер М., Iyem C., Akyer P. [et al.]. Variations in the high division of the sciatic nerve and relationship between the sciatic nerve and the piriformis [Text] // Turk. Neurosurg. – 2009. – 19. – P. 139–144.
4. Bruhn J., Van Geffen G. J., Gielen M. J. [et al.]. Visualization of the course of the sciatic nerve in adult volunteers by ultrasonography / Bruhn J., Van Geffen G. J., Gielen M. J. et al. // Acta Anaesth. Scand. – 2008. – 52. – P. 1298–1302.
5. Chan V. W., Nova H., Abbas S. [et al.]. Ultrasound examination and localization of the sciatic nerve: a volunteer study [Text] // Anesthesiology. – 2006. –104. – P. 309–314.
6. Sener RN, Alper H, Ozturk L, Ozer H, Falakali S. Retroperitoneal part of the femoral nerve. Normal ultrasound features. Neuroradiology. 1991;33(2):159–61.
7. Vloka J., Hadzic A., Drobnik L. [et al.] Anatomical landmarks for femoral nerve block: a comparison of four needle insertion sites [Text] / Anesth. Analg. – 1999. – Vol. 89. – P. 1467–1472.
8. Mehmood S, Coleman M, Egan M. [et al.] Study of the anatomical position of the femoral nerve by magnetic resonance imaging in patients with fractured neck of femur: relevance to femoral nerve block [Text] / J. Clin. Anesth. –2010. – Vol. 22. – N 2 (Mar). – P. 122–125.
9. Niazi A. U, Prasad A., Ramlogan R. [et al.] Methods to ease placement of stimulating catheters during in-plane ultrasound-guided femoral nerve block [Text] / Reg. Anesth. Pain Med. – 2009. – Vol. 34. – P. 380–381.
10. Dolan J., Williams A., Murney E. [et al.]. Ultrasound guided fascia iliaca block: a comparison with the loss of resistance technique [Text] // Reg. Anesth. Pain Med. – 2008. – 33. – P. 526–531.
11. Demiryurek D., Bayramoglu A., Erbil M. [et al.]. Bilateral divided piriformis muscle together with the high division of the sciatic nerve [Text] // Gazi Med. J. – 2002. – 13. – P. 41–44.
12. Frerk C. M. Palsy after femoral nerve block [Text] // Anaesthesia. – 1988. –43. – P. 167–168.
13. Ugrenović S., Jovanović.I, Krstić V. [et al.] The level of the sciatic nerve division and its relations to the piriform muscle [Text] / Vojnosanit. Pregl. –2005. Vol. 62. P. 45–49. (Serbian).
14. Bubnov RV, Abdullaiev RIa. [Main sonographic parameters of regional anesthesia conduction in the lower extremities under ultrasound guidance]. Lik Sprava. 2010 Oct-Dec;(7–8):97–107. Ukrainian.

## The brachial plexus

**The brachial plexus** is formed by the union of the anterior branches of the four lower cervical and first thoracic nerves. It extends from the lateral part of the cervical spine to the axilla. The upper trunk is classically formed by the joining of roots C5 and C6. The middle trunk is the continuation of root C7. The lower trunk is formed by the joining of roots C8 and T1. The three trunks are formed at the lateral border of the interscalene triangle. Each trunk divides into an anterior and a posterior division. The lateral cord is formed by the anterior divisions of the upper and middle trunks and the medial cord by the anterior division of the lower trunk. The posterior cord is formed by the posterior divisions of all the trunks. Just lateral to the pectoralis minor muscle, the cords divide into the five terminal branches (median nerve, ulnar nerve, musculocutaneous nerve, axillary nerve, and radial nerve).

Visualization of the brachial plexus by means of sonography has been reported [1, 2].

Demondion et al. suggest sonographic mapping of the brachial plexus [3], and distinguish following part of plexus: 1) the extraforaminal part of nerve roots and the deep cervical artery; 2) the nerve roots at the interscalene triangle; 3) the trunks of the brachial plexus; 4, the cords of the brachial plexus by a supraclavicular approach; 5) the cords of the brachial plexus by an infraclavicular approach; and 6) the cords of the brachial plexus at the retropectoralis minor space.

Interscalene view is presented on Fig. 5., 3D reconstruction – on Fig. 6.

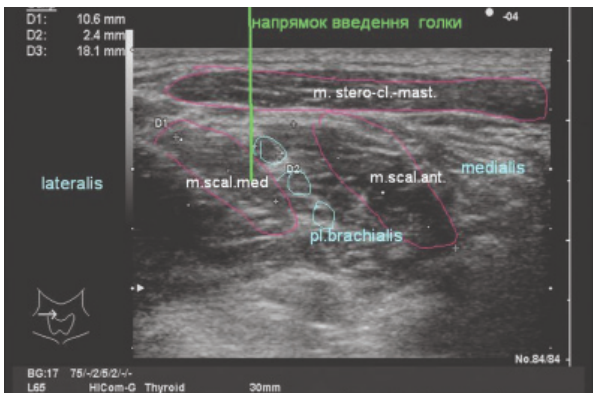


**Fig. 5.** Ultrasound anatomy of brachial plexus block performed in interscalene space. In transverse scan between the anterior and middle scalene muscles hypoechoic bundles of plexus are visualized.

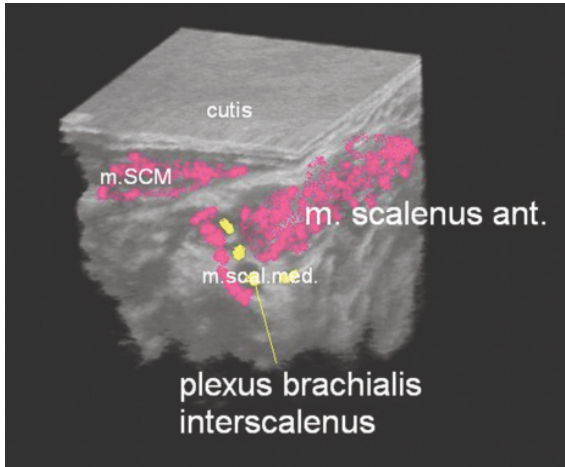


**Fig. 6.** 3D-reconstruction of the brachial plexus area

***The brachial plexus block of the under sonography guidance***

The brachial plexus block is used for anesthesia during surgical interventions on the upper extremity, followed by postoperative programmable pain management. Regional anesthesia is sufficient to perform a wide range of surgical procedures on the upper extremity and the next programmed postoperative pain. Benefits ultrasonographic control for brachial plexus block are in precision of puncture free from external anatomical landmarks, the ability to perform puncture at different facets of the neck and anatomic variants of the brachial plexus structure. Use of extra-long linear probes can effectively evaluate punctured structure with facets of the neck.

The brachial plexus block can be performed by supraclavicular [4,5], subclavian [6, 7] and axillar accesses [4]. It is believed that the subclavian access is not gained popularity because of the lack of clear anatomical landmarks and because of the relatively greater pain treatments. Most researchers currently preferred supraclavicular access [8].

Reported two possible pathways of anesthetic: the first in which the anesthetic dislocate plexus bundles to the periphery, while another – evenly distributed between the beams [9].

We use all methods depending on the clinical problem and the ability to access.

There are two possible pathways of anesthetic: the first, in which the anesthetic depresses brachial plexus to the periphery, in the other – is evenly distributed between the beams. We believe that a necessary condition for quality anesthesia infiltration anesthesia to her own case of facial nerve plexus. When this experience is recorded on the expected «needlepoint».

Appropriate combination of transverse and longitudinal scans to visualize the structure of a complete plexus and localization needles and catheters, although the insertion of the needle used transverse scanning, the verification provisions of the catheter supplemented longitudinal. Ultrasound control for catheterization of the brachial plexus block anesthesia in combination with nerve stimulation can reliably localize the site of injection of anesthetic, to minimize the possibility of damage to adjacent structures (the phrenic nerve, the jugular vein, carotid artery, esophagus) and the possibility of needlestick injuries beams of the plexus, reduces the number of attempts puncture and the number of complications, shortens the procedure.

**Methodics.** Operator's position is behind of the head of patient, manipulation is performed in aseptic conditions of operating room. The patient's head is turned in the opposite direction. External anatomic plexus landmarks are: annular cartilage, the outer edge of the sterno-cleido-mastoid muscle, interscalenal recess. Under ultrasound control with supraclavicular access along the course plexus bundles needle is introduced to plexus, injected anesthetic should infiltrate around the bundles, then special catheter is installed. The "free hand" method and combined transverse longitudinal scan plexus during visual assistance to people. The use of ultrasound monitoring catheterization of neural structures for regional anesthesia in real time provides visualization of the target nerve bundle, surrounding anatomical structures before and during puncture. With ultrasonography the needle moves, the path of anesthetics propagation, its distribution in the plexus projection, and estimated the location of catheter are precisely visualized. The use of neurostimulator reliably establish the accuracy of anesthesia and to determine the possibility of early surgical intervention (Fig. 7).

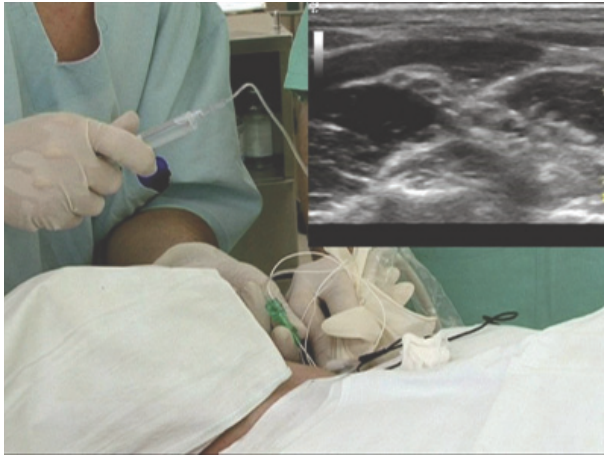


**Fig. 7.** Manipulations of regional anesthesia – brachial plexus block under ultrasound control. Overview

The radial nerve should be searched on posterior surface of the shoulder to the point of attachment of the distal fibers of the deltoid muscle. Inner forearm rotation helps for better visualizing the deltoid muscle contours. The nerve is fixed to the humerus with the fibrous strand. The normal width of the radial nerve is on average 4.6 mm anteroposterior size – 2.3 mm (Fig. 8).

The sonogram scans of nerves of the upper limb are presented in Fig. 9–13.



**Fig. 8.** The skin projection of the radial nerve

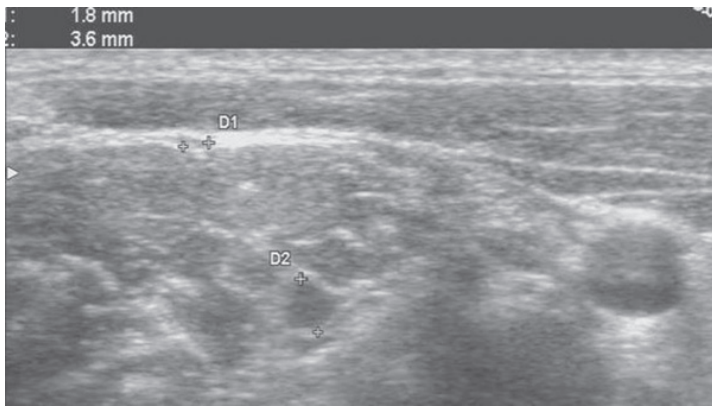


**Fig. 9.** Diaphragmal nerve on the anterior surface of the anterior scalene muscle

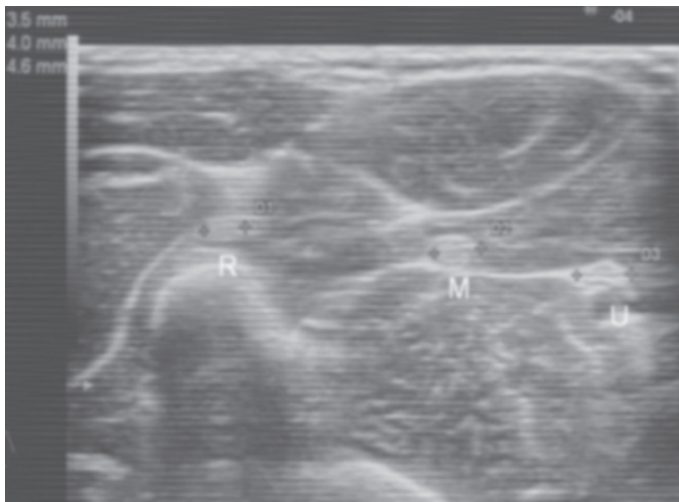


**Fig. 10.** A cross section of the median nerve in the middle third of the forearm



**Fig. 11.** Longitudinal section of the median nerve in the middle third of the forearm.

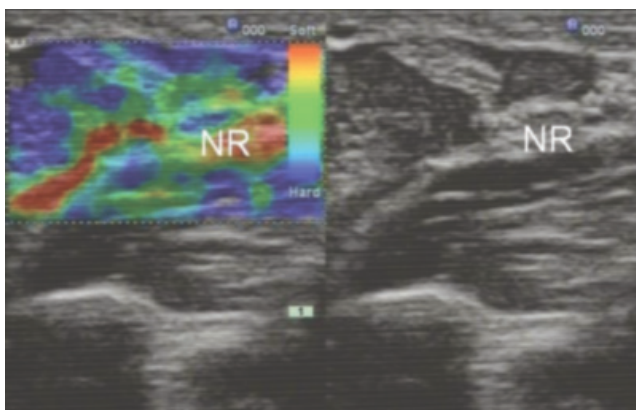


**Fig. 12.** Sonoelastography of radial nerve (NR) – denser than the surrounding tissue

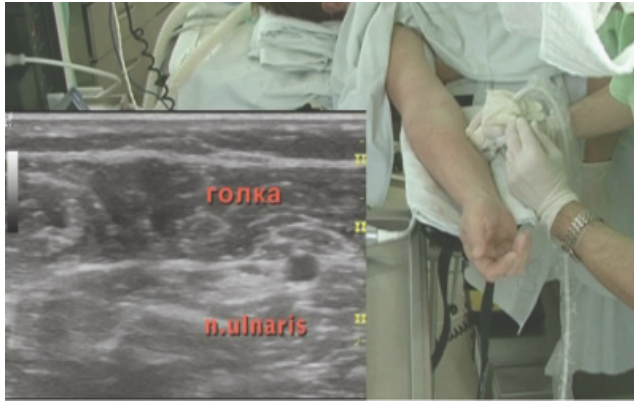


**Fig. 13.** The block of the ulnar nerve under ultrasound

### *References*

1. Gray H. Cervical nerves and brachial plexus. In: Gray's Anatomy Descriptive and Surgical, 10th ed. London: Longman, Green, and Co.;1883:533–541
2. Yang WT, Chui PT, Metreweli C. Anatomy of the normal brachial plexus revealed by sonography and the role of sonographic guidance in anesthesia of the brachial plexus. *AJR Am J Roentgenol* 1998;171:1631–1636Kapral S, Krafft P, Eibenberger K, et al. Ultrasound-guided supraclavicular approach for regional anesthesia of the brachial plexus. *Anesth Analg* 1994;78:507–13.
3. Demondion X, Herbinet P, Boutry N, Fontaine C, Francke JP, Cotten A. Sonographic Mapping of the Normal Brachial Plexus *Am. J. Neuroradiol.* August 1, 2003 24:1303–1309.
4. Williams SR, Chouinard P, Arcand G, et al. Ultrasound guidance speeds execution and improves the quality of supraclavicular block. *Anesth Analg* 2003;97:1518–23.
5. Ootaki C, Hayashi H, Amano M. Ultrasound-guided infraclavicular brachial plexus block: An alternative technique to anatomical landmark-guided approaches. *Reg Anesth Pain Med* 2000;25:600–4.
6. Sandhu NS, Capan LM. Ultrasound-guided infraclavicular brachial plexus block. *Br J Anaesth* 2002;89:254–9.
7. Arcand eT al. Ultrasound-Guided Infraclavicular Versus Supraclavicular Block *Anesth Analg* 2005;101:886–90.
8. Chan et al. Ultrasound-Guided Supraclavicular Brachial Plexus Block *Anesth Analg* 2003;97:1514–7.
9. Spencer S. Liu, and Francis V. Salinas Continuous Plexus and Peripheral Nerve Blocks for Postoperative Analgesia *Anesth Analg* 2003;96:263–72.

# Chapter 10

## Novel approaches of physical therapy and pain management

*Lev Kalika*  
*NY Dynamic Neuromuscular Rehabilitation &*  
*Physical Therapy Clinic. <https://nydnrehab.com/>*

### ***Biofeedback Motor Control Training and Analysis***

#### **Biomechanical Analysis With Real Time Force Plate Technology**

Biomechanical analysis can register the forces involved with athletic movement. When these forces exceed normal there is excessive stress to joints, muscles and ligaments. The excessive forces are always the result of poor muscle coordination, improper technique (motor control) and muscular weakness. The in depth biomechanical analysis allows differentiation of these factors and provides proper strategy to reduce injury and improve performance.

### ***Biofeedback Motor Control Training***

We've made it our mission to help our patients find the pathway to recovery as quickly as possible, providing them with a better quality of life and improved functioning. Biofeedback motor control training offers a groundbreaking approach that has had promising results for our patients with lower extremity disorders. If you are the victim of a host of injuries involving the knees or hips due to an active lifestyle, biofeedback motor control could be the answer you are looking for as you journey the road to rehabilitation.

## *AIM aka anatomy in motion*

A breakthrough solution for pain

Anatomy in Motion is a revolutionary approach to the problem of chronic pain. It's designed to systematically assess your gait and map out specific problems with the way you walk.

Once corrections are made and postural balance is restored, you'll find yourself moving with optimal efficiency and grace. Best of all, you'll walk without pain.

Possible causes of postural imbalance leading to pain include the following:

- Previous injuries
- Scar tissue
- Overworked muscles
- Structural abnormalities
- Degenerative changes from aging
- Improper exercise
- The wrong shoes, a heavy handbag or anything that adversely affects walking
- Ordinary stress

Over the years, influences like those listed above have changed the way you walk. An unnatural gait has become habitual. It would be set in stone if not for AiM.

After your initial consultation, which requires about two hours, sessions will include the following:

- Foot analysis using both digital and analog technology (Fig. 1–3)
- Video analysis to assess your gait and track your anatomy in motion (Fig. 4–7)
- Postural, structural and biomechanical assessments
- Soft tissue evaluation
- AiM techniques for correcting imbalance
- Additional techniques if necessary

Anatomy in Motion is the wave of the future for ending chronic pain. Schedule an assessment to get your gait and your life back in balance. You'll be walking tall again in no time.

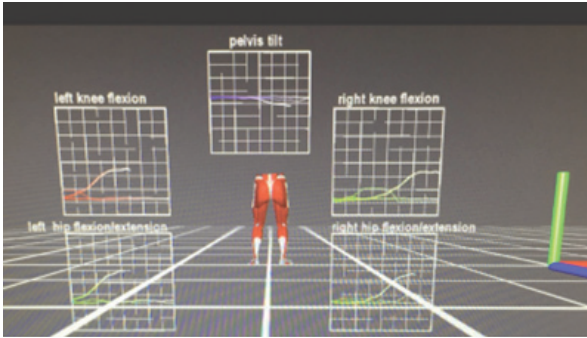


**Fig. 1–3.** Foot analysis using both digital and analogue technology

### ***Computer Assisted Rehabilitation Environment (CAREN)***

Computer Assisted Rehabilitation Environment (CAREN) is a versatile, multi sensory Virtual Reality system for treatment and rehabilitation of the human locomotion (walking), back pain, posture, balance, spinal stability and motor control integration. A physical therapist can name every muscle in the body, but if they asked you to put more force on the deltoid or the adductor longus muscle, would you know what they meant? The fact is that physical therapy is a constant back-and-forth interaction between the patient and the therapist. The therapist has to communicate the right motions to strengthen and move the muscles, the patient has to take that command and execute the required motion. The therapist must then evaluate the motion and decide whether the exercise served its purpose or the motion needs to be adjusted. In this scenario, it can be hard for the patient to understand how to move properly and the therapist may not be able to see which muscles were used to complete the motion. If a patient favors one muscle group over another, it may be that the ones that actually need the work never get the appropriate attention. Now, with a revolutionary tool for physical therapy sessions that use a Computer Assisted Rehabilitation Environment (CAREN), these types of issues are no longer a concern. This virtual reality tool creates a simulated environment whereby people who have suffered an injury can receive physical therapy in a way that makes it clear what muscles are being activated. The computer assisted rehabilitation environment is like walking into a Star Trek holodeck in its ability to immerse the patient in a variety of virtual environments with games or exercises programmed to help with specific motor actions. The floor of the deck consists of a circular platform, three meters in diameter, that integrates a treadmill and a force plate to measure the movements on the platform. The patient is strapped into a harness to remove any fear of falling. Then, sensors and reflective strips are put on the body. Twelve cameras sit around the platform getting a 360 degree view of the motion as the patient attempts to do the exercises or run through the virtual program which plays on the screen in front of them. These measurements can then provide real-time feedback during the program to help the patient improve their performance.



**Fig. 4–6.** CAREN. Video analysis of the posture to assess the gait and track anatomy in motion



**Fig. 7.** CAREN. Video analysis of the posture to assess the gait and track anatomy in motion

CAREN captures their motion with 12 infrared cameras and provides real-time feedback. By removing human error from physical therapy, we save time and can deliver unparalleled results.

CAREN is a virtual reality environment that takes force measurements as the patient is engaging a program on the screen. These precise measurements can then be mapped along the body in front of the patient to show which muscles were used. If a muscle is red, it shows that the muscle was at rest during the exercise. With this type of visual feedback, when the therapist asks them to exercise a particular muscle, the patient can now see in front of them which one they mean. This provides an excellent way to address a variety of issues in physical therapy including:

**Balance** – Since there is six degrees of freedom in the system, the patient is challenged to maintain balance during the routines. The sensors will also be able to track the range of motion and give real-time feedback to adjust the posture to maintain a better balance during the routines.

**Force** – The plate at the bottom can measure force and will provide feedback on how well the patient is doing. The treadmill can be adjusted as the patient gains more strength to keep challenging them to progress further.

**Individual Muscles** – If only one muscle needs to be stimulated, the routine can be changed to do more repetitions on that one muscle and be able to measure it accurately. With the muscle mapping program, the patient can pick out visually the muscle that needs to be exerted to turn the red color to blue or green.

**Cognitive Feedback** – CAREN works well with brain injury patients as well because it provides the cognitive feedback in real-time, making it easier for these patients to adjust their motions within the session. Since it does it automatically, the patient can receive that feedback instantly and have more time to process the changes, versus trying to remember complicated instructions after the fact.

**Muscle Groups** – The environment can also be programmed to include sophisticated routines that will help a patient exercise a group of muscles, not just one, if that is needed. Routine Boredom – Since the routines are done within a virtual environment, the programs can be exciting and novel. They include such scenarios as being a sailor on a ship having to maneuver a boat with your hips or a game where you have to hit some balls with your hands while avoiding others. The patient is completely immersed in the virtual reality program to the point where they are fully engaged with their physical therapy session, unlike other routines which don't have this type of environment. It can treat a variety of people and conditions including:

- Brain injuries
- Motor injuries
- Back pain
- Bone injuries
- Stroke patients
- Orthopedic disorders
- Neurological disorders
- Sports injuries
- Balance disorders
- Posture-related conditions
- Prosthetic patients

This ingenious new computer assisted therapy originated in Holland and was typically limited to military hospitals or even research facilities, with a few lucky professional sports teams making use of it now and then. However, now the technology is available to the general public for anyone in need of help with human locomotion. With this type of

real-time feedback available to both the therapist and the patient, it has been shown to decrease the amount of time in rehabilitation and speed up recovery. With the use of the harness and professional therapists, the CAREN is a safe and effective way to treat a multitude of problems dealing with balance, injury, or lack of motion. If you're interested in trying out this new and revolutionary approach to physical therapy, please contact us for more information. Up to now CAREN has only been used by military hospitals, research universities and few fortunate professional sports teams. CAREN systems consist of 6 DOF (Degrees of Freedom), motion base, motion capture, a projection screen, D-flow software and HBM (Human Body Model Software).

- CAREN enables measurements of motion of a subject in detail as a response to a perturbation from the computer driven motion platform. The system works in real-time and enables the creation of a variety of situations in a controlled and repeatable environment by using principals of virtual reality, highly instrumented perturbing platform and variety of feedback and feed forward simulators.
- CAREN creates a rehabilitation environment that provides precise therapeutic strategies through virtual immersion.
- The effects of treatment by CAREN can not be attained by any physical therapy methods. Treatment by CAREN greatly reduces rehabilitation
- CAREN has wide range of applications from treatment of back pain, orthopedic and neurological disorders, sports medicine and balance disorders.
- CAREN has been successfully used for enhancement of athletic performance by some of the worlds elite athletes. Testimonial for Computer Assisted Rehabilitation Environment (CAREN) from Dr. Jean Pier Farcy, MD Video below demonstrates how CAREN creates a rehabilitation environment that provide better therapeutic strategies through virtual reality.

### ***Dynamic Neuromuscular Stabilization (DNS)***

#### **The foundation of DNS\***

DNS is based on developmental kinesiology. Developmental kinesiology is a science of maturation of the human movement system during the time of early development from birth until the child starts walking.

### *Physiological principles*

The position acquired by the child during development is the process in which the human brain and musculoskeletal system starts to cooperate in order to overcome gravity and establish posture and locomotion (walking).

Human movement is based on transferring body weight over for support. Proper support allows optimum dynamic stability.

Optimum stability allows maximum mobility with no expense to support structures such as disks, ligaments, etc. (Fig.8,9). No expense literally means that load and force distribution acting on the body from inside and outside are in balance.

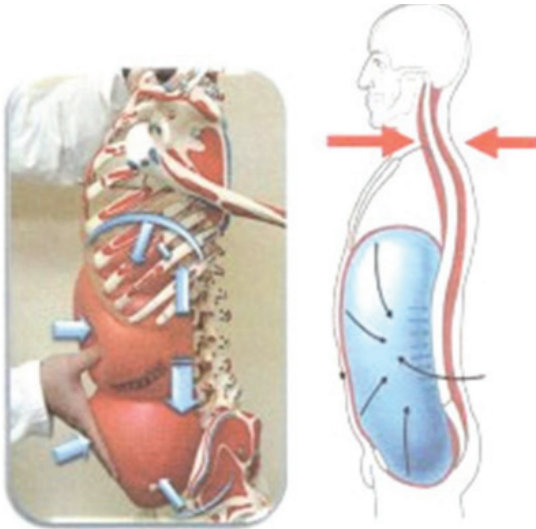


**Fig 8, 9.** Muscles responsible for neuromuscular stabilization\*

\*Origin: Prague school of rehabilitation <https://www.rehabps.com/>

### *Methodology*

dNS is a combination of manually assisted exercises and reflex stimulation. The patients movement patterns could include; dysfunction, misalignment, loss of control and postural deviations (Fig. 10). Based on these and the overall movement of the patient, a therapist chooses a position from early development in which proper support though the hip, shoulders and spine could be established (Fig. 11).



**Fig. 10.** Determining the model of optimal patients movement patterns



**Fig. 11.** The system at DNR has an immersive semi-cylindrical projection to correct movement patterns. In the picture Dr. Kalika at work with patients

Special manual joint centration by the therapist reinforces different movement strategy based on preprogrammed ideal movement patterns in brain. All joint mobilization and soft tissue manipulations are also performed in these positions with the only goal of preparing the body to be able to handle this position. The doctor or therapist follows developmental progression to different higher positions in which support and stability is more demanding.

### *Reflex locomotion aka vojta therapy*

Reflex locomotion is used when a certain global or local movement patterns are unavailable to patients on regular cuing physical therapy exercises. The therapist can start this particular movement pattern by manual reflex stimulation of zones in developmental positions such as creeping or turning (Fig. 12,13).

The reflex stimulation is also an excellent method to use with acute conditions. Some of these conditions include sciatica, radiculopathy and herniated disc. There can also be situations where the patient has poor body awareness and cannot use his muscles properly upon the therapist's command.

Although DNS is an all inclusive methodology clinicians are required to be proficient at soft tissue manipulation and joint mobilization approaches (Fig. 14–17.).

### *DNS advantage*

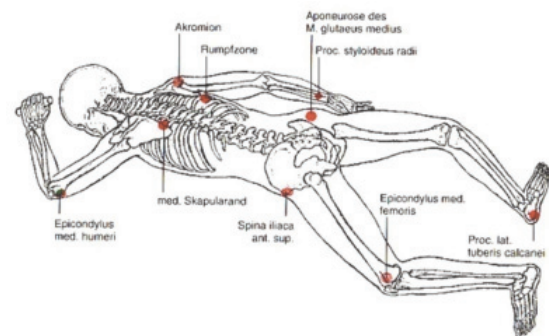


**Fig. 12,13.** Clue zones for therapy by manual reflex stimulation to optimize movement pattern; considering multiple factors including abdominal pressure (the model)



**Fig. 14, 15.** The general view of the DNS procedure (Dr.L Kalika performance)



**Fig. 16.** The general view of the DNS procedure (Dr.L Kalika performance)

The superiority of the DNS lies in its ability to invoke ideal or close to ideal movement patterns from the nervous system based upon genetical coding.

DNS, or dynamic neuromuscular Stabilization, involves a manual rehabilitative approach that is designed to stimulate movement control centers located in the brain. Through therapeutic techniques, neurons are activated in the same way that occurs naturally through planned an automatic movements. When there is a problem in the communication network of the central nervous system, DNS helps the brain and body to communicate more effectively. Structural and postural problems often cause or are the result of back conditions and other orthopedic conditions. The goal of DNS therapy is to restore proper functioning of the body, improving range of motion, flexibility, and stability along the way.

While DNS methods of treatment are being implemented around the world, it is still a relatively new approach that is only available on a limited basis. DNS is a manual rehabilitative approach based on developmental movement principles (ontogenesis). It is designed to activate the body's stabilizing system by stimulating movement control centers in the brain. The neuronal network activated during therapy is the same neuro-

nal pool representing sub-cortical centers responsible for automatic movements of the human body such as; movement executed during human gait (walking) and other planned movements such as prehension etc... This neuronal network is naturally programmed in an infant at birth by human genetic coding and it matures and develops during first year of life. Through the connection and growth of many different neurons a child will naturally develop movement stereotypes enabling him to move against gravity as the child learns to turn, crawl and finally walk. Thereafter motor maturation and an acquisition of an ability to walk this system (software like neuronal network) remains in place through adulthood to provide a foundation for most basic yet most complex movements such as gait. Posture follows movement like the a “shadow” as stated by Prechtl. This shadow is the system we are describing. This function was discovered by one of the worlds famous neurologists Professor V6clav Vojta. The method helps to restore the structural and postural alignment of the body’s neuromuscular system by invoking a full body “global” motor pattern. Global motor patterns form the foundation of human movement. They are activated in the specific sequence of increasing complexity during the postural development in the first months of a child’s life. The global motor pattern remains essential for control of posture and stability of the spine – the pivotal center of the entire locomotive system throughout the life of the individual. Dynamic Neuromuscular Stabilization therapy reactivates patient’s dormant global motor pattern and, exploits the plasticity of the brain, establishing new physiological connections. The spinal-joint manipulation, muscle relaxation and the soft tissue release procedures are all conducted in the postural positions of ideal movements of an infant (crawling and turning). In these positions of support the maximum spinal stability and joint centration of the entire body are achieved.

During DNS therapy, gentle pressure is applied to the body while the patient is situated in a ideal movement position. This pressure stimulates a global motor reaction which minimizes muscle imbalances, relieves painful muscle spasms, improves spinal stability, and encourages postural awareness. Over time, through repetition of the DNS exercises, spinal stability becomes habitual and unconscious. The results achieved by DNS are superior to conventional methods used by chiropractors and physiotherapists, who tend to address the problem “locally”. DNS therapy prepares the body for gentle, non-forceful manipulation producing faster and more stable improvement of function and, therefore, long-lasting pain relief.

# Chapter 11

## Introduction to sonosurgery

*Zbigniew Pilecki, Grzegorz Pilecki*

**Introduction.** The dynamic development of minimally invasive techniques in surgery was based on access to imaging equipment, endoscopic sets and surgeons huge passion. Looking back on the development of surgery we can conclude that this discipline is developing in the direction for minimizing damage during the intervention. This is the reason for the development of minimally invasive techniques in surgery. With the appearance of opportunities imaging in real time conditions were created for the performance of invasive procedures in ultrasound imaging. As a first evolved puncture techniques, which became the starting point for the development of sonosurgery [1, 2].

**Sonosurgery.** Sonosurgery is a collection of minimally invasive surgical techniques performed with continuous ultrasound imaging and the use of endoscopic tools. It's a surgical discipline and requires compliance of aseptic and medical art conditions and should be performed in the operating unit by experienced personnel. By medical art we understand mastery in surgical techniques and ability to perform ultrasound examination by a physician. However, the simplicity and minimal tissue trauma during sonosurgical procedures will lead to execute them in operating room similar to procedures in interventional ultrasonography [3].

Sonosurgical techniques are techniques performed in the conventional surgery and orthopedics, but the use of ultrasound equipment can reduce operating approach and reduce invasive procedure to the affected tissue. The use of proven surgical techniques used in minimally invasive surgery is desirable, because it does not fill signs of a medical experiment. Widespread is the use of prepared sets [4]. The strength of sonosurgery lies in the phenomenon of complementarity, which is supplementation of the various stages of sonosurgical procedure by each other. Logic of such proceedings during surgery allows it to make it simple and friendly for the surgeon and patient.

### *Stages in sonosurgical procedures.*

We (Z. Pilecki et al.) perform sonosurgery successfully for three years systematically increasing range of operations. All procedures in sonosurgery are performed in aseptic, have specific steps, as follow (Fig. 1–5):

- I. Performing of a sonotopogram;
- II. Preparations techniques:
  - 1) using liquid – needle technique (Fig. 2–5);
  - 2) using tools;
  - 3) using electrotols (Fig. 6);
  - 4) balloon techniques;
  - 5) mixed techniques (Fig. 7, 8);
- III. Endoscopic tools;
- IV. Sewing.



**Fig. 1.** In the treatment with skin discontinuity aseptics should be strictly complied

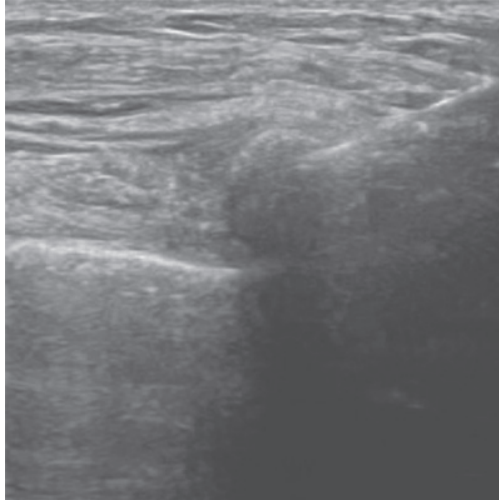


**Fig. 2.** Evacuation of urate deposits



**Fig. 3.** Evacuation urate deposits in technique 2 in 1



**Fig. 4.** Anesthesia under ultrasound control

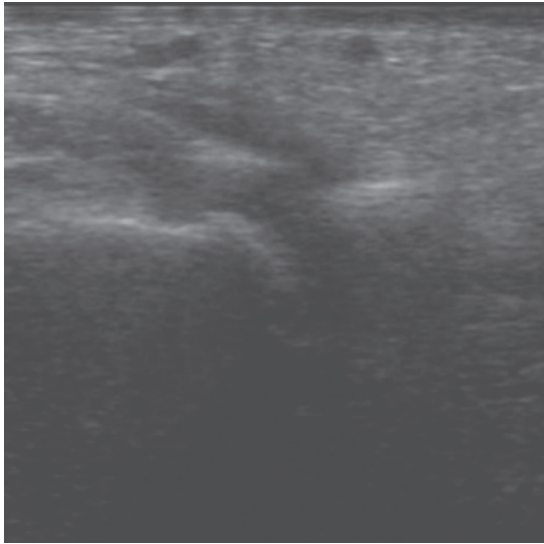


**Fig. 5.** Administration of the interphalangeal joint.



**Fig. 6 a.** Koblation by Topaz electrode (view of the operative field)

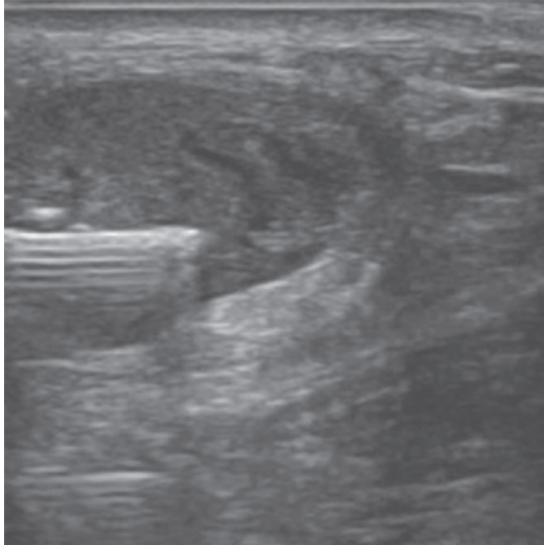


**Fig. 6 b.** Koblation of Achilles tendon by Topaz electrode

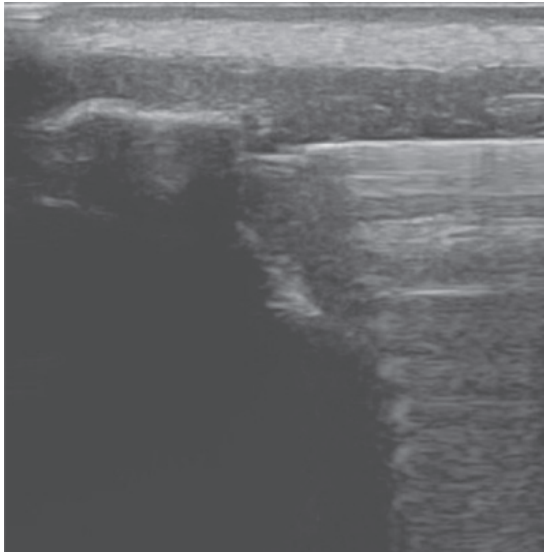


**Fig. 7.** Bone biopsy (“2 in 1” technique)

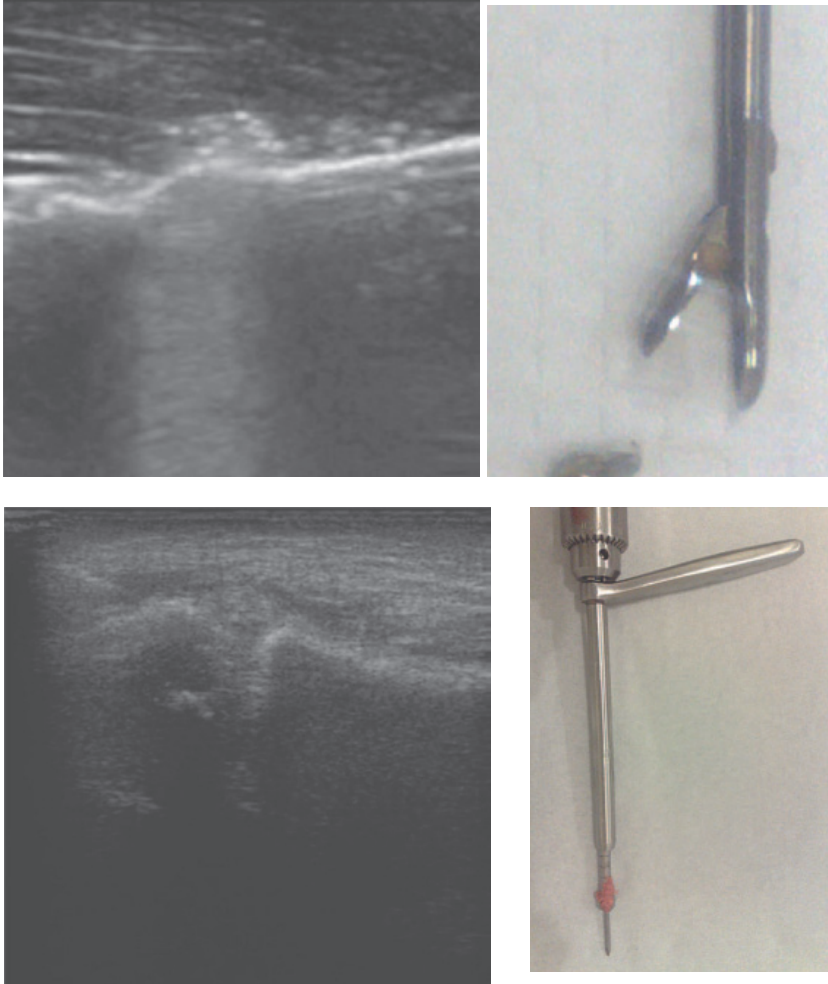


**Fig. 8.** Example of tools for techniques “*All in 1*”

Thus use of ultrasound imaging allows a very precise, atraumatically and aseptically perform surgery. Surgery performed in sonosurgical technique has all the characteristics of minimall invasive treatment: good cosmetic result, minimal tissue trauma, low pain, the possibility of taking early rehabilitation and a very good final result.

The programs utilizing sonosurgical techniques can facilitate building safe and modern hospital [5]. An essential element of any medical

procedures are the costs of its implementation, which are systematically counted [6]. The total cost of sonosurgical treatment, compared to procedures performed in classical techniques is low, because of minimal amount of materials used for the treatment, the number of staff and the way of anesthesia. Operations are performed in one-day procedure. The cost of ultrasound imaging amortization is low. Using ultrasound imaging, we can often control the course of healing of the operated structures. This is not a threat to the patient and the costs are also low. We are able, based on ultrasound images to determine the effectiveness and the time needed to heal the sick organ, which is enormous practical information. We are always concerned when we write about medical procedures only in superlatives, as in this article. But sonosurgery is exactly this. The only downside, which we should pay attention again is high hardware requirements and very experienced surgical team. We want to emphasize once again at the end strongly that the ultrasound device should be available in every operating room and handled by an experienced physician. This is necessary if we want to build safe and modern hospital [5].

## Chapter 12

# Clinical Application and Efficacy of Ultrasound in Combat-Related Neuropathies

### Introduction

Combat-related injuries often present complex clinical scenarios involving neuropathies, fractures, and musculoskeletal abnormalities. This chapter explores the clinical application of ultrasound in diagnosing and managing such intricate cases. The multifaceted nature of combat injuries necessitates a comprehensive approach for accurate diagnosis and effective intervention.

## **ULTRASONOGRAPHY IN THE DIAGNOSIS OF COMBAT NERVE INJURIES AND TREATMENT USING ULTRASOUND-GUIDED CONTROLLED DRY NEEDLING**

Combat trauma causes both myofascial and neuropathic pain, with neuropathy potentially leading to functional deficits. Dry needling under ultrasound guidance (DN-US) has been shown to effectively reduce myofascial pain and neuropathy symptoms, as well as improve posture. In this study, the efficacy of ultrasound for diagnosing combat nerve injuries and DN-US for targeted treatment was evaluated in 20 male patients with combat injuries to the extremities and pelvis. All patients had signs of neuropathy and neuropathic pain, and were examined through various imaging, laboratory, neurologic, and orthopedic tests. Neuromuscular ultrasound was used to evaluate nerves and motion in specific areas, and DN of myofascial trigger points (MTrP) was administered under US guidance. Ultrasound surveys were conducted at the levels of predicted nerve injury, and visual analogue scale and neuropathic symptom scores were measured before and after the intervention. The study found that neuropathy was present in all patients at various levels, including in the ulnar and median nerves, brachial plexus, sciatic nerve, tibial and peroneal nerves, and nerve roots. Multiple small hyperechoic bodies were also found in muscles, fascias, and skin, with changes observed in the nerve itself. Muscle spasticity and scars were targeted for US-DN, resulting in a decrease in fascicle diameter and improvements in nerve structure, motility, and contractility. Ultrasound was found to be a reliable tool for targeting interventions, with DN-US effectively reducing neuropathy and neuropathic pain in combat injuries. In

conclusion, combat nerve injuries and neuropathic pain can be diagnosed through ultrasound, with fascicle diameter being an important parameter for fast diagnosis. Ultrasound information is most reliable for targeting interventions, and DN-US is among the most relevant techniques for combat injuries.

## **Ultrasound for Diagnosis and Dry Needling under Ultrasound Guidance for Treating Combat Neuropathy**

**Introduction:** Combat trauma can lead to myofascial and neuropathic pain, often resulting in disability. Neuropathic pain requires continuous medication. Dry needling under ultrasound guidance (DN-US) is an effective therapeutic approach for myofascial pain and can also be used for neuropathic pain caused by muscle spasticity. This study aims to assess the utility of ultrasound in diagnosing combat-related nerve injuries, with a particular focus on nerve fascicle diameter increase as a major sign of neuropathy detected by US and its reversibility with targeted DN-US. Additionally, the study emphasizes DN-US as a very effective first-line therapeutic rehabilitation option for combat trauma, including cases with nerve damage and mechanical irritation from foreign objects like metal fragments.

### **Methods:**

20 male patients aged 22-46 with combat injuries that had wounds in the extremities, spine shoulders and pelvis.

All patients exhibited signs of neuropathy and neuropathic pain.

Diagnostic tests included imaging, laboratory, neurologic, and orthopedic evaluations.

Precise physical tests and neuromuscular ultrasound using M-mode were conducted to assess nerves and motion in various areas.

Patients received DN of **Myofascial Trigger Points (MTrP) under US guidance.**

MTrP were identified based on clinical examination, referred pain pattern, and US identification.

Single fine (28G) steel needles were used for DN under US guidance.

Ultrasound surveys were conducted at predicted nerve injury levels.

Visual Analogue Scale (VAS, 0-10) and Leeds Assessment of Neuropathic Symptoms and Signs (LANSS) scores were measured before, immediately after, 24 hours, and 7 days after the intervention.

## **Results:**

Neuropathy was diagnosed in all patients at various levels, including extremities and nerve roots.

Researchers visualized the site of injury and nerve changes, with a specific emphasis on increased nerve fascicle diameter as a sign of neuropathy.

Certain foreign objects (bullets, shrapnel, metal, bone fragments) were poorly visible on US near vascular and nerve structures.

Multiple small hyperechoic bodies were found in muscles, fascias, and skin, with cystic formations and encapsulation processes at later stages.

Muscle spasticity and scars were detected and treated with US-DN.

After treatment, the nerve fascicle diameter decrease was observed immediately, along with improvements in nerve structure, motility, and contractility during functional tests and walking.

## **Conclusion:**

- Combat-related nerve injuries and neuropathic pain can be detected using ultrasound.
- The increase in nerve fascicle diameter, as detected by US, is a major sign of neuropathy, and its reversal is achieved through targeted DN-US.
- DN-US is an extremely effective first-line therapeutic rehabilitation option for combat trauma patients, including cases with nerve damage and mechanical irritation from foreign objects like metal fragments.
- DN-US offers rapid improvements in neuropathic symptoms and serves as a versatile and successful approach for managing combat-related neuropathy across a spectrum of injuries.

## **It is crucial to emphasize two important points:**

**1. Nerve Fascicle Diameter Increase as a Major Sign of Neuropathy** Detected by US and its Reversibility with Targeted DN-US: One major finding in your study is that the increase in nerve fascicle diameter, as detected by ultrasound (US), serves as a significant sign of neuropathy in combat trauma patients. It's crucial to highlight that this increase in fascicle diameter is not only indicative of neuropathy but also that it is reversible through targeted Dry Needling under Ultrasound Guidance (DN-US). Furthermore, you found that the effects of DN-US on reducing nerve fascicle diameter can be rapid, with improvements seen immediately after the procedure.

**2. DN-US as a Highly Effective First-Line Therapeutic Rehab Option for Combat Trauma, Including Amputees and Mechanical Irritation:** Another key point to underscore is that DN-US proves to be a highly effective first-line therapeutic rehabilitation option for combat trauma patients. This effectiveness extends to cases where patients have suffered nerve damage, including amputees, and where mechanical irritation from foreign objects like metal fragments is a contributing factor to neuropathic pain. DN-US emerges as a versatile and successful approach for managing combat-related neuropathy across a spectrum of injuries.

By emphasizing these points, study provides a clear message about the diagnostic and therapeutic potential of DN-US in combat-related neuropathy, including its rapid impact on nerve fascicle diameter and its suitability for various types of injuries, including those involving amputations and mechanical irritation.

# Case series: combat neuropathy ultrasound

## Case Report 1: Comprehensive Case Report on Multifaceted Neuropathy, Fracture Management, and Complex Medical Associations

*This case report explores a 26-year-old male military personnel with combat-related neuropathy symptoms, a history of fractures, and complex medical conditions. Ultrasound examinations revealed neuropathic conditions in the right forearm and left sciatic nerve, with prominent involvement of the peroneal nerve. X-ray findings showed multi-fragmentary fractures and surgical fixation. The report discusses the challenges of diagnosing and managing neuropathy in the context of fractures and complex medical history, emphasizing the importance of a multidisciplinary approach.*

**Patient Information:** Male, 26 years old, military personnel

**Clinical History:** The patient presented with combat-related neuropathy symptoms and a history of fractures and surgical interventions in both forearms and left knee. The patient's medical history included infectious episodes, sepsis, purulent wounds, a left-sided pneumothorax, multiple brachial plexus blocks in suboptimal conditions, and distinctive medical findings related to lymph nodes and spleen.

**Introduction:** This comprehensive case report explores the intricate interplay between combat-related neuropathy, fractures, complex medical conditions, and the influence of suboptimal medical interventions. The diagnostic intricacies underscore the challenges of deciphering multifaceted clinical presentations and demand a multidisciplinary approach.

**Clinical Presentation:** The patient's complex clinical presentation included symptoms suggestive of neuropathy, fractures, and a medical history marked by sepsis, purulent wounds, left-sided pneumothorax, and multiple brachial plexus blocks.

### Ultrasound Examination:

Lower Limbs: The ultrasound assessment of the patient's sciatic nerves yielded critical insights:

Left Sciatic Nerve:

- Nerve thickening up to 1.5 mm at the knee level.

- Localized thickening of the tibial portion up to 1.5 mm, extending to 15 mm.
- Localized thickening of the peroneal portion ranging from 2 to 2.5 mm.

#### Right Sciatic Nerve:

- Predominantly intact structure, with minimal fascicle thickening (1-1.2 mm).
- Localized thickening in the tibial portion (up to 1 mm) and peroneal portion (up to 1.8 mm).
- Identification of a hypoechoic formation (5x4 mm).

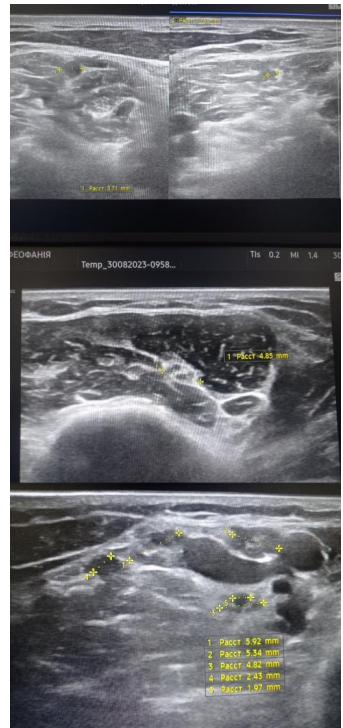
#### N. Suralis Visualization:

- Distal segments exhibited consistent structural patterns.
- Ankle-level segments displayed relatively unchanged structures.

Right Forearm: Ultrasound evaluation of the right forearm provided multifaceted findings:

#### Right Ulnar Nerve:

- Post-surgical state after multi-fragmentary fracture of the right ulnar bone.
- Surgical intervention involving plate fixation with screws and additional osteotomy of the distal radius.
- Presence of a loose fragment in soft tissues.

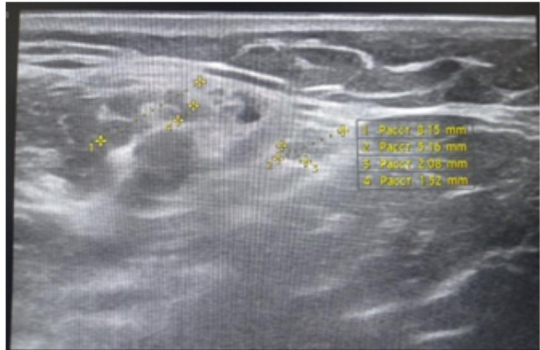


#### Median and Radial Nerves:

- Nerve thickening in both nerves (5 to 10 mm).
- Fascicles exhibited thicknesses of 1-2.5 mm.

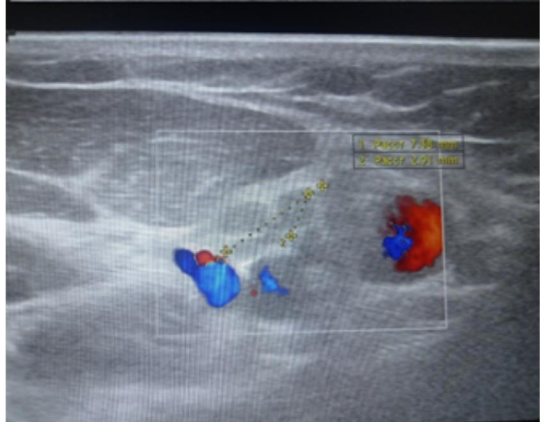
### All Nerves at Shoulder Level:

- Notable thickening ranging from 5 to 10 mm.
- Fascicle thicknesses ranging from 2 to 2.5 mm.



### Brachial Plexus:

- Axillary level nerves exhibited significant thickening.
- Inter-scalene space showed varying degrees of thickening.



### Conclusion from Ultrasound:

The ultrasound findings portrayed a complex neuropathic condition in the right forearm, suggestive of widespread neuropathy and plexopathy on the right side. The assessment indicated a post-surgery status following multi-fragmentary fracture of the right ulnar bone. Neuropathic manifestations were also discernible in the left sciatic nerve, with prominent involvement of the peroneal nerve.

**X-ray Findings:** The X-ray findings unveiled multi-fragmentary fracture of the right ulnar bone, surgical fixation, and a slowly consolidating femoral fracture in the left knee.

**Ultrasound Findings:** The abdominal ultrasound examination revealed additional intriguing findings:

- Hepatic abnormalities with increased echogenicity, but no focal changes.
- Enlarged spleen, normal parenchyma.

- Lymphadenopathy.
- Enlarged thyroid gland with a colloid nodule.

**Discussion and Analysis:** The convergence of neuropathy, fractures, and complex medical conditions demands a holistic approach. Infectious history, sepsis, lymph node changes, splenomegaly, and suboptimal brachial plexus blocks contribute to the intricate clinical landscape. The potential association between infections, immune responses, medications, and neurological complications adds further complexity.

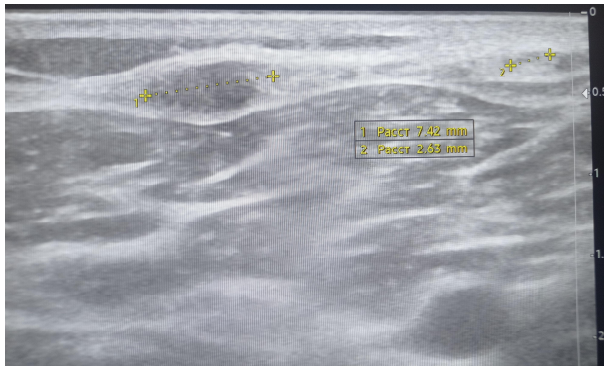


**Figure n. Suralis neurinoma (leg)**

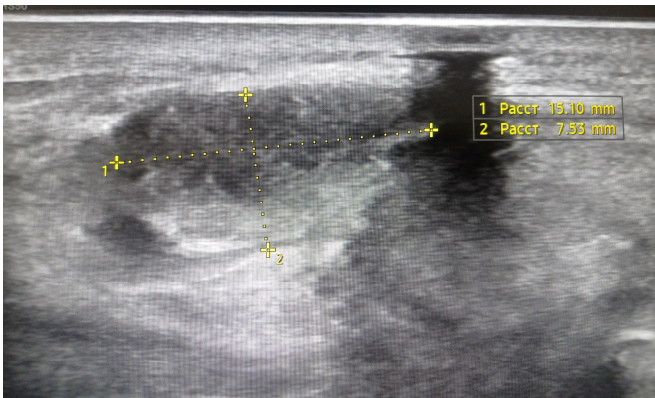
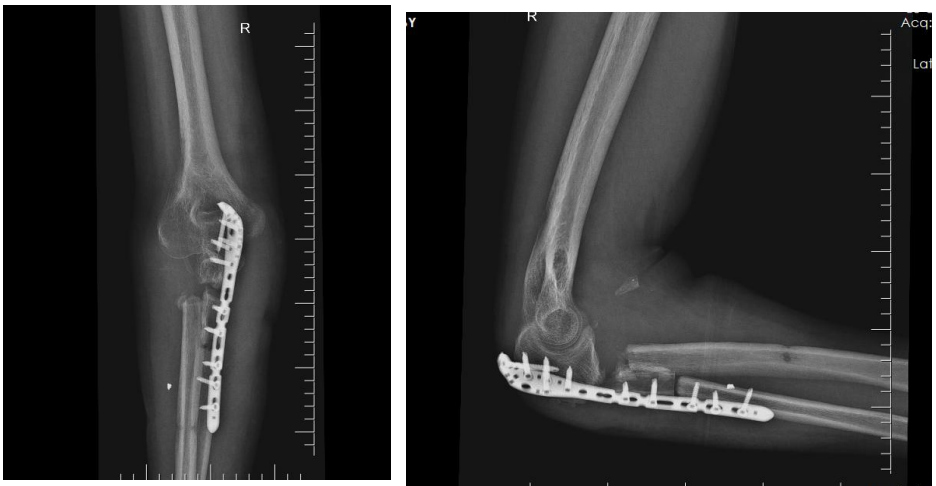


**Figure n. suralis neurorrhaphy at forearm level, autotransplant to the ulnar nerve. Damaged ulnar nerve, neurinoma.**

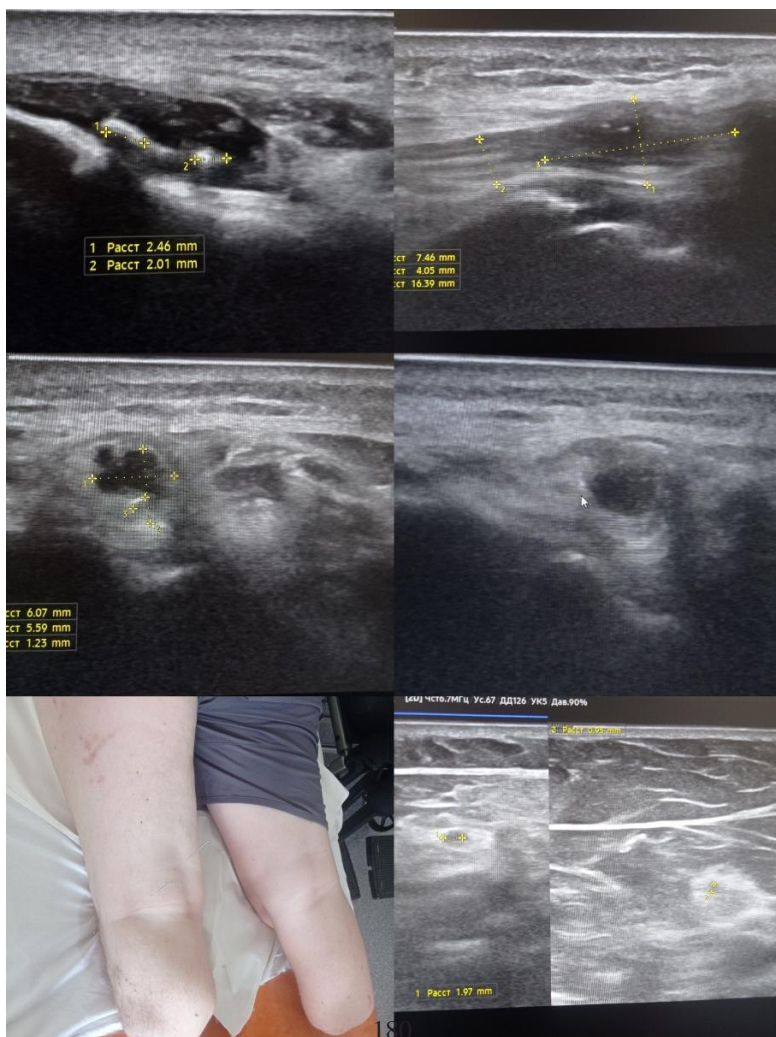
**N. Suralis Neurorrhaphy and Neurinomas:** Of particular importance in this comprehensive case is the role of the n. suralis, which underwent neurorrhaphy as an autotransplant to the ulnar nerve. This surgical intervention aimed to address the multifaceted neuropathic manifestations. However, ultrasound imaging revealed intriguing findings along the n. suralis. Lesions in the form of neurinomas were evident at the level of the nerve cut and suture, shedding light on the complexities of peripheral nerve repair. This discovery adds another layer of intricacy to the patient's condition, emphasizing the challenge in managing multiple neuropathic manifestations and their dynamic interactions within the broader clinical context.

**Conclusion:** This multifaceted case underscores the interconnectedness of neuropathy, fractures, infectious history, and complex medical conditions. The clinical puzzle mandates interdisciplinary collaboration, astute diagnostic interpretation, and holistic patient care. The complexities highlight the essential role of a multidisciplinary approach in unraveling intricate medical narratives and guiding comprehensive patient management.



## Case Report 2: Dry Needling under US-Guidance for Neuropathic Pain and Spasticity in a Bilateral Amputee Combatant

This case report presents the successful treatment of neuropathic pain and spasticity in a 38-year-old bilateral amputee combatant using dry needling under ultrasound guidance. The intervention aimed to alleviate pain, improve movement, and enhance sensitivity for effective prosthesis use. The report details the patient's presentation, treatment, and positive outcomes, highlighting the potential benefits of dry needling in managing neuropathic pain in amputees.



**Introduction:** Neuropathic pain is a challenging condition to manage, especially in patients with limb amputations. In this case report, we present the successful treatment of neuropathic pain and spasticity in a bilateral amputee combatant using dry needling under ultrasound guidance. The aim of the intervention was to alleviate pain, improve movement, and enhance sensitivity to facilitate the use of a prosthesis effectively.

**Case Presentation:** A 38-year-old male combatant with bilateral amputations (both lower limbs) presented with severe neuropathic pain in the left stump. The patient reported difficulty in using a prosthesis due to the intensity of the pain and associated spasticity. Upon examination, areas of spasticity and trigger points were identified near the affected nerves, including the left sciatic nerve and ulnar nerve.

**Treatment and Intervention:** The patient underwent targeted dry needling under ultrasound guidance to address the areas of spasticity and trigger points. Precise needle placements were made based on ultrasound imaging to ensure accurate targeting of the affected nerves and muscles.

**Outcome:** Following the dry needling sessions, the patient reported a significant improvement in neuropathic pain in the left stump. Notably, the movement and sensitivity in the 4th and 5th fingers of the left hand also improved. Ultrasound imaging post-treatment showed a reduction in fascicle size of the left sciatic nerve, where previously enlarged.

**Discussion:** This case report demonstrates the potential benefits of dry needling under ultrasound guidance in managing neuropathic pain and spasticity in amputees. The precise targeting of affected nerves and muscles likely contributed to the positive outcomes observed in this patient. The reduction in nerve fascicle size seen on ultrasound imaging suggests an improvement in nerve structure, supporting the notion that dry needling may have a positive impact on nerve health.

**Conclusion:** Dry needling under ultrasound guidance appears to be a valuable treatment option for managing neuropathic pain and spasticity in bilateral amputees. The reported improvements in pain, movement, and sensitivity, along with the reduction in nerve fascicle size, indicate the potential efficacy of this intervention. Further research and larger studies are warranted to validate the findings and determine the broader applicability of this treatment modality in complex neuropathic pain cases in amputees.

## **Case Report 3: Combat-Related Neuropathy and Fracture Management**

Patient Information: Male, 26 years old, military personnel

Clinical History: The patient presented with combat-related neuropathy symptoms and a history of fractures and surgical interventions in both forearms and left knee.

Introduction: Combat injuries can result in complex medical presentations involving both orthopedic and neurological complications. This case report delves into the intricate interplay between nerve injuries and fracture management, underscoring the diagnostic challenges and multidisciplinary approach required for effective patient care.

Clinical Presentation: A 26-year-old male military personnel presented with symptoms suggestive of neuropathy, possibly linked to combat-related injuries. Additionally, the patient had a history of fractures in both forearms and the left knee, necessitating surgical interventions.

Ultrasound Examination:

Lower Limbs:

Left Sciatic Nerve: Ultrasound imaging of the left sciatic nerve revealed several abnormalities indicative of neuropathy:

Thickening of fascicles by up to 1.5 mm at the knee level.

Tibial portion displayed localized thickening of up to 1.5 mm, extending to 15 mm.

Peroneal portion exhibited localized thickening ranging from 2 to 2.5 mm.

Right Sciatic Nerve: Contrasting with the left side, the right sciatic nerve maintained a predominantly intact structure:

Minimal thickening of fascicles, measuring up to 1-1.2 mm.

Tibial portion demonstrated localized thickening up to 1 mm.

Peroneal portion displayed localized thickening of up to 1.8 mm.

A hypochoic formation, measuring approximately 5x4 mm, was identified.

N. Suralis Visualization: The n. suralis was visualized at different levels:

Distal segments exhibited consistent structural patterns.

Ankle-level segments displayed relatively unchanged structures.

Right Forearm: The ultrasound examination of the right forearm unveiled a complex picture:

Right Ulnar Nerve:

Multi-fragmentary fracture aftermath observed in the right ulnar bone.

Surgical intervention involving a plate fixed by 10 screws to the distal ulna.

Satisfactory alignment of fracture fragments.

Additional osteotomy of distal radius, accompanied by a loose fragment in soft tissues.

Median and Radial Nerves:

Nerve thickening observed, ranging from 5 to 10 mm.

Fascicles demonstrated thicknesses of 1-2.5 mm.

All Nerves at Shoulder Level:

Notable thickening observed, ranging from 5 to 10 mm.

Fascicle thicknesses ranging from 2 to 2.5 mm.

Brachial Plexus:

Axillary level nerves exhibited significant thickening.

Inter-scalene space demonstrated varying degrees of thickening.

Conclusion from Ultrasound: The ultrasound findings unveiled a complex neuropathic state in the right forearm, reflective of widespread neuropathy and plexopathy on the right side. Furthermore, the examination indicated a post-surgery status following multi-fragmentary fracture of the right ulnar bone. Neuropathic signs were also evident in the left sciatic nerve, with predominant involvement of the peroneal nerve.

X-ray Findings:

Right Elbow:

Multi-fragmentary fracture of the right ulnar bone.

Plate fixation with 10 screws to the distal ulna.

Additional osteotomy of the distal radius with a loose fragment in soft tissues.

Left Knee:

Removal of a fixation device (AZF) after displaced fracture.

Proximal femoral fracture with incomplete consolidation.

Bone callus forming along the back surface of the metaphysis.

Discussion and Analysis:

The diagnostic complexity in this case stems from the intricate interplay between neuropathy and fractures. The ultrasound findings provided a comprehensive view of nerve structural changes, contributing to the understanding of the patient's neuropathic condition. The differing presentations of the left and right sciatic nerves highlight the importance of comparative analysis. The X-ray data further underscore the orthopedic challenges, especially in relation to fracture management.

Conclusion: This case demonstrates the complex landscape of combat-related neuropathy and fractures, necessitating a multidisciplinary approach. Accurate diagnosis and effective patient care require skilled interpretation of imaging data, collaboration among medical specialties, and a comprehensive understanding of the patient's clinical history. The interdependence of nerve injuries and orthopedic conditions emphasizes the significance of holistic patient management.

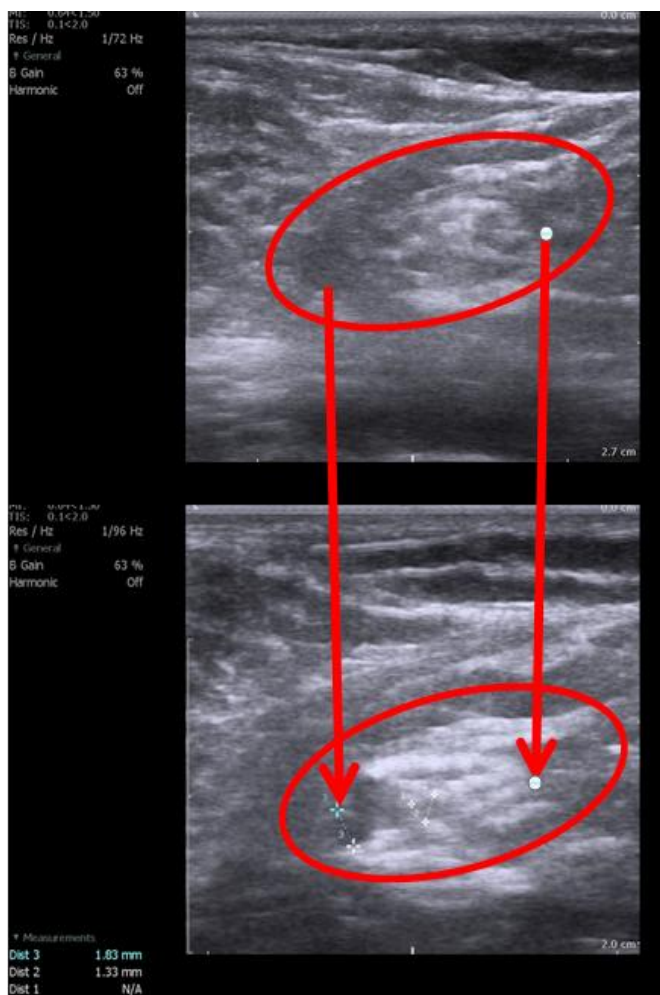


**Figure Patient, 28 years old.** The patient has multiple partial fractures in the left hip joint, as well as small metal fragments in bone and soft tissue structures near the fractures. CT scan results confirm the location and size of the fractures, while ultrasound shows signs of sciatic nerve neuropathy on the left side with disruption of the contour of the hip joint structures, hip bone, acetabulum and femoral head. Muscle areas adjacent to the injury sites and the sciatic nerve also show spasms. Ultrasound-guided dry needling of the affected muscles results in a reduction in the diameter of the sciatic nerve bundles on the left side, especially in the tibial and fibular portions. This suggests that ultrasound-controlled dry needle therapy may be an effective treatment option for neuropathy associated with hip fractures.

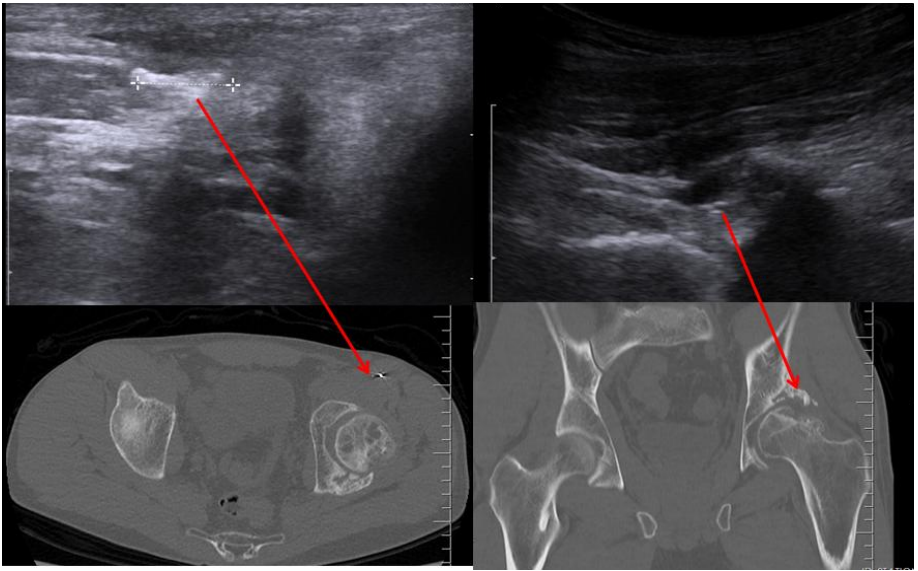


**Fig. Patient, 45 years old, injured, lower back pain.** The ultrasound and CT findings in this case indicate significant injury to the lumbar vertebrae and hip acetabulum on the right side, with the presence of bone fragments and scarring. Based on the ultrasound and CT findings, there were numerous bone fragments and scar formation. In addition, detected muscle trigger points in the multifidus muscles near the splinters were an additional cause of pain and a target for treatment. However, with the use of ultrasound-guided dry needling, these points could be effectively located and treated, greatly helping to relieve the pain.

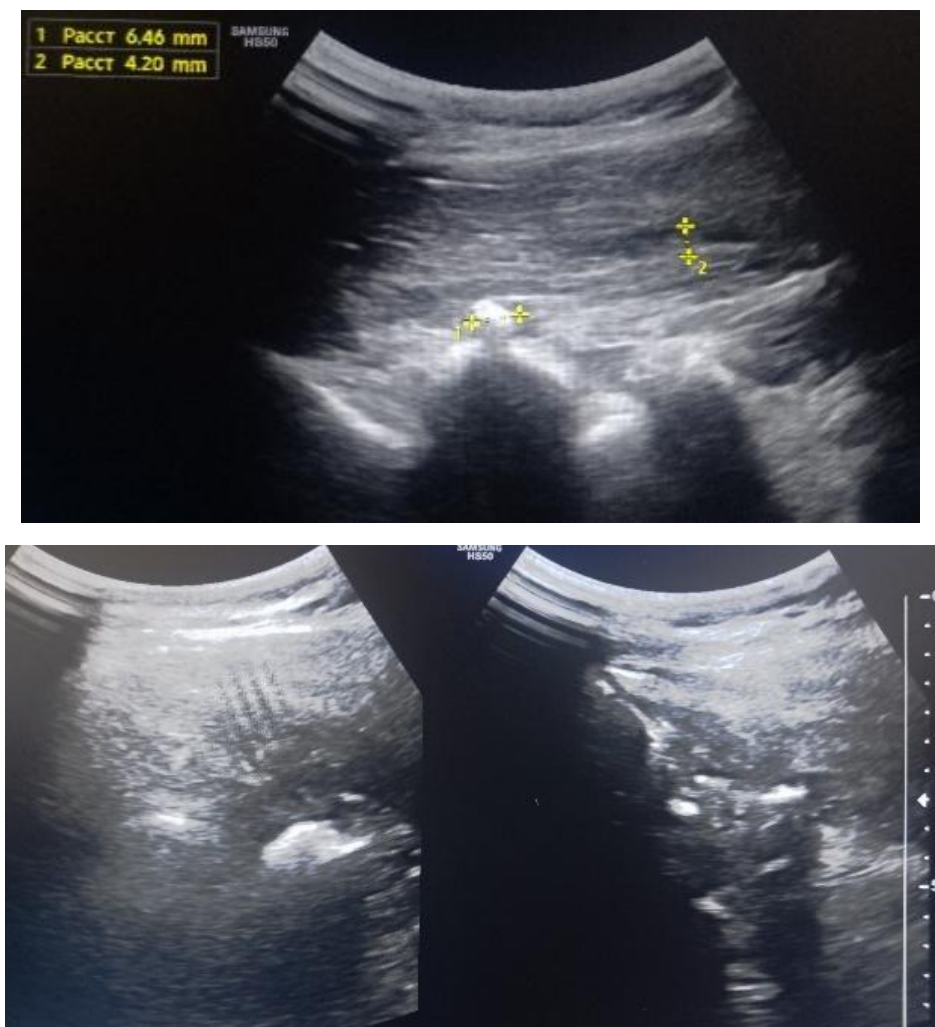
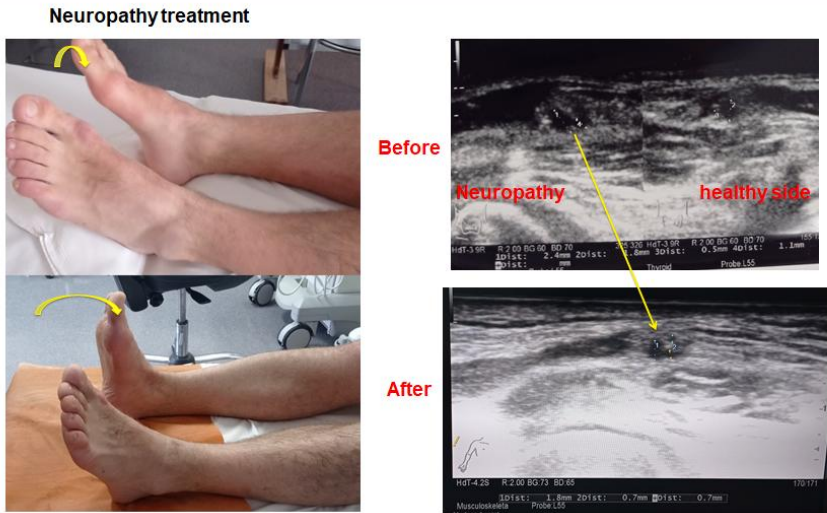


Fig. Multiple bone fragments and damage to the right transverse process of L5 were observed at the level of the L5-4 vertebrae. Near the left transverse processes of the L5-4 vertebrae, a hyperechoic inclusion with a diameter of 5 mm was observed. Muscle trigger points were noted near the bone fragments.



**Fig. Symptoms of traumatic neuropathy of the ulnar nerve.** On ultrasound examination of the tissues on the medial surface of the right arm, a fluid structure measuring 50x60 mm in transverse dimensions and filled with hypoechoic content was identified. Next to it, in the third medial location, a hyperechoic formation measuring 11x9 mm was also found. On the medial surface of the right arm, an area of damage extending into the adjacent muscles up to 18 mm in length was detected, with no signs of pathological inclusions. The ulnar nerve was located nearby: on the distal side from the injury, the nerve had thickened dimensions of up to 8x5 mm and fiber bundle diameter of up to 1.4 mm; on the proximal side, the nerve had transverse dimensions of up to 5x4 mm and fiber bundle diameter of up to 0.8-1 mm. Upper image - above the injury (nerve in a circle); Middle - the site of injury passes into the muscle (arrow); Lower image - nerve below the injury (nerve in a circle, bundle diameter increased).

## Case 5. DN-US effectively treat peroneal neuropathy - clinical and imaging improvement



Peroneal neuropathy treatment at knee level

Local muscle spasticity / trigger points near peroneal nerve (A,B)

Restoring nerve structure on US (C)

Clinical improvement after one single session (left)

## Discussion

injury site can cause spasticities in various regions. In some cases, the nerve may be injured directly (e.g., by a bullet) or indirectly by spastic muscles, trigger points, and associated scar tissue. Ultrasound imaging can visualize these nerve injuries and related tissue changes, which can be effectively treated by dry needling (DN) under ultrasound guidance.

DN of trigger points is a technique that involves inserting a thin needle into the muscle tissue to stimulate the trigger point and relieve pain. The mechanism behind the effectiveness of DN for nerve injuries and swollen fascicles is not yet fully understood, but it is believed to involve several factors. The needle stimulation can help to reduce muscle tension and spasticity, leading to improved blood flow and oxygenation to the affected area. This can promote the healing process and reduce inflammation, which can relieve pressure on the nerve and decrease the size of the swollen fascicles.

In the cases discussed in this paper, ultrasound imaging was used to identify nerve injuries and related tissue changes in combat bullet injuries. DN of trigger points was then performed under ultrasound guidance to effectively treat the injuries. The immediate decrease in the diameter of the swollen fascicles seen on ultrasound imaging following DN suggests that this technique may be an effective treatment option for combat-related nerve injuries.

The pathophysiology behind the visualization of nerve injuries on ultrasound and the effectiveness of DN in treating these injuries involves complex interactions between the nervous system, muscle tissue, and other factors. Further research is needed to fully understand the mechanisms involved and to optimize the use of DN for nerve injuries in combat medicine.

It is worth noting that the finding of nerve pathology on ultrasound below the site of injury is not uncommon. This phenomenon is known as "distal axonal sensorimotor neuropathy" and can occur due to the mechanical stress and ischemia that the nerve fibers experience at the site of injury. This can lead to swelling, impaired blood flow, and ultimately axonal degeneration that spreads distally along the nerve. Therefore, ultrasound examination of nerves both proximal and distal to the injury site can provide valuable information on the extent and severity of nerve damage.

### **Distal injury**

When a nerve is injured, the nerve fibers distal to the injury site begin to degenerate, leading to muscle atrophy and loss of sensory function. This degeneration is known as Wallerian degeneration. As the nerve fibers begin to degenerate, the myelin sheath around them also begins to break down, resulting in the formation of debris that can be seen on ultrasound imaging as hypochoic or anechoic foci.

In addition, when a nerve is injured, there is an inflammatory response that can lead to the accumulation of fluid and other cellular debris around the site of injury. This can result in the formation of a hematoma or other fluid-filled structure that can also be visualized on ultrasound.

When performing an ultrasound examination of a nerve, it is important to examine the entire length of the nerve, from the injury site distally to the nerve terminal. This is because, as I mentioned earlier, nerve pathology is commonly visualized distal to the injury site due to Wallerian degeneration.

In summary, ultrasound imaging is a valuable tool for evaluating nerve injuries, as it can help identify the extent of the injury, visualize the formation of hematomas or other fluid-filled structures, and assess the progression of Wallerian degeneration distal to the injury site.

### **Conclusion**

Combat nerve injuries and neuropathic pain are detectable on ultrasound and should be diagnosed during neuromuscular combat trauma. Main parameters for fast diagnosis are fascicle diameter, and changes should be searched for lower than the injury. Detecting scars, muscle spasticity, and gunshot wounds close to the nerve is important. Ultrasound information is most reliable for targeting interventions, and DN is among the most relevant techniques. Dry needling under US guidance effectively reduces neuropathy and neuropathic pain in combat injuries.

### **Learning objectives**

- Neuropathic signs, as in neuropathy, are detectable on ultrasound and need to be diagnosed during neuromuscular combat trauma.
- The main parameters for fast diagnosis are fascicle diameter, and changes should be searched for lower than the injury.
- Detecting scars, muscle spasticities, and gunshot wounds close to the nerve is important.
- Ultrasound information is most reliable for targeting interventions, and DN is among the most relevant techniques.

## LITERATURE

1. Bubnov R.V. The use of trigger point “dry” needling under ultrasound guidance for the treatment of myofascial pain (technological innovation and literature review). *Lik Sprava*2010, 5-6:56-64.
2. Bubnov RV: Evidence-based pain management: is the concept of integrative medicine applicable? *EPMA J*2012, 3(1):13.
3. Bubnov RV. Ultrasonography diagnosis of peripheral neuropathy. The initial experience. *Ultrasound Med Biol.* 2011;37(Suppl 1):S144–S145
4. Bubnov R, Kalika L. EFFECTIVE RESTORING MOTION AND EFFECTIVE TREATMENT OF MYOFASCIAL AND NEUROPATHIC LOW BACK PAIN BY TARGETED DRY NEEDLING USING ULTRASOUND GUIDANCE. *Annals of the Rheumatic Diseases* 2019;78:1921-1922. <http://dx.doi.org/10.1136/annrheumdis-2019-eular.5533>
5. Pilecki Z, Pilecki G, Bubnov R. Introduction to sonosurgery. *EPMA J.* 2014 Feb 11;5(Suppl 1):A66. doi: 10.1186/1878-5085-5-S1-A66. PMID: PMC4125956.
6. Bubnov R, Kalika L, Pilecki Z, Pilecki G. Badanie skuteczności ultrasonografii w diagnozowaniu urazów nerwów powstałych na polu walki i ich leczenia za pomocą suchego igłowania pod kontrolą ultrasonografii. Doniesienie wstępne. Materiały konferencji naukowej "Spersonalizowane metody leczenia wad rozwojowych i schorzeń u dzieci", Zabrze 2023: 99-106.
7. Bubnov R, Kalika L, Pilecki G, Pilecki Z. Ultrasound-guided dry needling for combat nerve injuries and neuropathic pain: A case series. *Journal of the Neurological Sciences* 2023, 455 (suppl): 122698. <https://doi.org/10.1016/j.jns.2023.122698>

### *References:*

1. Pilecki Z., Hrazdira L., Pilecki G., Bubnov R., Jakubowski W. Techniki punkcyjne w ultrasonografii. *Ultrasonografia* 2011, 11(45):38–45.
2. Pilecki Z, Pilecki G, Bubnov R. Introduction to sonosurgery. *The EPMA Journal*. 2014;5(Suppl 1): A66. doi:10.1186/1878–5085–5-S1-A66.
3. Pilecki Z., Pilecki G., Ciekalski J., Dzielicki J.; Sonochirurgia w leczeniu schorzeń i urazów narządu ruchu. *Ultrasonografia* 2010.42:53–58.
4. Tyloch J.; Ultrasonografia w diagnostyce i leczeniu chorób gruczołu krokowego. *Ultrasonografia* nr 40, 2010; 90–108.
5. Pilecki G. Pilecki Z. Ciekalski J. Wąsikowska-Kutaj H. et al. Bezpieczeństwo pacjentów z uszkodzeniem ścięgna Achillesa leczonych sonochirurgicznie. *Ultrasonografia* 2010; Sup 1/2010:64.
6. Akhmetov I, Bubnov RV. Innovative payer engagement strategies: will the convergence lead to better value creation in personalized medicine? *EPMA J*. 2017 Feb 13;8(1):5–15. doi: 10.1007/s13167–017–0078–6. eCollection 2017 Dec. Review.



Atlas - monograph

Vitaliy **Tsybalyuk**  
Rizvan **Abdullaiev**  
Igor **Lurin**  
Irina **Dikan**  
Rostyslav **Bubnov**  
Olena **Grechanyk**

**Ultrasound  
of the spine, peripheral nerves  
and for pain management**

Editor T. P. Martyniak  
Computer layout by N. Kopytko

Signed for printing on January 9, 2024. Format 60x84/16.  
Chalked paper. Offset printing. Printed Sheet. 12.62.  
Circulation of 500 copies.

Produced at FOP V. E. Gudzinskyi  
Ukraine, 61072, Kharkiv, st. August 23.  
Phone/fax: (057)340-52-26.

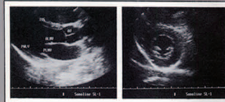
State registration certificate: series No. 269 dated November 23, 2010.

Р. Я. Абдуллаев, С. Левит, Ю. С. Соболев  
**Комплексная эхография**  
*Comprehensive echography*



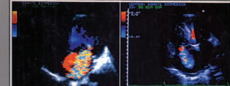
Р. Я. Абдуллаев, О. Ю. Атьков, Ю. С. Соболев

**АТЛАС**  
УЛЬТРАЗВУКОВОЙ ДИАГНОСТИКИ  
ATLAS OF ULTRASONIC DIAGNOSTICS



Р. Я. Абдуллаев, Ю. С. Соболев  
Н. В. Швалер, Э. Фестер

**Современная  
эхокардиография**  
*Advanced Echocardiography*



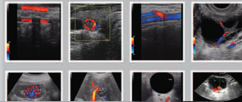
Р. Я. Абдуллаев

**Клиническая  
эхокардиография  
при ишемической  
болезни сердца**



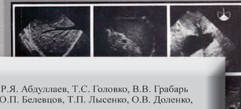
Р. Я. Абдуллаев, Т. С. Головкин

**Ультрасонография**



Р. Я. Абдуллаев, М. А. Белоусов

**АТЛАС**  
УЛЬТРАЗВУКОВОЙ ДИАГНОСТИКИ  
ATLAS OF ULTRASONIC DIAGNOSTICS



Т. С. Головкин, Р. Я. Абдуллаев  
С. Ю. Склад, Л. П. Крахмалова,  
А. С. Крахмалова, И. Н. Сорокин

**Лучевая диагностика  
опухолевых заболеваний  
грудной железы**



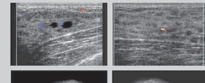
Р. Я. Абдуллаев, С. Г. Ефименко,  
Б. С. Сорокин, Б. С. Фадеев

**УЛЬТРАЗВУКОВАЯ  
ДИАГНОСТИКА  
ПРИ  
ТРАВМЕ  
ЖИВОТА**



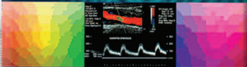
Р. Я. Абдуллаев, Т. С. Головкин, В. В. Грабарь,  
Ю. П. Белевцов, Т. П. Лысенко, О. В. Доленко

**Лучевая диагностика  
неопухолевых заболеваний  
грудной железы**



Р. Я. Абдуллаев, В. Г. Марченко, Л. А. Кадирова

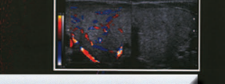
**ДОПЛЕРОГРАФІЯ  
В НЕВРОЛОГІЧНІЙ  
ПРАКТИЦІ**



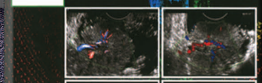
**ДОПЛЕРОГРАФІЯ  
В НЕВРОЛОГІЧЕСЬКІЙ  
ПРАКТИКЕ**

Р. Я. Абдуллаев, Е. И. Герасименко, А. В. Рогов,  
Б. В. Эпштейн, О. А. Сидельникова

**УЛЬТРАЗВУКОВАЯ  
ДИАГНОСТИКА  
НЕТИРЕОИДНЫХ  
ЗАБОЛЕВАНИЙ  
ЩИТОВИДНОЙ  
ЖЕЛЕЗЫ**



**МОЖЛИВОСТІ СУЧАСНОЇ  
УЛЬТРАЗВУКОВОЇ  
ДІАГНОСТИКИ  
ЗАХВОРЮВАНЬ  
ТОВСТОЇ КІШКИ**



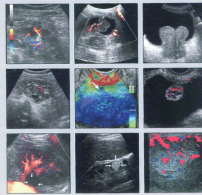
Р. Я. Абдуллаев, И. Н. Сафонова,  
И. С. Луцканина, В. В. Грабарь

**ДОПЛЕРОМЕТРИЯ  
СОСУДОВ  
ФЕТОПЛАЦЕНТАРНОГО  
КОМПЛЕКСА**



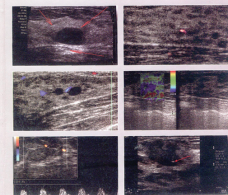
Р. Я. Абдуллаев, В. Н. Лесовой  
С. А. Возняков

**УЛЬТРАЗВУКОВАЯ  
ДИАГНОСТИКА  
ОПУХОЛЕЙ  
МОЧЕПОЛОВОЙ СИСТЕМЫ**



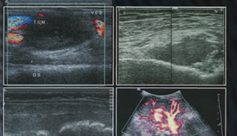
R.Y. Abdullayev, I.Q. Mammadov

**SÜD VƏZİLƏRİNİN  
ULTRASƏS MÜAYİNƏSİ**




Р.Я. Абдуллаев, Т.С. Головию, А.Н. Ханиско, В.Г. Марченко, В.Е. Моздуров, И.И. Давлат

**УЛЬТРАЗВУКОВАЯ ДИАГНОСТИКА ОПУХОЛЕЙ ОПОРНО-ДВИГАТЕЛЬНОГО АППАРАТА**

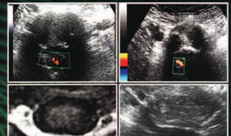


**УЛЬТРАЗВУКОВАЯ ДИАГНОСТИКА ЗАБОЛЕВАНИЙ КОЛЕННОГО СУСТАВА**



Р.Я. Абдуллаев, А.Н. Ханиско, Л.А. Дзюк, В.Г. Марченко, В.В. Голышев, Б.С. Фарад

**УЛЬТРАЗВУКОВАЯ ТОМОГРАФИЯ ПОЗВОНОЧНОГО ДВИГАТЕЛЬНОГО СЕГМЕНТА**



**УЛЬТРАЗВУКОВАЯ ДИАГНОСТИКА ПРИ ШЕЙНОМ ОСТЕОХОНДРОЗЕ**



**ТРАНСВАГИНАЛЬНАЯ ДОПЛЕРОГРАФИЯ ПРИ ЭНДОКРИННОМ БЕСПЛОДИИ**



**ДОПЛЕР-ЭХОКАРДИОГРАФИЯ ПЛОДА ДИАГНОСТИКА НОРМЫ**



**ДОПЛЕРОГРАФИЯ МАГИСТРАЛЬНЫХ СОСУДОВ ШЕИ**



**УЛЬТРАЗВУКОВАЯ ДИАГНОСТИКА ПРИ ПОЯСНИЧНОМ ОСТЕОХОНДРОЗЕ**



Р.Я. Абдуллаев, Н.И. Пилипенко, Ф. Горлачу

**УЛЬТРАЗВУКОВАЯ ДИАГНОСТИКА ОЧАГОВЫХ ПОРАЖЕНИЙ ПЕЧЕНИ**

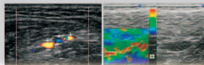


Р.Я. Абдуллаев, Г.В. Дзюк, Т.А. Душкин, Р.В. Бубинов

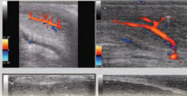
Р.Я. Абдуллаев, В.Н. Лесовой

Р.Я. Абдуллаев, В.В. Грабарь, Т.П. Лысенко, И.Н. Сафонова, В.Д. Деджо

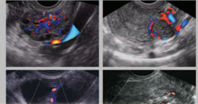
**УЛЬТРАСОНОГРАФИЯ ТАЗОБЕДРЕННОГО И ГОЛЕНОСТОПНОГО СУСТАВОВ**



**Ультрасонография в андрологии**



**Доплерография в гинекологии**

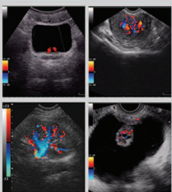


Р.Я. Абдуллаев, В.Н. Лесовой, Н.И. Пилипенко, Т.С. Головию

Р.Я. Абдуллаев, Г.В. Дзюк, А.Н. Ханиско, Т.А. Душкин, Р.В. Бубинов, А.А. Фарад

Д.А. Аллев Р.Я. Абдуллаев

**Ультрасонография в уронефрологии**



**УЛЬТРАСОНОГРАФИЯ В АРТРОЛОГИИ**

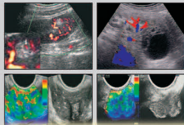


**УЛЬТРАСОНОГРАФИЯ В ОНКОЛОГИИ**



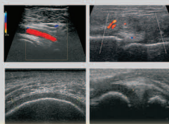
Р.Я. Абдуллаев, В.Н. Лесовой  
Р.В. Бубнов, Ю.А. Винник

### УЛЬТРАСОНОГРАФИЯ В ОНКОУРОЛОГИИ



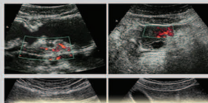
Р.Я. Абдуллаев, Г.В. Дзяк  
Т.А. Душик, А.А. Фельцо

### УЛЬТРАСОНОГРАФИЯ КОЛЕННОГО СУСТАВА



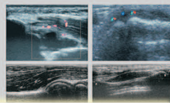
Р.Я. Абдуллаев, В.В. Гавченко,  
М.И. Спунжик, Ю.А. Винник

### Ультрасонография желудка и 12п кишки



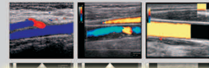
Р.Я. Абдуллаев, Т.А. Душик,  
А.А. Фельцо, М. Тазар

### УЛЬТРАСОНОГРАФИЯ ЛОКТЕВОГО, ЛУЧЕЗАПЯСТНОГО И СУСТАВОВ КИСТИ



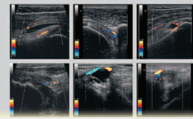
Р.Я. Абдуллаев, В. Г. Марченко, Л. А. Дзяк,  
А. А. Фельцо, В. С. Фельц, Г. В. Бубнов

### УЛЬТРАСОНОГРАФИЯ В НЕВРОЛОГИИ



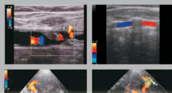
Р.Я. Абдуллаев, Г.В. Дзяк  
Т.А. Душик

### УЛЬТРАСОНОГРАФИЯ ПЛЕЧЕВОГО СУСТАВА



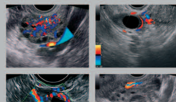
Р.Я. Абдуллаев

### ДОПЛЕРОГРАФИЯ СОСУДОВ ШЕИ И ГОЛОВЫ



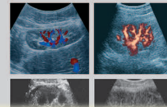
Р.Я. Абдуллаев

### ДОПЛЕРОГРАФИЯ ПРИ ЭНДОКРИННОМ БЕСПЛОДИИ



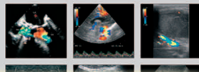
Р.Я. Абдуллаев, А.В. Лесовая

### КЛИНИЧЕСКАЯ УЛЬТРАСОНОГРАФИЯ ПРИ НЕФРИТАХ



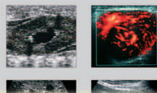
Р.Я. Абдуллаев, З.Н. Мыттык,  
А.А. Фельцо, Г.К. Бубнов

### УЛЬТРАСОНОГРАФИЯ ПРИ ИНФЕКЦИОННЫХ ЗАБОЛЕВАНИЯХ



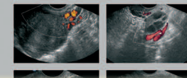
Р. Я. Абдуллаев, З. Н. Мыттык, А. А. Фельцо

### УЛЬТРАСОНОГРАФИЯ ПРИ ТУБЕРКУЛЕЗЕ И СПИДЕ



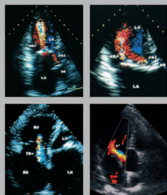
Р.Я. Абдуллаев

### ТРАНСВАГИНАЛЬНАЯ ЭХОГРАФИЯ ПРИ ВОСПАЛЕНИИ МАТКИ И ПРИДАТКОВ



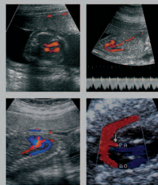
Р.Я. Абдуллаев

### ЭХОКАРДИОГРАФИЯ ПРИ ИНФЕКЦИОННЫХ ЗАБОЛЕВАНИЯХ СЕРДЦА



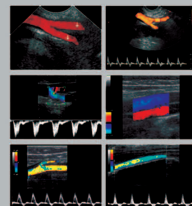
Р.Я. Абдуллаев

### ЭХОКАРДИОГРАФИЯ ПЛОДА



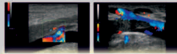
Р.Я. Абдуллаев

### ДОПЛЕРОГРАФИЯ АРТЕРИЙ НИЖНИХ КОНЕЧНОСТЕЙ



Р.Я. Абуллаев

### ДОПЛЕРОГРАФИЯ ВЕН НИЖНИХ КОНЕЧНОСТЕЙ



СПУЖИК М.И., ШАРМАЗАНОВА С.П.,  
АБДУЛЛАЕВ Р.Я., СПУЖИК С.М.,  
ФЕДОРОВИЧ В.О.

## КОЛІННИЙ СУГЛОБ

ПРОМЕНЕВА АНАТОМІЯ,  
МЕТОДИ ДОСЛІДЖЕННЯ,  
ПРОМЕНЕВА ДІАГНОСТИКА  
ЗАХВОРОВАНЬ



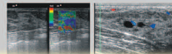
Р.Я. Абуллаев

### ДОПЛЕРОГРАФИЯ АБДОМИНАЛЬНЫХ СОСУДОВ



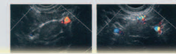
Р.Я. Абуллаев, В. И. Калашников  
В. Г. Марченко, Л. А. Сисуи

### ДУПЛЕКСНЕ СКАНУВАННЯ В ДІАГНОСТИЦІ КАРОТИДНОГО АТЕРОСКЛЕРОЗУ



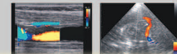
Р.Я. Абуллаев, М.И. Спужик  
Е.П. Шармазанова

### УЛЬТРАСОНОГРАФИЯ ШЕЙНОГО ОТДЕЛА ПОЗВОНОЧНИКА



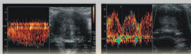
Р.Я. Абуллаев, В. И. Калашников  
В. Г. Марченко, Л. А. Сисуи

### УЛЬТРАЗВУКОВЕ ДОСЛІДЖЕННЯ МАГІСТРАЛЬНИХ АРТЕРІЙ ГОЛОВИ ТА ШІЙ



Р. Я. Абуллаев, В. Г. Марченко  
И. Г. Мамедов

### ДУПЛЕКСНОЕ СКАНИРОВАНИЕ ПРИ ПОЯСНИЧНОМ ОСТЕОХОНДРОЗЕ



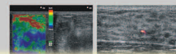
Р.Я. Абуллаев, В.Г. Марченко  
А.А. Фелько, Л.А. Сисуи

### ДОПЛЕРОГРАФИЯ ПРИ ИШЕМИЧЕСКОМ ИНСУЛЬТЕ



Р.Я. Абуллаев, А. А. Фелько  
Д. Ю. Гульмечко

### УЛЬТРАСОНОГРАФИЯ ПРИ МАСТОПАТИЯХ



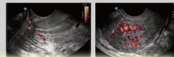
Р.Я. Абуллаев, С.Г. Кереман  
А.И. Ханов, В.Г. Марченко

### УЛЬТРАСОНОГРАФИЯ МЯГКИХ ТКАНЕЙ ОПОРНО-ДВИГАТЕЛЬНОГО АППАРАТА



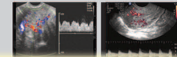
Р. Я. Абуллаев

### НОРМАЛЬНАЯ ТРАНСВАГИНАЛЬНАЯ ЭХОГРАФИЯ МАТКИ И ПРИДАТКОВ



Р. Я. Абуллаев, С. М. Карташов,  
А. А. Михановский, Е. Н. Сухина

### УЛЬТРАЗВУКОВАЯ ДИАГНОСТИКА ЗЛОКАЧЕСТВЕННЫХ ОПУХОЛЕЙ МАТКИ



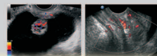
Р. Я. Абуллаев, В. В. Каминский  
О. В. Грищенко, А. Х. Сибханкулов

### ТРАНСВАГИНАЛЬНАЯ ЭХОГРАФИЯ ПРИ ПАТОЛОГИИ ШЕЙКИ МАТКИ

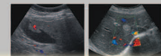


Р. Я. Абуллаев, В. Н. Лесовой  
Ю. В. Думанский, Ю. А. Винник

### УЛЬТРАЗВУКОВАЯ ДИАГНОСТИКА ОПУХОЛЕЙ ОРГАНОВ МАЛОГО ТАЗА

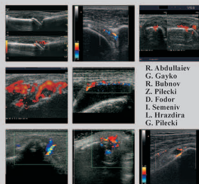


### УЛЬТРАЗВУКОВАЯ ДИАГНОСТИКА ОПУХОЛЕЙ АБДОМИНАЛЬНЫХ ОРГАНОВ



Р. Я. Абуллаев, Г. В. Гайко, Р. В. Бубинов  
З. Пилейский, Д. Флор, И. П. Сомовин  
Л. Грацира, Г. Пилейский

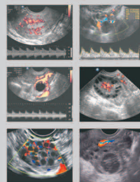
### УЛЬТРАСОНОГРАФИЯ СУСТАВОВ ULTRASONOGRAPHY of the joints



Р. Абуллаев  
С. Гайко  
Р. Бубинов  
З. Пилейский  
Д. Флор  
И. Сомовин  
Л. Грацира  
Г. Пилейский

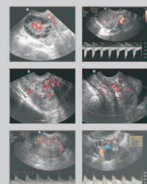
Р.Я. Абуллаев Ю.П. Виноченко  
Н.Ю. Воронско А.И. Мухомор А.А. Фелько

### УЛЬТРАЗВУКОВАЯ ДИАГНОСТИКА В РЕПРОДУКТИВНОЙ ГИНЕКОЛОГИИ



Р.Я. Абуллаев В.Н. Запорожан  
Ю.И. Гульмечко

### УЛЬТРАСОНОГРАФИЯ в ГИНЕКОЛОГИИ



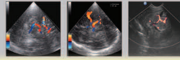
Р.Я. Абуллаев, В.Н. Лесовой  
С.А. Вельяминов

### УЛЬТРАЗВУКОВАЯ ДИАГНОСТИКА ОПУХОЛЕЙ МОЧЕПОЛОВОЙ СИСТЕМЫ



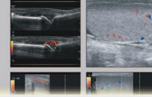
Р.Я. Абуллаев, Е.Г. Пестриченко,  
В.Н. Цымбалюк, В.Г. Марченко, И. Е. Пашинюк,  
Е.И. Савиных, А.И. Морозов

### ТРИПЛЕКСНОЕ СКАНИРОВАНИЕ в НЕВРОЛОГИИ и НЕЙРОХИРУРГИИ

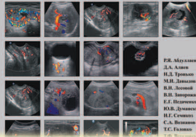


Р. Я. Абуллаев, В.Н. Лесовой

### ЭХОГРАФИЯ МУЖСКИХ ПОЛОВОЙ ОРГАНОВ



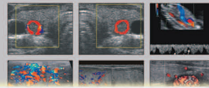
### УЛЬТРАЗВУКОВАЯ ДИАГНОСТИКА в онКОЛОГИИ



Р.Я. Абуллаев  
Д.А. Алиев  
И.А. Третьяков  
В.В. Лысенков  
В.Н. Цымбалюк  
В.И. Давыдов  
В.Г. Марченко  
И.Е. Пашинюк  
С.А. Вельяминов  
С.Г. Ефименко

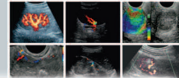
Р. Я. Абуллаев, А. Д. Алиев

### ЭХОГРАФИЯ ЩИТОВИДНОЙ ЖЕЛЕЗЫ



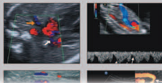
Р. Я. Абуллаев, В.Н. Лесовой  
А.В. Лесовая

### ЭХОГРАФИЯ почек, мочевого пузыря и предстательной железы



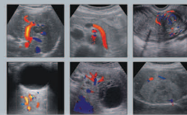
### ПРЕНАТАЛЬНАЯ ЭХОГРАФИЯ

#### АНОМАЛИИ СЕРДЕЧНО- СОСУДИСТОЙ СИСТЕМЫ



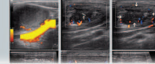
Р. Я. Абуллаев

### ЭХОГРАФИЯ



Р.Я. Абуллаев, А.Д. Алиев  
С.Г. Ефименко, В.В. Лысенков

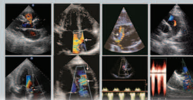
### Эхография челюстно-лицевой зоны



Р.Я. Абуллаев

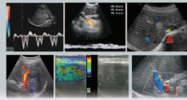
### Эхокардиография

#### Врожденные пороки сердца



Р. Я. Абуллаев

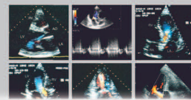
### ЭХОГРАФИЯ печени



Р.Я. Абуллаев

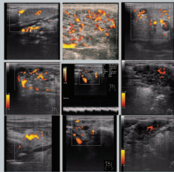
### ЭХОКАРДИОГРАФИЯ

#### Инфекционные заболевания сердца



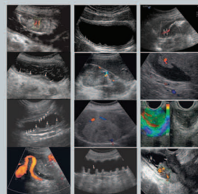
Р.Я. Абуллаев, А.Д. Алиев  
С.Г. Ефименко, В.В. Лысенков

### УЛЬТРАСОНОГРАФИЯ СЛОННЫХ ЖЕЛЕЗ



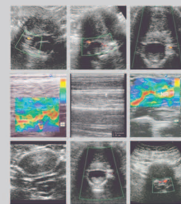
Д.А. Алиев, Р.Я. Абуллаев, А.Д. Алиев

### УЛЬТРАСОНОГРАФИЯ в АБДОМИНАЛЬНОЙ ОНКОЛОГИИ



Р.Я. Абуллаев, В.Н. Цымбалюк  
В.Г. Марченко, Р.В. Бубнов

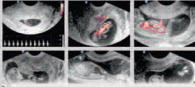
### Ультрасонография периферических нервов и спинного мозга



Р.Я. Абдуллаев

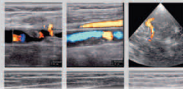
**ПРЕНАТАЛЬНАЯ ЭХОГРАФИЯ**

Первый триместр. Скрининг  
в 12-14 недель беременности



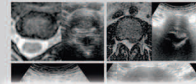
Р. Я. Абдуллаев, В. Н. Цымбалюк,  
В. Г. Марченко, Л. А. Сысуи

**Допплерография  
при атеросклерозе каротидных  
и церебральных артерий**



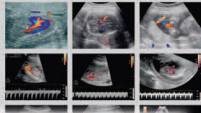
Р.Я. Абдуллаев, В.Н. Цымбалюк,  
А.Н. Хансиков, В.Г. Марченко

**УЛЬТРАЗВУКОВАЯ, КОМПЬЮТЕРНАЯ  
И МАГНИТНО-РЕЗОНАНСНАЯ  
ТОМОГРАФИЯ ПРИ ОСТЕОХОНДРОЗЕ**



Р.Я. Абдуллаев

**ДУПЛЕКСНОЕ  
СКАНИРОВАНИЕ  
В АКУШЕРСТВЕ**



А. А. Опарин, А. Г. Опарин, Р. Я. Абдуллаев,  
А. Н. Корж, Г. И. Кочуев, Н. В. Лаврова,  
Ю. Н. Дюшккина, М. Н. Кочуева

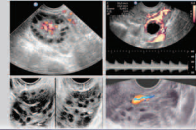
**Комплексная  
диагностика  
и лечение заболеваний  
СЕРДЦА**

МОНОГРАФИЯ



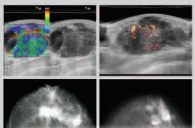
Р.Я. Абдуллаев, Т.Ф. Татарчук  
О.В. Грищенко

**УЛЬТРАСОНОГРАФИЯ  
В ЭНДОКРИННОЙ  
ГИНЕКОЛОГИИ**



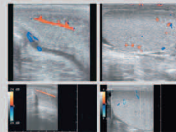
Т.С. Головкин, Р.Я. Абдуллаев  
А.С. Крахмалёва

**УЛЬТРАЗВУКОВАЯ И РЕНТГЕНОВСКАЯ  
МАММОГРАФИЯ В ДИАГНОСТИКЕ  
ОПУХОЛЕВЫХ ЗАБОЛЕВАНИЙ  
МОЛОЧНОЙ ЖЕЛЕЗЫ**



Р.Я. Абдуллаев, В.Н. Лесовой

**ЭХОГРАФИЯ  
МУЖСКИХ ПОЛОВЫХ  
ОРГАНОВ**



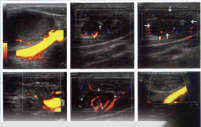
Р. Я. Абдуллаев, А. А. Опарин,  
А. Г. Опарин, А. В. Бильченко

**Комплексная  
электро-  
и эхокардиографическая  
диагностика  
заболеваний  
СЕРДЦА**



Р.Я. Абдуллаев, А.Д. Алиев  
С.Г. Ефименко, В.В. Лысенко

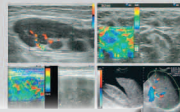
**Эхография  
челюстно-лицевой зоны**



Р.Я. Абдуллаев

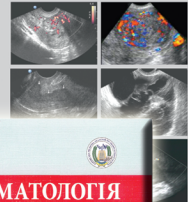
**ЭХОГРАФИЯ**

Инфекционные заболевания



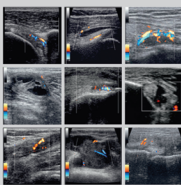
Р. Я. Абдуллаев, О. В. Грищенко  
Т. П. Лысенко

**ЭХОГРАФИЯ  
в онкогинекологии**



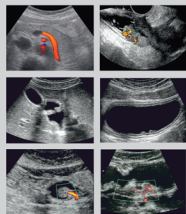
Р. Я. Абдуллаев, А. Н. Хансиков  
В. Г. Марченко, А. Н. Хансиков

**ЭХОГРАФИЯ  
мягких тканей скелета**



Р.Я. Абдуллаев, Р.А. Мамедов

**УЛЬТРАЗВУКОВАЯ  
ДИАГНОСТИКА  
ЗАБОЛЕВАНИЙ  
ЖЕЛУДОЧНО-КИШЕЧНОГО  
ТРАКТА**



**ТРАВМАТОЛОГИЯ  
І ОРТОПЕДІЯ**

для практиці сімейного лікаря

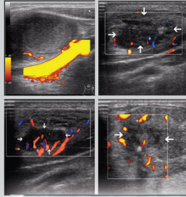
Керівництво



Харків  
2016

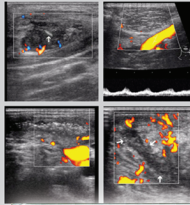
Р.Я. Абдуллаєв, О.В. Шербіна  
Н.О. Савичук, С.Г. Єфіменко

### ЕХОГРАФІЯ СЛИННИХ ЗАЛОЗ



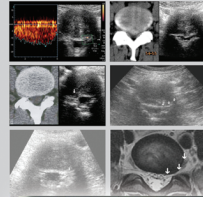
Р.Я. Абдуллаєв, О.В. Шербіна  
П.О. Король, Н.О. Савичук, С.Г. Єфіменко

### УЛЬТРАЗВУКОВА ЩЕЛЕПНО-ЛИЦЬОВОЇ ЗОНИ



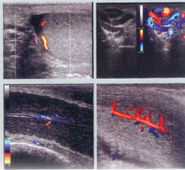
Р.Я. Абдуллаєв, І.О. Вороньжєв  
Т.М. Козарєнко, Ю.А. Коломичєнко  
Н.С. Лисєнко

### УЛЬТРАЗВУКОВА ДІАГНОСТИКА ПОПЕРЕКОВОГО ОСТЕОХОНДРОЗУ



Р.Я. Абдуллаєв, В. М. Лісовий,  
В.В. Рюєв

### УЛЬТРАЗВУКОВА ОРГАНІВ МОШОНКИ ТА ПЕНІСА



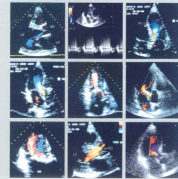
В.Я. Кляєв, Р.Я. Абдуллаєв, Г.В. Цігуєв, С.О. Король,  
О.О. Бєз, Д.О. Сєвєрєнов, М.Г. Гєрєшєв

### НАРИСИ ПРОМЕНЕВОЇ ДІАГНОСТИКИ ГОСТРИХ ЗАХВОРЮВАНЬ ТА БОЙОВОЇ ТРАВМИ ЖИВОТА



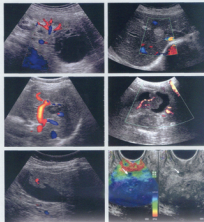
Р.Я. Абдуллаєв, В.А. Капустинєв

### УЛЬТРАЗВУКОВА ДІАГНОСТИКА ЗАПАЛЬНИХ ЗАХВОРЮВАНЬ СЕРЦЯ



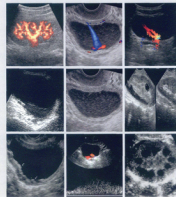
Р.Я. Абдуллаєв, М.Д. Трєньєво,  
О.К. Толєстєнов, О.В. Шербіна,  
В.М. Мішєлєвєв, В.В. Рюєв, П.О. Король

### ЕХОГРАФІЯ В ОНКОЛОГІЇ



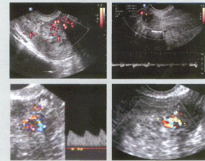
Р.Я. Абдуллаєв, В. М. Лісовий,  
В.А. Капустинєв, В.В. Рюєв

### ЕХОГРАФІЧНА ДІАГНОСТИКА ЗАПАЛЬНИХ ЗАХВОРЮВАНЬ СЕЧОВИДИЛЬНОЇ СИСТЕМИ



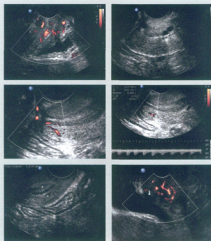
Р.Я. Абдуллаєв, О.В. Шербіна  
Т.М. Козарєнко, П.О. Король

### УЛЬТРАЗВУКОВА ДІАГНОСТИКА ЗЛОЯКІСНИХ ПУХЛИН МАТКИ



Р.Я. Абдуллаєв, В.В. Князьєвський

### УЛЬТРАЗВУКОВА ДІАГНОСТИКА ШИЙКИ МАТКИ



Медицина XXI століття



## ОРТОПЕДІЯ І ТРАВМАТОЛОГІЯ

Харків  
2018

В. М. Ждан, Р. Я. Абдуллаєв  
С. О. Пономарєнко, Г. В. Іваньєвський

### УЛЬТРАЗВУКОВА ДІАГНОСТИКА У ПРАКТИЦІ СІМЕЙНОГО ЛІКАРЯ

